Project THEMIS

Technical Report No. 24

THE STABILITY OF PARALLEL, QUASI-PARALLEL AND STATIONARY FLOWS

by

René A. Kahawita

and

Robert N. Meroney

Prepared under

Office of Naval Research

Contract No. N00014-68-A-0493-0001

Project No. NR 062-41416-6-68(Code 438)

U.S. Department of Defense

Washington D.C.

Fluid Dynamics and Diffusion Laboratory
College of Engineering
Colorado State University
Fort Collins, Colorado

September, 1973

CER73-74-RK-RNM12

ABSTRACT

The methods of linear perturbation theory have been used to study the stability of various flows, among them being

(i) The stability of boundary layers along concave heated walls;

(ii) The stability of boundary layers along concave walls with suction;

(iii) The stability of wall jets along concave and convex walls;

(iv) The spin up of a two-dimensional cylinder in an infinite medium;

(v) The stability of stationary layers of fluid with arbitrary temperature stratification;

(vi) The stability of natural convection flow along inclined plates.

During the course of this work, three different solution techniques were employed; one of them was an approximate analytic technique, the remaining two were numerical. Three-dimensional spatially and temporally amplifying disturbances were considered in this study.

The results indicated that the normal velocity component of the mean flow in a boundary layer, although much smaller than the stream-wise component had a profound effect in reducing the stability of the flow. On the other hand, suction at the wall improved the stability characteristics. For the flow of parallel layers of fluid along heated walls with small curvature, it was found that a unique stability curve for neutral disturbances may be obtained if the quantity plotted along the abscissa is $Ra + K_s N_G^2$ where Ra is the Rayleigh number, N_G is the Goertler number and K_s is a constant which expresses the relative importance of the mean temperature and velocity profiles.

It was demonstrated also that wall jets are unstable on concave as well as convex walls.

The results obtained for the stability of the spin up of a cylinder in an infinite medium are in qualitative agreement with experiment.

The dependence of the onset of convective overturning in an unstable layer of fluid with a nonlinear basic temperature profile and bounded above by fluid of varying stability on Rayleigh number was established.

The angle at which the two-dimensional wave instability passes into the three-dimensional mode in natural convection along an inclined plate was calculated. The result was found to be in good agreement with experiment. Other results obtained for this flow were in good qualitative agreement with experiment.

Finally, some simple wind tunnel experiments with boundary layers along curved heated walls were performed. Photographic evidence of longitudinal vortices was obtained together with some qualitative data.

ACKNOWLEDGMENTS

Financial support for this research study was provided by the Office of Naval Research by Contract No. N00014-68-A-0493-0001. The author gratefully acknowledges this support.

TABLE OF CONTENTS

TABLE OF CONTENTS (Continued)

LIST OF TABLES

LIST OF FIGURES

LIST OF FIGURES (Continued)

LIST OF FIGURES (Continued)

LIST OF SYMBOLS

Note: These symbols do not include those in Appendices A, B and C. They are independently defined there.

English

A	Dimensionless wavenumber
B	Dimensionless amplification factor
C_p	Dimensionless pressure perturbation
G	Dimensionless parameter defined in Chapter 8
G_r	Grashof Number based on δ
Gr_x	Grashof Number based on x [Chapter 8]
K	Dimensionless Curvature
N_G	Goertler Number
P_r	Prandtl Number
R_a	Rayleigh Number
R	Longitudinal radius of curvature
R_d	Reynold's Number
T_1	Dimensionless mean temperature
T	Temperature. Also dimensionless temperature perturbation
T_p	Temperature perturbation
T_w	Wall temperature
T_∞	Free stream temperature
U, V, W	Mean velocities in the three respective coordinate directions
U_∞	Characteristic velocity (Generally Free Stream)
U_m	Velocity scale; also velocity maximum in wall jet profile
U_o, V_o, W_o	Dimensionless mean velocity components

LIST OF SYMBOLS (Continued)

a	Cylinder radius in spin up problem
a_1 to a_5, b_1 to b_4, c_1 to c_3, d_1 to d_4	Constants defined in Chapter 6
c	Characteristic chord length. Also penetration coefficient in Chapter 5
d	Total height of disturbances in Chapter 5
$f = \frac{U}{U_m}$	Dimensionless velocity profile for wall jet calculations
g	Gravitational acceleration
$k = \frac{1}{R}$	Curvature
p_p	Pressure perturbation
r	Radial coordinate in spin up problem
t	Time
u,v,w	Coordinate velocity components. Also dimensionless velocity perturbations
u_p, v_p, w_p	Perturbation velocity components
x,y,z	Streamwise, vertical and lateral directions respectively.

Greek

α	Wavenumber
β	Amplification factor
δ	Characteristic boundary layer length scale
γ	Fluid volumetric expansion coefficient
κ	Thermal diffusivity
ν	Kinematic viscosity
η	Dimensionless vertical (y) coordinate
λ	Decay parameter in wall jet calculations

LIST OF SYMBOLS (Continued)

$\tau = \frac{\nu t}{a^2}$	Dimensionless critical time in spin up problem
$\Phi = c\phi$	Dimensionless wavenumber
ϕ	Dimensionless wavenumber
ξ	Dimensionless vertical (y) coordinate
λ_δ	Pohlhausen pressure parameter $-\frac{\delta^2}{\gamma}\frac{du}{dx}$
μ	Dynamic viscosity
ν	Kinematic viscosity
ρ	Density of fluid
σ	Free stream flow parameter $\frac{1}{(x_s-x_o)}[\int_{x_o}^{x_s} t\, C_p \frac{dC_p}{dt}]^{1.2} / \frac{1}{(t_s-t_o)} \int_{x_o}^{x_s} C_p d_t$
σ^2	Variance
ψ	Stream function $\int_o^y udy$
ψ_i	Stream function in the inner layer
τ	Shear stress
τ_w	Shear stress at wall

Suffixes

o	Conditions at the position of the peak velocity
'	Velocity fluctuations
'	Derivative with respect to x
'	Denotes value for the comparison profile of constant pressure in flat plate case
s	Denotes value evaluated at separation
t	Denotes value evaluated at transition position
w	Denotes value evaluated at the wall

Chapter 1

INTRODUCTION

The onset of instability in fluid layers is of considerable interest owing to it's wide application in the various technological fields and in the disciplines of Geophysics and Astrophysics.

Recently, there has been considerable interest in transition phenomena in boundary layers as evidenced by the large amount of material published within the last decade. The ultimate goal, is the ability to make accurate predictions regarding the transition from laminar to turbulent flow, since important flow properties like the wall friction, heat transfer rate and separation characteristics deviate considerably in the turbulent regime from their laminar values.

Research into Short Takeoff and Landing (STOL) Aircraft has now become of vital necessity if the concept of downtown airports is to be a reality. Their low takeoff and landing speeds and correspondingly high lift coefficients require sophisticated methods of boundary layer control which in turn demand an increased understanding of boundary layer stability.

Heat transfer experiments relating to forced convection reveal surprising increases in heat transfer when vortical disturbances are superimposed on the boundary layer. A study of the stability of boundary layers on heated walls, would therefore be expected to yield useful information pertaining among other things to the design of efficient heat exchangers.

In the realm of Geophysics, certain cloud patterns revealed by weather satellites are characteristic manifestations of large scale convective motion. The driving force here, may be attributed to a variety of instability mechanisms in the planetary boundary layer. Since such convection on the atmospheric scale considerably modifies the vertical transport of heat, moisture and momentum, a need exists for suitable analyses from which at least qualitative inferences may be made.

Convective instability is also of Astrophysical interest. There is sufficient evidence to indicate that certain regions within stars may become gravitationally unstable and lead to steady convective overturning. The criteria for the onset of such convective activity is of importance among other reasons, because of the role it plays in the construction of stellar models.

The examples mentioned so far may be classified as belonging to that branch of Fluid Mechanics denoted as Hydrodynamic Stability. About fifteen years ago, enough information was available about the various manifestations of instability in a continuous medium to formulate three main catagories. These are, first, the oscillations of parallel flows, or nearly parallel (quasi-parallel) flows: channel flows, boundary layers, jets and wakes. Second, there is the class with curved streamlines, such as vortices between rotating cylinders or boundary layers along curved walls. In the third catagory are placed those cases where the mean flow is truly zero: Bénard cells and convective instabilities being the chief examples. The first category contains the classical examples of inviscid instabilities which are generally damped when friction becomes significant. However, it also contains outstanding examples of resistive instability. It is well known that resistive instability can occur in electrical as well as mechanical systems. It is still surprising however, that fluid systems can also display the same type of instability.

This discourse restricts itself to the second and third classes of the Hydrodynamic Stability Problem: the stability of parallel and quasi parallel flows with curved streamlines and unstable stratification, and the stability of stationary flows with heating at the lower boundaries. The disturbances in these flows, generally manifest themselves as parallel rows of streamwise oriented vortices when a mean flow is present. In the stationary case, columnar type convection is observed.

Although only disturbances in stationary layers of fluid are conventionally referred to as convective instabilities, throughout this report the term will also be used to describe the disturbances generated in curved flows due to centrifugal effects.

The purpose of this investigation is twofold: to investigate the stability of boundary layers under the combined influence of curvature and heating, and to examine the onset of convective activity in arbitrarily stratified fluid layers. The first has wide application in aeronautics and heat transfer; the second will hopefully increase understanding of convective mechanisms in the atmosphere and in stellar structures.

Chapter 2

REVIEW OF CONVECTIVE INSTABILITY PHENOMENA IN FLUID LAYERS

2.1 Hydrodynamic Instability Caused by Unstable Thermal Stratification

This section is devoted to a review of thermally induced convective instability in fluid layers under both stationary and mean shear conditions.

2.1.1 Experimental observations

The earliest recorded study of convective instabilities in a layer of fluid heated flow below was that of Benard (1900). He observed the now familiar pattern of hexagonal cells in a thin layer of preheated spermaceti cooling slowly in a shallow vessel. These experiments were elaborated on by Terada et al. (1928, 1929), Avsec (1930), Graham (1933) and Chandra (1937). Avsec made a detailed study of the instability in layers of air contained between two conducting plates and heated from below under stationary as well as mean shear conditions. The onset of convection was determined by a flow visualization technique involving the injection of tobacco smoke along the lower plate. At the onset of instability, the smoke collected into wavelike crests, ultimately forming steady rectangular cellules. As the thickness of the air layer was reduced, a critical thickness of about 8 mm was reached where the two dimensional columnar convection passed into the three dimensional hexagonal mode. On imposing a shear on the flow, he discovered that for small velocities, transverse rolls were formed while for larger velocities, longitudinal rolls with periodic spanwise spacing completely dominated the flow. These results were confirmed by Graham (1933). Schmidt and Milverton (1935) obtained precise measurements of the onset of convective motion in stationary fluid layers. They incorporated a principle for it's detection which is so direct and simple that it has served as the basis for all later experiments in this subject. We will briefly outline the method here, for details the reader is referred to Chandrasekhar (1961). Suppose a fluid layer contained between two planes is heated from below; in order to maintain a given temperature gradient a constant heat flux must be maintained at the lower boundary. In the Schmidt-Milverton experiments, the lower boundary was heated by an electric current, which in the absence of heat losses and in the conductive regime, increases with the square root of the temperature difference between the two plates. As soon as convection sets in, the current required increases with temperature difference. If a graph of the square of the current versus temperature difference is plotted, one observes a break in the curve corresponding to the point of instability. This has come to be known as the Schmidt-Milverton principle. Silveston (1958) utilized the same principle to obtain the critical point for various liquids.

Optical methods have also been used to examine convective phenomena in liquids. Silveston (1958) as well as Schmidt and Milverton (1935) and Schmidt and Saunders (1938) have obtained photographic evidence of thermal instability by the so called "Schlieren" method. In this method the variability of the refractive index of a medium with density and temperature is utilized. Further details of these experiments are discussed by Chandrasekhar (1961). In recent times, Berg, Boudart and Acrivos (1966) have obtained Schlieren photographs of convective motions in pools of evaporating liquids at various depths. A review of nearly a century's research on convective phenomena in fluid layers heated from below has been published by Ostrach (1955) and the interested reader is directed there.

So far, we have mentioned only briefly the appearance of longitudinal rolls in fluid layers heated from below and subjected to a mean shear. Terada and his co-workers (1928, 1929), who used thin layers of alcohol flowing down inclined plates were able to observe the periodically spaced streamwise vortices by a dye injection technique. The unstable stratification in their experiments was achieved by the evaporative cooling of the alcohol surface thus creating the necessary 'top-heavy' requirement. More recently, Sparrow and Husar (1969) as well as Lloyd and Sparrow (1970) have obtained photographic evidence that longitudinal rolls are formed in the natural convection flow along inclined plates. They used water as the working fluid and a sensitive dye indicator technique for the flow visualization. Their principle observation was that the inclination angle of the plate from the vertical had to exceed a certain critical value of about 15° before longitudinal rolls would form. Once formed however, the rolls constituted a parallel system with periodic spacing which appeared independent of inclination angle. Quantitative measurements of mass transfer in inclined plate natural convection were taken very recently by Lloyd, Sparrow and Eckert (1972) who noticed a periodic spanwise variation in mass transfer due to the presence of the vortices. Table I provides a brief guide to experimental work published on thermo-convective rolls.

The main motivation for the study of convective phenomena in fluids was their analogy with similar phenomena in the atmosphere. For example, Idrac (1920) and Avsec (1939) among others, pointed out that the regularly spaced pattern of cumulii frequently formed in fair weather looked remarkably like a Benard Cell arrangement, although not truly hexagonal in shape. Terada (1929) pointed out the similarity between the cloud structure observed in parallel bands (cloud streets), and his laboratory experiments with thin alcohol layers. Recent satellite photographs of the earth's atmosphere (Krueger and Fritz 1961) have revealed that cloud streets as well as Benard cell type clouds are in fact a very common occurrence. Numerous research efforts relating to these geophysical phenomena have been published, chief among these being the works of Kuettner (1959), Kuo (1963), Faller (1965), Faller and Kaylor (1966) and Lilly (1966). Faller (1969) has also discussed the various mechanisms by which longitudinal convective rolls may be formed. These include density convection, streamline curvature, two types of instability in rotating boundary layers (Ekman flow), advective instability and instability caused by wind-wave induced turbulence. Each of these mechanisms has a distinctive energy transfer process drawing upon one or another potential or kinetic energy source in the basic flow field.

2.1.2 Theoretical Analyses

A theoretical analysis regarding the onset of convection in fluid layers with unstable temperature stratification was first presented by Lord Rayleigh (1916). Jefferies (1926) and then Low (1929) later verified and extended Rayleigh's Analysis. All the analyses were based on a linear stability theory, the cell size and geometry being implicitly assumed in the calculation. The analyses yielded the interesting and fundamental result that an unstably stratified fluid layer was statically stable under the joint influence of viscosity and conduction until the vertical temperature gradient (assumed constant) became sufficiently large. The sole parameter governing stability was found to be the Rayleigh number defined as

$$Ra = \frac{g\ \gamma\ \Delta T\ \delta^3}{\kappa\ \nu}$$

where

- g is the gravitational acceleration
- γ the fluid volumetric expansion coefficient
- ΔT the temperature difference between the bounding surfaces
- δ a characteristic length scale, in this case the thickness of the fluid layer
- κ the thermal diffusivity
- ν the kinematic viscosity.

In retrospect, this result is easily explained in physical terms. Consider for example, an unstably stratified fluid layer and suppose that a fluid particle within it suffers a small vertical displacement from it's equilibrium position. If for example it was displaced upwards, it would find itself in a region where it's temperature (and therefore it's buoyancy) would be higher than that of the local environment. This would tend to increase it's vertical displacement leading to an unstable motion. Two factors attenuate this movement: one is the action of viscosity in retarding all relative motion, the other is the thermal diffusivity which tends to harmonize the temperature of the particle with it's surroundings, thus eliminating the net buoyancy force. If however, the vertical temperature gradient is sufficiently large, the potential energy released to the fluid element as a result of it's displacement from an equilibrium position, exceeds the damping force of the viscosity and the equalizing action of the thermal diffusivity, resulting in convective motion.

To investigate the stability of such a system, an analogous operation is performed mathematically. A small harmonic disturbance is superimposed on the system and it's response is calculated over a complete variation of wavenumbers. This is in essence the method of small or "infinitesimal" perturbation theory that is employed throughout this study. If the disturbance continues to grow in time, the system is deemed unstable and convective overturning will occur, if it is damped the system is stable -- at least to small perturbations. If a small input disturbance is neither damped nor amplified the system is on the verge of instability and is said to be marginally or neutrally stable.

Small perturbation theory has been notably successful in analyzing the stability of a variety of flows, chiefly because it permits linearization of the nonlinear equations of motion. However, it is important to realize that this linearized theory is subject to certain limitations. It does not, for example provide any information on the behavior of the flow once the disturbance grows to a certain size sufficient to cause non linear interaction with the mean flow. In many cases, the non linear interaction is sufficient to retard any further growth of the disturbance. This is frequently observed in the case of thermal convection between parallel plates (Whitehead 1971). After the onset of the convecting regime the Rayleigh number may be increased by several factors before the flow loses it's orderly, laminar movement and develops towards turbulent transition. Another limitation of small perturbation theory is it's failure to predict regions of instability or stability in certain fluid flows. The case of resistive instability in circular pipe flow under isothermal flow conditions is one such example, where a small perturbation analysis predicts the flow to be absolutely stable (Pretsch (1941)), Sexl and Spielberg (1958)). In reality however, the flow is stable to infinitesimal perturbations but unstable to finite perturbations. In cases where the theory may be applied however, it provides valuable design information since it indicates a lower bound below which the stability of the flow to small disturbances is guaranteed.

Nonlinear temperature profiles - Once a system becomes unstable, the linear temperature profile is distorted by the fluid's convective motion. Nonlinear profiles may also be generated by other means such as artificially stratifying a system in the laboratory or superimposing a flow or mixing motion on a stratified system. The resulting nonlinear profiles are of more practical importance than the linear profiles although the linear stratifications are significant in a conceptual and theoretical sense. Linear temperature profiles are the exception rather than the rule in Geophysical systems prior to the onset of convection. There is therefore a need to apply the methods of stability theory to study systems possessing nonlinear mean temperature profiles.

The stability of combined fluid layers with nonlinear temperature stratification was examined by Sparrow, Goldstein and Jonsson (1964).

Using the linearized equations of Goldstein (1959) two other independent investigators, Lick (1965) and Currie (1967) subsequently examined the effect of nonlinear temperature profiles on marginal stability. The principle assumption made by the latter two authors was the linearization of the temperature profile by application of an "equivalent" one. This equivalent linear profile was constructed so as to contain the same integrated area as the nonlinear one. Sparrow, Goldstein and Jonsson made no such assumptions, they solved the equations governing the stability of the system by approximate techniques.

Boundary conditions - The boundary conditions applied to the governing equations depend on the specific problem under consideration. Conventional choices include horizontal boundaries, both free and rigid with fixed temperature or constant flux across them. A rigid boundary implies that all velocities there are zero while a free boundary exerts no stress. In mathematical terms this may be expressed as

$$\text{Rigid Boundary:} \quad T_p = v_p = v_p' = w_p = 0;$$

$$\text{Free Boundary:} \quad T_p = v_p = w_p' = 0 \ ,$$

where primes denote differentiation with respect to the vertical coordinate, v_p , w_p are the vertical and lateral perturbation velocity components respectively, and T_p is the temperature perturbation. The early theoretical works referred to earlier considered only combinations of the two types of boundaries (free, rigid) just mentioned. Chandrasekhar (1961) has reviewed these works in great detail.

Unbounded or semi-infinite regions are also physically realistic conditions especially with respect to the atmosphere. For example, convection arising in an unstable layer of air may penetrate into a neighboring stable region. This is precisely the mechanism by which 'lifting' of an elevated inversion occurs (Lumley and Panofsky, 1964). The surface of the earth is warmed during the day by incident solar radiation and initiates convection in the layer of air next to it. This type of convection involving penetration into neutral or stably stratified fluid is termed penetrative convection. Besides the atmospheric example just mentioned, penetrative convection is thought to occur in the convection zones of stars, [K. Schwarzschild (1906), N. R. Lebovitz (1965), Whitehead (1971)], and in the thin layer at the surface of the oceans which is cooled by evaporation [(Lindberg (1970), Whitehead (1971)].

In order to model penetrative convection, there have been a series of theoretical studies which are concerned with models of several layers of fluid with different degrees of stability. Lick (1965) described a two-layer model with a time dependent temperature gradient. Gribov and Gurevich (1957) investigated the influence of the bordering stable layers on the considered layer and handled the special cases in which the bordering layers (a) are near the stability limit, or (b) possess considerable stability. Stix (1970) computed the critical Rayleigh numbers for a two layer model of fluid heated from below for two different cases: the upper layer was considered to possess (a) an infinite coefficient of heat conduction or (b) a large negative Rayleigh number corresponding to a strongly stable elevated inversion. Heikes (1971) developed an N-layer model for steady thermal convection in a stratified fluid with a general thermal boundary condition at the upper and lower limits of the system. The mechanical boundary conditions assumed were the classical rigid free type. The mathematical treatment was restricted to a consideration of linear temperature profiles only. However, the different layers of fluid were permitted different thermal diffusivities and kinematic viscosities, assumed constant throughout each layer. Ogura and Kondo (1970) studied the effect of the stability and depth of an upper stable or neutral layer for rigid-rigid, rigid-free and free-free dynamic boundary conditions.

The principle results from all these analyses may be summarized as indicating that the critical Rayleigh number for the onset of thermal convection is lowered by the nonlinearity of temperature profiles and removal of the upper boundary condition to infinity. The works just discussed are briefly summarized in Table II of this report. It is clear that an analysis incorporating semi-infinite boundary conditions and arbitrary temperature profiles is lacking.

Chapter seven of this study was motivated by the fact that in natural phenomena, the region of unstable equilibrium is often bounded by fluid in stable equilibrium with basic temperature (and therefore density) stratifications which are essentially nonlinear.

2.2 Centrifugal Instabilities

The effect of unstable stratification is by no means unique in achieving destabilization of fluid flows. For example, Chandrasekhar (1961) has treated cases of instability in fluids caused by magnetic fields. This section is restricted to a consideration of instability caused by centrifugal forces.

2.2.1 Experimental Observations

A familiar example of instability introduced by centrifugal effects is the instability of viscous flow between rotating concentric cylinders. This problem was first examined by Taylor (1923) who formulated the motion in mathematical terms, analyzed it's stability and verified the analysis in quite conclusive fashion. The instability, which manifests itself in the form of toroidal vortices in the annular space between the cylinders, is due to the apparent "buoyancy" (just as in the Bénard Problem) caused by the centrifugal forces. That is, the radial displacement of a fluid element from it's equilibrium position results in a net imbalance between the radial pressure and the centrifugal forces acting on it. If the net force on the particle causes it to increase it's radial displacement, the flow is unstable and the familiar Taylor vortices are formed.

The criteria for stability of such systems was first postulated by Rayleigh (1917) who confined himself to inviscid flows. It states that in the absence of viscosity, the necessary and sufficient condition for a distribution of angular velocity to be stable is that the square of the circulation decrease monotonically outward. Taylor (1923) of course, considered viscous effects in his analysis and discovered not surprisingly that viscosity tends to delay the onset of instability. In fact, viscosity plays a dual role in suppressing instability: it damps any tendency of a fluid element to change it's radial position with respect to it's environment, and in case it's radial position is altered as the result of a small disturbance it causes the circumferential velocity of the fluid particle to equalize with it's new surroundings thus reducing the imbalance between the pressure and centrifugal forces to zero. If however, the radial stratification of angular momentum is sufficiently strong to overcome viscous effects, Taylor instability sets in. There is thus a close analogy between thermally driven convective instability and instability caused by curvature effects. The former is due to unstable temperature stratification while the latter is caused by an unstable stratification of angular momentum. In thermal instability, viscosity and thermal diffusivity play a stabilizing role, while in centrifugal instability viscosity plays the additional role of thermal diffusivity as well.

The recent experiments of Donnelly and Schwartz (1965) and Snyder and Lambert (1965) combine to give a satisfactory picture of axially symmetric Taylor Vortices. Laminar flow visualization techniques used have been aluminum flakes or dye suspended in an aqueous medium. The experiments of Coles (1965) have indicated secondary instabilities caused by non-linear effects in which circumferential travelling waves superimposed on the Taylor Vortices have been observed. A review of these works may be found in the article by Segal (1965). Kirchner and Chen (1970) have experimentally observed the formation of Taylor Vortices in the transient case when the inner cylinder is spun up from rest. Goertler (1940) investigated the vortex mode of motion in a boundary layer along a concave, curved plate and showed that a system of streamwise oriented, parallel counter-rotating vortices were formed. Furthermore, he was able to theoretically derive the condition that the plate should have concave curvature for the flow to be unstable. The mechanism in operation here is identical to the one in Taylor's Problem. The parameter of interest in the Goertler flow is the so called Goertler number defined as $R_d \sqrt{\delta/R}$ where δ is a characteristic boundary layer thickness, R is the radius of curvature of the plate and R_d is the Reynold's number based on δ . Liepmann (1943) experimentally verified the importance of the Goertler number in governing the stability of viscous flows over concave surfaces, as did Clauser and Clauser (1937). In recent times, McCormack et al., (1969) have made laboratory measurements that indicate that in the presence of Goertler Vortices, an increase of over 60 percent in the heat transfer rate is observed over the simple flat plate value. Possible application to the design of high efficiency heat exchangers is therefore obvious. The convective nature of the vortices make them an efficient mechanism for transporting high temperature boundary layer fluid into the free stream region.

2.2.2 Theoretical Analyses

As in the case of thermal convection, linearized perturbation theory has been very successful in analysing the stability of Goertler type flow. Nonlinear methods have recently been used with increasing frequency and are summarized by Segal (1967). The discussion here is limited to linear theories.

Taylor (1923) as well as Goertler (1940), Meksyn (1950), Hammerlin (1955) and Smith (1954) obtained the differential equations for the disturbances on the basis of linear perturbation theory. However, methods of obtaining solutions to the differential equations have varied widely, just as have solutions to the celebrated Orr-Sommerfeld equation governing two-dimensional resistive instability. Goertler (1940) integrated the equations by transforming them into two simultaneous integral equations, and then solving them approximately at a few points within the boundary layer. Goertler's analysis was a simplified one since his primary objective was to ascertain whether flows along concave walls were unstable. Consequently he treated the case of weak curvature with time varying disturbances and was able to drop a large number of terms. Since he assumed that the flow was parallel the normal velocity component in the boundary layer was also neglected. His analysis did show however, that vortex instability could only exist in boundary layers along walls with concave curvature and that the Goertler number was the controlling parameter.

Meksyn (1950) essentially re-solved Goertler's equations by the method of asymptotic expansions. His result however for the critical point disagreed considerably with Goertler's. Hammerlin (1955) also re-solved Goertler's stability equations by different methods and obtained very accurate solutions. He established the peculiar result that the minimum Goertler number for neutral stability occurred at a spanwise wavenumber of zero thus implying a vortex of infinite size. In such a case, the disturbances will extend far outside the boundary layer having a finite size even at infinity. Smith (1955) performed a refined analysis of the Goertler problem in which:

(a) It was assumed that the disturbances were amplifying spatially in the streamwise direction;

(b) The normal velocity component in the Blasius boundary layer was incorporated into the analysis thus accounting for it's quasi-parallel nature;

(c) The flow was assumed to possess finite curvature, thus requiring retention of a large number of extra terms in the analysis. These extra terms will hereafter be referred to as the "finite curvature terms."

The equations obtained were solved by the Galerkin method which is an analytic approximation technique. His result confirmed the result of Goertler and disagreed with that of Hammerlin's. In other words, the curve of critical Goertler number versus wavenumber displayed a minimum at a finite value of the wavenumber and did not decrease monotonically to zero as did Hammerlin's. Di Prima and Dunn (1956) performed a parallel flow analysis of the stability of liquid layers along curved, heated or cooled walls. They accounted for the temperature dependence of the viscosity and thermal conductivity but neglected density variations. Their analysis apparently indicated that cooling the wall destabilized the flow, while heating stabilized it.

Hammerlin (1961) subsequently extended his own analysis to include cases of compressible flow over heated walls. This new analysis assumed (as had Di Prima and Dunn) that viscosity and thermal conductivity were functions of temperature, but did not incorporate the additional buoyancy force caused by density effects. A refinement in this analysis was that the streamline curvature was assumed to decay exponentially with increasing distance from the wall. The decay constant in the exponential term was empirically specified from the measurements of Witting (1958). Hammerlin's rationale for this was as follows: He argued that away from the wall, the streamlines tended to decrease in curvature until at large distances from the wall they were parallel. Hence additional damping of the disturbances by the decreasing streamline curvature would be expected. The new critical stability curve did display a minimum (apparently confirming Hammerlin's reasoning) which however was higher than that obtained by Smith (1955).

Sandmayr (1966) used the new coordinate system devised by Hammerlin in constructing solutions for the case of a turbulent boundary layer along a concave curved wall. Following Smith (1955), he used Galerkin's method to solve the differential equations governing the perturbations.

A recent analysis by Chang and Sartory (1968) in which solutions were obtained to the equations governing neutral disturbances confirmed the earlier (1955) result of Hammerlin. On retention of the normal flow velocity component into the equations they obtained critical conditions of zero Goertler number at zero wavenumber. Since their analysis had neglected the finite curvature terms, it was presumed that these terms must somehow serve to limit the size of the disturbances. The discrepancy between their results which were obtained by numerical integration and that of Smith (1955), was explained mainly on the grounds that the Galerkin method which he used was subject to inaccuracies unless certain precautions were followed. Smith (1955) apparently assumed the solution to have the form of a polynominal times an exponential factor which decayed far from the wall. The coefficients of the polynominal were calculated in solving the problem, but the exponential decay rate was assumed mainly on the basis of numerical experimentation. Since at that time Smith did not have access to high speed digital computers, his numerical experimentation was understandably of limited scope. Chang and Sartory (1968) indicate that Smith's answers could be incorrect by over an order of magnitude at the lower wavenumbers. Sandmayr (1966) in fact noticed the same difficulty with Galerkin's method; increasing the number of starting functions appeared to decrease the characteristic eigenvalue without limit. Accordingly, he claims an accuracy for his results to perhaps an order of magnitude only since a limited number of starting functions in his approximate solution appeared to decrease the characteristic eigenvalue without limit.

Recently, Rintel (1971) has extended the Goertler problem to include cases where the free stream above the unstable boundary layer has a stable stratification of angular momentum. This is analogous to penetrative convection in the thermal sense. An example of such a situation would be the case of the flow between counter-rotating concentric cylinders. In such a case, the fluid nearest to the inner cylinder is in unstable equilibrium while the outer flow is stable. Rintel (1971) considered only parallel flows and neglected all finite curvature terms. The analysis assumed the simple fixed-free mechanical boundary conditions; that is, the lower boundary was considered fixed while the upper boundary was assumed stress free. The solution technique applied was an expansion in eigenfunctions satisfying the boundary conditions.

2.3 Analogy Between Flows with Concave Curvature and Those Possessing an Unstable Temperature Stratification

An analogy exists between various types of flows with concave curvature and buoyancy due to unstable stratification. This has already been pointed out in a physical sense to some extent in the preceding sections of this chapter. The analogy was first indicated in mathematical terms by Goertler (1959) and more recently by Bradshaw (1969) who considered it in "turbulent shear flow" terms with meteorological applications. In a theoretical sense, neglecting the finite curvature terms for Goertler instability in parallel layers of fluid result in a system of equations very similar to those for Bénard Convection.

Although this analogy between Goertler flow and thermal convection exists, there does not appear to have been an analysis of Goertler instability with thermal buoyancy effects, which is clear from an examination of Table III. Chang and Sartory (1968) have however, investigated the different but parallel case of Hydromagnetic Goertler Instability.

Chapter 3

THEORETICAL DEVELOPMENT

In this chapter, the governing equations of motion are developed for the particular flows under consideration. Linearized perturbation theory is used, and the differential equations governing the perturbations are obtained. In section (3.1) we consider flows over heated curved walls and develop the general, relevant equations.

Section (3.2) is devoted to a study of the onset of convective overturning in stationary layers of fluid with arbitrary temperature stratification and of semi-infinite extent. The governing equations are presented, detailed development being relegated to Appendix A.

3.1 General Equations Governing the Stability of Quasi-Parallel Flows Along Curved, Heated Boundaries

Consider a stratified flow along a curved surface. In keeping with the generality of the analysis, the unstable layer is considered to be bounded above by fluid possessing an arbitrary distribution of temperature and angular momentum. Following Smith (1955), the Navier–Stokes equations and the Energy Equation are expressed in a curvilinear coordinate system (Fig. 1). The primary reason for this is that the analysis is then not restricted to flows with constant curvature. The fluid is assumed incompressible within the framework of the Boussinesq approximation and with constant properties. The equations are then

$$\frac{1}{1-ky}\, u\frac{\partial u}{\partial x} + v\frac{\partial u}{\partial y} + w\frac{\partial u}{\partial z} - \frac{kuv}{1-ky} = -\frac{1}{\rho(1-ky)}\frac{\partial p}{\partial x} +$$

$$\nu[\nabla^2 u - \frac{2k}{(1-ky)^2}\frac{\partial v}{\partial x} - \frac{k^2 u}{(1-ky)^2} - \frac{k}{(1-ky)}\frac{\partial u}{\partial y} - v\frac{dk}{dx}\frac{1}{(1-ky)^3}] \qquad (3.1A)$$

$$\frac{1}{1-ky} u \frac{\partial v}{\partial x} + v \frac{\partial v}{\partial y} + w \frac{\partial v}{\partial z} + \frac{ku^2}{1-ky} - g\gamma(T-T_\infty) = -\frac{1}{\rho}\frac{\partial p}{\partial y} +$$

$$\nu[\nabla^2 v + \frac{2k}{(1-ky)^2}\frac{\partial u}{\partial x} - \frac{k^2 v}{(1-ky)^2} - \frac{k}{(1-ky)}\frac{\partial v}{\partial y} + u\frac{dk}{dx}\frac{1}{(1-ky)^3}]$$

(3.1B)

$$\frac{1}{1-ky} u \frac{\partial w}{\partial x} + v \frac{\partial w}{\partial y} + w \frac{\partial w}{\partial z} = -\frac{1}{\rho}\frac{\partial p}{\partial z} + \nu[\nabla^2 w - \frac{k}{1-ky}\frac{\partial w}{\partial y}] \qquad (3.1C)$$

$$\nabla \cdot \underset{\sim}{v} \equiv \frac{1}{1-ky}\frac{\partial u}{\partial x} + \frac{\partial v}{\partial y} + \frac{\partial w}{\partial z} - \frac{kv}{1-ky} = 0 \qquad (3.1D)$$

$$\frac{u}{1-ky}\frac{\partial T}{\partial x} + v\frac{\partial T}{\partial y} + w\frac{\partial T}{\partial z} = \frac{\nu}{P_r}\{\nabla^2 T - \frac{k}{1-ky}\frac{\partial T}{\partial y}\} \quad . \qquad (3.1E)$$

Here k is the curvature $(= \frac{1}{R})$, where R is the radius of curvature.

$$\nabla^2 \equiv \frac{1}{(1-ky)^2}\frac{\partial^2}{\partial x^2} + \frac{\partial^2}{\partial y^2} + \frac{\partial^2}{\partial z^2} + \frac{1}{(1-ky)^3} y \frac{dk}{dx}\frac{\partial}{\partial x} \, .$$

The sign convention followed is a positive sign for concave curvature. u, v, w, p and T are the three coordinate velocity components, pressure and temperature respectively. The coordinate axes are oriented so that $x, y,$ and z are the streamwise, vertical and spanwise directions respectively. Pr and ν are the Prandtl number and kinematic viscosity respectively. The instantaneous velocity, pressure and temperature components are now represented by a steady (mean or base flow) part and a fluctuating component of small amplitude. Formally we write

$$u = U + \tilde{u}$$

$$v = V + \tilde{v}$$

$$w = \tilde{w}$$

$$p = p_o + \tilde{p}$$
$$T = T_o + \tilde{T}\ .$$

Substitution of these expressions into equations (3.1) and subtraction of the mean flow boundary layer equations results in the differential equations governing the perturbations. The mean flow is assumed two-dimensional. The standard linearizing assumption of neglecting second order products of the perturbations is made. The justification for this is that provided the amplitudes of the disturbances are sufficiently small, cross terms such as $\tilde{u}\tilde{v}$ serve only to generate higher harmonics with greatly reduced amplitudes. However, although the amplitudes of the fluctuations are assumed small, they can be subject to large amplification rates. The purpose of linearized perturbation theory is to determine the range of frequencies for which arbitrary disturbances are either attenuated, remain at constant amplitude, or are amplified.

As a result of the previous operation, the following differential equations governing the perturbations are obtained

$$\frac{1}{1-ky}\left(\tilde{u}\,\frac{\partial U}{\partial x} + U\,\frac{\partial \tilde{u}}{\partial x}\right) + V\,\frac{\partial \tilde{u}}{\partial y} + \tilde{v}\,\frac{\partial U}{\partial y} - \frac{k}{1-ky}\,(U\tilde{v} + \tilde{u}V)$$

$$= -\frac{1}{\rho}\,\frac{1}{(1-ky)}\,\frac{\partial \tilde{p}}{\partial x} + \nu\left[\nabla^2\tilde{u} - \frac{2k}{(1-ky)^2}\,\frac{\partial \tilde{v}}{\partial x} - \frac{k^2\tilde{u}}{(1-ky)^2}\right.$$

$$\left. - \frac{k}{1-ky}\,\frac{\partial \tilde{u}}{\partial y} - \tilde{v}\,\frac{dk}{dx}\,\frac{1}{(1-ky)^3}\right] \tag{3.2A}$$

$$\frac{1}{1-ky}\left(\tilde{u}\,\frac{\partial V}{\partial x} + U\,\frac{\partial \tilde{v}}{\partial x}\right) + V\,\frac{\partial \tilde{v}}{\partial y} + v\,\frac{\partial V}{\partial y} + \frac{2kU\tilde{u}}{1-ky}$$

$$- g\gamma\,\tilde{T} = -\frac{1}{\rho}\,\frac{\partial \tilde{p}}{\partial y} + \nu\left[\nabla^2\tilde{v} + \frac{2k}{(1-ky)^2}\,\frac{\partial \tilde{u}}{\partial x}\right.$$

$$\left. - \frac{k^2\tilde{v}}{(1-ky)^2} - \frac{k}{1-ky}\,\frac{\partial \tilde{v}}{\partial y} + \tilde{u}\,\frac{1}{(1-ky)^3}\,\frac{dk}{dx}\right] \tag{3.2B}$$

$$\frac{1}{1-ky} U \frac{\partial \tilde{w}}{\partial x} + V \frac{\partial \tilde{w}}{\partial y} = - \frac{1}{\rho} \frac{\partial \tilde{p}}{\partial z} + \nu[\nabla^2 \tilde{w} - \frac{k}{1-ky} \frac{\partial \tilde{w}}{\partial y}] \tag{3.2C}$$

$$\frac{1}{1-ky} \frac{\partial \tilde{u}}{\partial x} + \frac{\partial \tilde{v}}{\partial y} + \frac{\partial \tilde{w}}{\partial z} - \frac{k\tilde{v}}{1-ky} = 0 \tag{3.2D}$$

$$\frac{1}{1-ky} (\tilde{u} \frac{\partial T_o}{\partial x} + U \frac{\partial \tilde{T}}{\partial x}) + \tilde{v} \frac{\partial T_o}{\partial y} + V \frac{\partial T}{\partial y} =$$

$$\frac{\nu}{Pr} [\nabla^2 \tilde{T} - \frac{k}{1-ky} \frac{\partial \tilde{T}}{\partial y}] . \tag{3.2E}$$

Mathematical Description of the Disturbance - Goertler (1940) in his classical work followed Taylor (1923) in describing the vortex motion in the boundary layer by means of the following equations, in which all quantities are real numbers.

$$\tilde{u} = u_p(y)\ e^{\beta t} \cos\alpha z$$
$$\tilde{v} = v_p(y)\ e^{\beta t} \cos\alpha z$$
$$\tilde{w} = w_p(y)\ e^{\beta t} \sin\alpha z$$
$$\tilde{p} = p_p(y)\ e^{\beta t} \cos\alpha z$$

In the above

u_p , v_p , w_p , p_p are the amplitudes of the superimposed disturbance functions

α is a wavenumber = $\frac{2\pi}{\lambda}$ where λ is the lateral wavelength of the vortex spacing

β is a measure of the rate of growth of the disturbance as a function of time. Physically, the use of a time varying disturbance in the present case implies that at a given location in the flow the vortices are varying in size with time. In fact, the experiments of Liepmann (1943), Tani (1962) indicate that the vortices are stationary in time, but only vary with streamwise distance. Therefore, following Smith (1955) we postulate a spatially varying disturbance in the following form

$$\tilde{u} = u_p(y)\, e^{\int \beta dx} \cos\alpha z$$
$$\tilde{v} = v_p(y)\, e^{\int \beta dx} \cos\alpha z$$
$$\tilde{w} = w_p(y)\, e^{\int \beta dx} \sin\alpha z$$
$$\tilde{p} = p_p(y)\, e^{\int \beta dx} \cos\alpha z$$
$$\tilde{T} = T_p(y)\, e^{\int \beta dx} \cos\alpha z$$

In this formulation, the exponent $\int \beta dx$ is introduced in order to account for any changes in β that occur with x. This would be the case for example, if the curvature k varied in the x direction. The solutions obtained throughout this report however, have assumed a constant curvature and hence a constant β. Substituting the set (3.3) into equations (3.2) results in

$$\frac{1}{1-ky}\left(u_p \frac{\partial U}{\partial x} + U u_p \beta\right) + V u_p' + v_p \frac{\partial U}{\partial y} - \frac{k}{1-ky}(U v_p + V u_p)$$
$$= -\frac{1}{\rho}\frac{1}{(1-ky)} p_p \beta + \nu\Big[\frac{1}{(1-ky)^2}\left(u_p \beta^2 + u_p \frac{d\beta}{dx}\right)$$
$$+ u_p'' - u_p \alpha^2 + \frac{1}{(1-ky)^3}\, y \frac{dk}{dx} u_p \beta - \frac{2k}{(1-ky)^2} v_p \beta$$
$$- \frac{k^2}{(1-ky)^2} u_p - \frac{k}{1-ky} u_p' - v_p \frac{dk}{dx}\frac{1}{(1-ky)^3}\Big] \tag{3.4A}$$

$$\frac{1}{(1-ky)}\left(u_p \frac{\partial V}{\partial x} + U v_p \beta\right) + V v_p' + v_p \frac{\partial V}{\partial y} + \frac{2k}{1-ky} U u_p$$
$$- g\gamma T_p = -\frac{1}{\rho} p_p' + \nu\Big[\frac{1}{(1-ky)^2}\left(v_p \beta^2 + v_p \frac{d\beta}{dx}\right)$$
$$+ v_p'' - v_p \alpha^2 + \frac{1}{(1-ky)^3}\, y \frac{dk}{dx} \beta v_p + \frac{2k}{(1-ky)^2} \beta u_p$$
$$- \frac{k^2}{(1-ky)^2} v_p - \frac{k}{1-ky} v_p' + \frac{1}{(1-ky)^3} u_p \frac{dk}{dx}\Big] . \tag{3.4B}$$

$$\frac{1}{1-ky} U w_p\beta + V w_p' = \frac{1}{\rho} \alpha p_p + \nu[\frac{1}{(1-ky)^2} w_p(\beta^2 + \frac{d\beta}{dx})$$

$$+ w_p'' - \alpha^2 w_p + \frac{1}{(1-ky)^3} y \frac{dk}{dx} \beta w_p$$

$$- \frac{k}{1-ky} w_p'] \ . \tag{3.4C}$$

The continuity equation for the perturbations becomes

$$\frac{1}{1-ky} u_p\beta + v_p' + \alpha w_p - v_p \frac{k}{1-ky} = 0 \ , \tag{3.4D}$$

while the energy equation is

$$\frac{1}{1-ky} (u_p \frac{\partial T_o}{\partial x} + U T_p\beta) + v_p \frac{\partial T_o}{\partial y} + V T_p'$$

$$= \frac{\nu}{P_r} \{ \frac{1}{(1-ky)^2} (\beta^2 T_p + T_p \frac{d\beta}{dx}) + T_p'' - \alpha^2 T_p$$

$$+ \frac{1}{(1-ky)^3} y \frac{dk}{dx} \beta T_p - \frac{k}{1-ky} T_p' \} \ . \tag{3.4E}$$

Equations (3.4) are made dimensionless with the following scaling lengths, velocities and temperatures

$$U = U_o u_\infty$$

$$V = V_o U_\infty$$

$$T_o = T_1 \Delta T$$

$$T_p = T \Delta T$$

$$u_p = u\, U_m$$

$$v_p = v\, U_m$$

$$\frac{dk}{dx} = \frac{1}{c^2} \frac{d(ck)}{d(x/c)}$$

$$y = \eta\delta$$

$$p_p = C_p \frac{1}{2} \rho U_m^{\,2}$$

$$R_d = \frac{U_\infty \delta}{\nu}$$

$$K = k\delta$$

$$B = \beta\delta$$

$$w_p = w\, U_m$$

$$A = \alpha\delta$$

In the above:

U_∞ is a characteristic velocity, generally the free stream velocity for a boundary layer. It will be explicitly defined for each flow studied in this report.

δ is a characteristic boundary layer thickness.

c is a chord length in the streamwise direction

$U_m = \frac{\nu}{\delta}$ is a velocity scale chosen such that under zero mean flow conditions, the equations reduce correctly to those of thermal convection.

R_d is the Reynold's number of the flow $(= \frac{U_\infty \delta}{\nu})$ based on the characteristic velocity and boundary layer thickness.

$\Delta T = T_w - T_\infty$ is the temperature difference between the wall and the free stream.

Utilization of these dimensionless quantities in the equations (3.4) results in

$$\frac{d^2u}{d\eta^2} - [V_o\ R_d + \frac{K}{1-K\eta}]\ \frac{du}{d\eta} + [\ \frac{B\eta}{(1-K\eta)^3}\ \frac{\delta^2}{c^2}\ \frac{d(ck)}{d(x/c)}$$

$$- A^2 - \frac{K^2}{(1-K\eta)^2} + \frac{1}{(1-K\eta)^2}\ (B^2 + \frac{\delta}{c}\ \frac{dB}{d(x/c)}) - \frac{V\ U_o\ R_d}{1-K\eta}$$

$$+ R_d\ \frac{dV_o}{d\eta}]\ u - [\ \frac{2\ K\ B}{(1-K\eta)^2} + \frac{1}{(1-K\eta)^3}\ \frac{\delta^2}{c^2}\ \frac{d(ck)}{d(x/c)}$$

$$+ R_d\ \frac{dV_o}{d\eta} - \frac{K\ V_o\ R_d}{(1-K\eta)}\ ]\ v = \frac{B}{1-K\eta}\ \frac{C_p}{2}\ . \tag{3.5A}$$

$$\frac{d^2v}{d\eta^2} - [V_o\ R_d + \frac{K}{1+K\eta}]\ \frac{dv}{d\eta} + [\ \frac{1}{(1-K\eta)^2}\ (B^2 + \frac{\delta}{c}\ \frac{dB}{d(x/c)})$$

$$- A^2 + \frac{B\nu}{(1-K\eta)^3}\ \frac{\delta^2}{c^2}\ \frac{d(ck)}{d(x/c)} - \frac{K^2}{(1-K\eta)^2} - \frac{B\ U_o\ R_d}{(1-K\eta)} - R_d\ \frac{dV_o}{d\eta}\ ]\ v$$

$$- [\ \frac{1}{(1-K\eta)}\ R_d\ \frac{\delta}{c}\ \frac{d\ V_o}{d(x/c)} + \frac{2\ K\ V_o\ R_d}{(1-K\eta)} - \frac{2KB}{(1-K\eta)^2} - \frac{\delta^2}{c^2}\ (1-K\eta)^3$$

$$\frac{d\ (ck)}{d\ (x/c)}\ ]\ u = \frac{1}{2}\ \frac{dC_p}{d\eta} - G_r\ T\ . \tag{3.5B}$$

$$\frac{d^2w}{d\eta^2} - [V_o\ R_d + \frac{K}{1+K\eta}]\ \frac{dw}{d\eta} + [\ \frac{1}{(1-K\eta)^2}\ (B^2 + \frac{\delta}{c}\ \frac{dB}{d(x/c)})$$

$$- A^2 + \frac{\delta^2}{c^2}\ \frac{B\eta}{(1-K\eta)^3}\ \frac{d(ck)}{d(x/c)} - \frac{B\ V_o\ R_d}{1-K\eta}\ ]\ w = - \frac{A}{2}\ C_p\ . \tag{3.5C}$$

$$\frac{1}{1-K\eta}\ Bu + \frac{dv}{d\eta} + A\ w - \frac{K}{1-K\eta}\ v = 0\ . \tag{3.5D}$$

$$\frac{d^2T}{d\eta^2} - [V_o\ P_r\ R_d + \frac{K}{1-K\eta}]\ \frac{dT}{d\eta} + [\ \frac{1}{(1-K\eta)^2}\ (B^2 + \frac{\delta^2}{c^2}\ \frac{dB}{d(x/c)} - A^2 +$$

$$\frac{\delta^2}{c^2}\ \frac{B}{(1-K\eta)^3}\ \frac{d(ck)}{d(x/c)} - B\ U_o\ P_r\ R_d]\ T = \frac{\delta}{c}\ P_r\ u\ \frac{d\ T_1}{d(x/c)}$$

$$+ v\ P_r\ \frac{dT_1}{d\eta} \tag{3.5E}$$

where the terms $\frac{k\ V}{1-ky} - \frac{1}{1-ky}\frac{\partial U}{\partial x}$ have been replaced with $\frac{\partial V}{\partial y}$ from the continuity equation for the mean flow. This provides an analytical representation of the quasi-parallel nature of the boundary layer. The following simplifications are now made to equations (3.5). Terms such as $\frac{1}{(1-K\eta)^n}$ are replaced by $1 + n\,K\eta$, the first term in a series expansion. The justification for this lies in the range of values that $K\eta$ achieves, typically from 0 to 0.1. With $K\eta = 0.1$, the simplification is accurate to 1%. The maximum value of K may be in the vicinity of 10^{-2} although throughout this work, a value of even 10^{-3} was never achieved. Consequently, terms of order K^2 and greater are neglected in this approximation. The ratio δ/c is very small since a characteristic chord length is generally several times a boundary layer thickness and is therefore neglected. Finally, the effect of variations of K and B with x are assumed small and are therefore neglected in the cases studied here. A detailed justification of this has been given by Smith (1955). With these simplifications the disturbance equations reduce to the following:

$$\frac{d^2u}{d\eta^2} - [V_o\,R_d + K]\frac{du}{d\eta} + [B^2 - A^2 - R_d(B\,U_o - \frac{d\,V_o}{d\eta})$$
$$+ K\eta\,B(2B - V_o\,R_d)]\,u - [R_d\frac{d\,V_o}{d\eta} + K(2B - U_o\,R_d)]\,v$$
$$= \frac{B}{2}\,C_p(1 + K\eta)\ . \qquad (3.6A)$$

$$\frac{d^2v}{d\eta^2} - [V_o\,R_d + K]\frac{dv}{d\eta} + [B^2 - A^2 + 2K\,B - B^2R_d\,U_o(1 + K\eta)$$
$$- R_d\frac{d\,V_o}{d\eta}]\,v - [2K\,R_d\,U_o - 2K\,B]\,u = \frac{1}{2}\frac{d\,C_p}{d\eta} - G_r\,T\ . \qquad (3.6B)$$

$$\frac{d^2w}{d\eta^2} - [V_o\ R_d + K]\ \frac{dw}{d\eta} + [B^2 - A^2 + 2K\ B^2\eta - B\ R_d\ U_o(1 + K\eta)]\ w$$

$$= -\ \frac{A}{2}\ C_p\ . \tag{3.6C}$$

$$Bu + K\ Bu\eta + \frac{dv}{d\eta} + Aw - Kv = 0\ . \tag{3.6D}$$

$$\frac{d^2T}{d\eta^2} - [V_o\ P_r\ R_d + K]\ \frac{dT}{d\eta} + [B^2 - A^2 + 2K\ B^2\ \eta$$

$$-B\ U_o\ P_r\ R_d(1 + K\eta)]\ T = P_r\ v\ \frac{dT_1}{d\eta}\ . \tag{3.6E}$$

Here Gr is the Grashof number defined as $Gr = \frac{g\ \gamma\ \Delta T\ \delta^3}{\nu^2} = Ra/Pr$. The system of five equations (3.17) to (3.21) have the boundary conditions

$\eta = 0\ ,\quad u,v,w,\ T = 0$

$\eta \to \infty\ ,\quad u,v,w,\ T \to 0$

In addition, the equation of continuity (3.6D) supplies an auxiliary boundary condition at the wall; $\eta = 0 \quad \frac{dv}{d\eta} = 0$. The boundary conditions at infinity imply that all disturbances must eventually die out with increasing distance from the wall since they originate in the unstable layer adjacent to it.

The system of equations (3.6) are homogeneous with homogeneous boundary conditions and therefore take on non-trivial solutions for only certain values of the parameters A, B, Gr and K . For the eigenvalue problem, uniqueness of the solutions does not exist; in actual fact there being an infinity of solutions (Keller 1967). The requirement is to obtain the variation of the minimum positive Grashof number Gr with respect to the wavenumber A of the disturbance, keeping values of the other parameters K and B fixed. Alternatively, Gr may be kept fixed and K treated as the eigenvalue. B as well as A could also be treated as eigenvalues in principle; however since they appear as nonlinear functions in the equations, difficulties with iterative techniques could be encountered. Accordingly, either Gr or K was treated as the eigenvalue, depending on the particular case under consideration.

For $K = 0$, the disturbance equations describe the stability of a boundary layer over a heated flat plate.

Throughout this report, equations (3.6) have been solved for a variety of flows involving curvature and thermal stratification. One of the objectives was to resolve the discrepancy between Hammerlin's (1955), and Chang and Sartory's (1968) results with those of Smith (1955), since here the finite curvature terms have been included. Accordingly, the stability calculations for a growing Blasius Boundary Layer on a Concave Curved Wall have been redone using a numerical method and the results compared with those of Smith (1955) and Hammerlin (1955).

In addition, the following problems in Hydrodynamic Stability have been investigated:

(a) the stability of the Blasius Profile on a curved heated wall,

(b) the stability of the asymptotic suction profile,

(c) the stability of wall jets on curved surfaces,

(d) the spin up of a cylinder in an infinite medium.

3.2 Penetrative Convective Instabilities in Stationary Stratified Fluid

The preceding perturbation analysis is conventionally used to study the onset of convective overturning in layers of fluid possessing unstable stratification. In this section, the relevant disturbance equations are presented. In principle, these disturbance equations may be obtained from the set (3.6) merely by setting $K = U_o = V_o = R_d = 0$. However, equations (3.6) were derived by assuming a disturbance that amplifies spatially; in the present context this of course is irrelevant. Equations (3.7) have therefore been derived assuming a temporal amplification of the disturbance. Equations (3.6) with the additional term $B = 0$ reduce correctly to equations (3.7) with $\sigma = 0$.

$$v'' - (\phi^2 + \sigma)v = C_p' - Gr\ T \tag{3.7A}$$

$$w'' - (\phi^2 + \sigma)w = -\phi C_p \tag{3.7B}$$

$$v' + \phi\ w = 0 \tag{3.7C}$$

$$T'' - (\phi^2 + \sigma)T = P_r\ v\ \frac{dT_1}{d\eta}\ . \tag{3.7D}$$

Primes denote differentiation with respect to η, ϕ is the dimensionless horizontal wavenumber and σ an amplification factor. The detailed development of equations (3.7) has been relegated to Appendix A. For the boundary conditions the surface $\eta = 0$ has been taken as a rigid surface. The fluid is considered unbounded in the vertical direction. Mathematically, the boundary conditions may be expressed as

$$\eta = 0\ , \quad v = v' = w = T = 0$$

$$\eta \to \infty\ , \quad v = w = T \to 0.$$

The equations together with the boundary conditions have been applied in this thesis, to study the onset of convective overturning in stratified layers of fluid under some particular conditions. The cases examined are:

(a) the stability of a layer of fluid in which the lower boundary is suddenly heated to a constant temperature,

(b) the stability of a layer of fluid in the presence of an elevated inversion.

This case was examined in order to simulate thermoconvective motion in the atmosphere. The unstable lower layer is assumed to have an exponentially decreasing temperature gradient while the inversion is considered as having a constant stable gradient. The stability of the system is studied as the inversion is raised or lowered and when the inversion height is kept fixed but the inversion strength varied. In the actual atmosphere of course, the situation is much more complex with such things as nonlinear eddy viscosities and latent heat release complicating the analysis. The solutions obtained here are intended to provide a qualitative picture only of the convective action in the atmosphere. We have assumed here that the fluid is of semi-infinite extent. For this reason and because of the use here of nonlinear temperature profiles the present study just discussed may be considered as an extension of the work of Heikes (1971), and Ogura and Kondo (1970).

Chapter 4

SOLUTION METHODS FOR TWO POINT BOUNDARY VALUE PROBLEMS

In this chapter, three methods of obtaining solutions to the Eigenvalue Problem are presented. Depending on the particular problem under consideration, one of these methods has been selected to obtain solutions to the differential equations. The intent here is to briefly discuss in turn each of the three methods and to indicate their relative merits in various areas of application. Not surprisingly, the methods employed here depend heavily on the use of high-speed digital computers to perform the tedious arithmetic.

The methods we discuss here are:

(i) An expansion in eigenfunctions satisfying the boundary conditions;

(ii) Direct numerical integration of homogeneous solution vectors with linear independence maintained by the Gram-Schmidt Process at certain intervals;

(iii) Numerical integration of the equations within the boundary layer which are matched at the boundary layer edge, to analytical solutions in the free stream.

(i) Expansion in eigenfunctions: - For this section we will require some definitions of a complete and closed set of functions. Churchill (1941) defines a complete set and a closed set of functions as follows:

Definition 4.1. The set of functions $\{f_n(x)\}$ is said to be complete if there is no function in the function space considered which is orthogonal to every $f_n(x)$ of the set.

Definition 4.2. Let $S_m(x)$ denote the linear combination, $S_m(x) = \sum_{n=1}^{m} C_n\phi_n(x)$, of a set of functions $\{\phi_n(x)\}$, where the C_n are constants. The sum $S_m(x)$ is said to converge in the mean to the function $f(x)$, or $f(x)$ is said to be approximated in the mean by $S_m(x)$, if

$$\underset{m\to\infty}{\mathrm{Lt}} \int_a^b [f(x) - S_m(x)]^2 \, dx = 0 .$$

Definition 4.3. The set of functions $\{\phi_n(x)\}$ is said to be closed if a function in the function space considered can be approximated in the mean by a linear combination of ϕ_1, ϕ_2, ...

In the solution of Hydrodynamic Problems it is often necessary to be able to expand the prevailing velocity and temperature field in a set of orthogonal functions which are complete over the entire solution space. It is not of course, necessary that the functions are orthogonal, only that they be linearly independent. King (1961) indicates various methods by which orthogonal functions may be synthesized from a linearly independent set. However, the usual expansions in terms of trigonometric or Bessel functions are not useful in problems involving viscous flow with plane boundaries, since the boundary conditions on a rigid wall for example, require not only the normal component, but also it's first derivative to vanish there.

Chandrasekhar (1961) has listed a sequence of orthogonal functions that satisfy four boundary conditions. They appear to form a closed set as long as the function being approximated satisfies the given boundary conditions. In Chapter 5 a similar sequence of functions have been used to obtain solutions to the characteristic equations governing the stability of parallel flows between curved heated walls. The functions employed there are a linearly independent set. The functions are continuous with continuous first and second derivatives over the interval considered. In order that they converge to the true solution of the characteristic equation the following theorem must be satisfied: [Hildebrand 1965]

Theorem 4.1: If a general real continuous function $f(x)$ is approximated by a sequence $f(x) \approx S_n = \sum_{k=1}^{n} a_k \phi_k(x)$ $(a < x < b)$ where the constants a_k are determined in such a way that the norm of the difference between the two members S_n and $f(x)$ is a minimum, then the sum of the series $S_n = \sum_{k=1}^{n} a_k \phi_k(x)$ will converge as $n \to \infty$ to the true function $f(x)$ provided that the ϕ_k are continuous and S_n converges uniformly in the interval (a,b).

It is also shown in Hildebrand (1965) that the best approximation in the least squares sense is obtained when the a_k are taken as the Fourier constants of $f(x)$ relative to $\phi_k(x)$. The criteria for the uniform convergence of a sequence of functions is given by the famous Weirstrass M-Test which we state here without proof: [Wylie 1966]

If a sequence of positive constants $\{M_n\}$ exists such that $|\phi_n(x)| \leqq M_n$ for all positive integers n and for all values of x in a given region R and if the series

$\sum_{n=1}^{\infty} M_n$ is convergent; then the series $\sum_{n=1}^{\infty} \phi_n(x)$ converges uniformly in R.

The above theorems have been used in Chapter 5 to show convergence of the approximating functions to the true solution of the characteristic equation.

There are other techniques for obtaining solutions to the differential equations. Galerkin's method is used extensively for problems in

Hydrodynamic Stability. In this method, some functional approximation to the solution (frequently a polynomial) is generally substituted into the differential equations and the function coefficients evaluated from the condition that the least squares of the error over the function space is minimized. Further details may be found in Kantorovich and Krylov (1955).

(ii) Numerical integration methods: - Small perturbation analysis relating to hydrodynamic stability usually result in two point boundary value problems. Throughout this report, the major effort is concentrated on obtaining solutions to the system of ordinary differential equations that describe the behavior of small perturbations in fluid layers. Numerical methods for the integration of ordinary differential equations are well known and will not be discussed in any detail here. However, the nature of the differential equations obtained in Chapter 2 is such, that considerable modification to the integration scheme is necessary. We now proceed to outline the technique that was used. This method was also employed for the solution of the equations pertaining to the onset of convective instability in stationary layers of fluid. The differential equations of Chapter 2 contain a large parameter $R_d \frac{dU_o}{d\eta}$. This can reach a value of several hundred within the boundary layer. The presence of this large parameter in the system of equations leads to a rapidly growing parasitic solution that dominates the true solution so that within a short integration interval, the answers are hopelessly inaccurate by several orders of magnitude (Fox 1960). Such differential equations containing a large parameter are termed "stiff."

In order to obtain accurate numerical results, a method first proposed by Godunov (1961) and later modified by Conte (1966) was used. The differential equations of Chapter 2 were rewritten as a system of nine first order equations; in general this can always be done. Since four unknown initial values exist at the wall, it is necessary to synthesize four linearly independent solution vectors, all combinations of which satisfy the given initial conditions. The simplest such system to synthesize is of course the vectors with zero components everywhere except at the missing initial conditions. The system is then integrated to a distant point in the boundary layer and a linear combination of the four homogeneous solution vectors taken so that the boundary conditions are satisfied. The boundary value problem is therefore converted into four initial value problems. This mathematically exact procedure leads to inaccuracies unless special precautions are taken. Due to the rapid buildup of the parasitic solution, the four solution vectors tend to become increasingly dependent. Geometrically, this is interpreted as a reduction from 90° of the angle between the solution vectors as integration proceeds towards the outer boundary. In addition, the numbers that belong to the components of each vector become extremely large so that exponential overflow in the computer occurs after a few integration steps. The method proposed by Conte (1966) suggests orthonormalization of the solution vectors after a certain criterion is exceeded. The vectors may readily be orthonormalized by the Gram-Schmidt process which is described in any elementary text book on linear algebra. One criterion would be to compute the angle between any two of the solution vectors at each integration step and orthonormalize when the angle becomes smaller than a certain value. An alternative criterion (used here since it consumes far less computer time) is to orthonormalize the vectors when the length of any vector exceeds a certain preassigned value. Using this technique, good numerical results for the eigenvalues and eigenfunctions were obtained. Hamming's Modified Predictor-Corrector method was used for the integration since it is faster than Runge-Kutta methods and has fifth order accuracy. The actual application of the procedure is detailed in Chapter 6. Since the second boundary condition occurs at infinity, it was necessary to integrate the system of equations to some distant point in the boundary layer and successively increase the integration interval until no further change in the eigenvalues resulted.

The technique of orthogonalization has been used increasingly in recent times in stability theory with good success. Wazzan et al. (1966) have applied it to incompressible two-dimensional flows with Reynold's numbers as large as 5×10^5.

(iii) Numerical 'inner' solutions matched to 'outer' analytic solutions: - For cases were the flowfield possesses a 'boundary layer' character, i.e., where the primary flow is changing within a thin boundary layer region and is essentially constant outside it, a variation of the numerical method may be employed. In the outer flow, the differential equations reduce to a constant coefficient type. This allows analytic solutions in terms of elementary functions to be obtained, these solutions being valid in the free stream. In particular, the validity of these solutions at the edge of the boundary layer is assumed. They may therefore be utilized to provide boundary conditions at the boundary layer edge, thus restricting the interval of numerical integration to the boundary layer thickness.

The numerical integration within the boundary layer may be performed in two ways: a) One could start at the wall and integrate outwards to the boundary layer edge, simultaneously adjusting the values for the missing initial conditions and the eigenvalue until a match at the boundary layer edge is obtained. This procedure was used successfully by Nachsteim (1963) in an analysis of the stability of natural convection flow on a vertical plate. However, the technique suffers from the drawback of requiring excessive amounts of computer core since a large number of equations need to be integrated simultaneously. For example, in the present case with nine first order equations and four missing initial conditions, thirty-six equations need to be integrated; b) the second method used here is to essentially convert the system into four initial value problems as in (ii) and integrate in the reverse direction from the edge of the boundary layer to the wall. This eliminates the iterations that refine the missing initial conditions and only an iteration on the eigenvalue is required. The correct eigenvalue causes the boundary conditions at the wall to be satisfied. Furthermore, since the integration proceeds in the direction in which the parasitic solution is decaying, the solution vectors are 'well behaved' in a numerical sense and no orthornormalization of the homogeneous solution vectors is required.

Relative Merits of the Three Methods - Approximate analytical methods such as those described in (a), require tremendous computer time if the integrals obtained cannot be evaluated analytically. This is because one obtains an infinite set of equations each containing an infinite number of terms and each term involving evaluation of an integral. There is the advantage however that the technique is convergent and does not lead to numerical instabilities. Method (b) is faster than Method (a) and has the advantage of producing accurate eigenfunctions. However, programming the necessary algorithms is somewhat complicated and sometimes numerical instability can result. Method (c) is fastest of all, since in essence it reduces the interval of integration to the width of the boundary layer. It can only be used however where the conditions at the boundary layer edge are known in functional form.

Chapter 5

PARALLEL FLOW ALONG CURVED HEATED WALLS

In this chapter, solutions to the stability equations for a parallel flow along a curved heated wall have been obtained under the following restrictions.

(i) The "finite curvature terms" (second order curvature terms) retained by Smith have been neglected.

(ii) The lower boundary is assumed rigid while the upper boundary is assumed free.

(iii) Only solutions for a neutral disturbance have been obtained.

Accordingly we set $B = 0$ and $V_o = 0$ in equations (3.6) and neglect the second order curvature terms. This results in the following simplified set of equations:

$$\frac{d^2u}{d\eta^2} - A^2u - R_d \frac{dU_o}{d\eta} v = 0$$

$$\frac{d^2v}{d\eta^2} - A^2v - 2K\, U_o R_d\, u = \frac{1}{2}\frac{dC_p}{d\eta} - Gr\, T$$

$$\frac{d^2w}{d\eta^2} - A^2w = -\frac{A}{2} C_p \tag{5.1}$$

$$\frac{dv}{d\eta} + A\, w = 0$$

$$\frac{d^2T}{d\eta^2} - A^2T = P_r\, v \frac{dT_1}{d\eta} \quad .$$

The lateral velocity fluctuation w and the pressure fluctuation C_p are now eliminated to give the system

$$(D^2 - A^2)^2\, v = A^2(2KU_oR_d\, u - G_rT)$$

$$(D^2 - A^2)u \quad = v\, R_d \frac{dV_o}{d\eta} \qquad (5.2)$$

$$(D^2 - A^2)\, T \quad = v\, P_r \frac{dT_1}{d\eta}$$

where $D \equiv \frac{d}{d\eta}$. The boundary conditions we assume here are those of a finite layer of fluid enclosed between a lower, rigid boundary, and an upper plane that exerts no stress. Accordingly, we must have

$\eta = 0$, $u, v, T, Dv = 0$

$\eta = 1$, $u, v, T, D^2v = 0$.

In this formulation $\eta = \frac{y}{\delta}$ where δ is taken as the thickness of the unstable layer. The disturbances originating in the unstable layer δ are assumed to penetrate to a total height d . In order to approximate penetrative convection with this crude model, we define a penetration coefficient $c = \frac{d}{\delta}$ where d is the total penetrated height attained by the fluctuations as denoted in fig. (2). Therefore a new dimensionless coordinate $\xi = \frac{\eta}{c}$ is defined, noting that $c = 1$, indicates zero penetration.

Transforming equations (5.2) in terms of the new coordinate ξ results in

$$(D^2 - \Phi^2)^2\, v = \Phi^2(2\, K_cU_oR_{cd}u - \frac{Gr_c}{C}\, T)$$

$$(D^2 - \Phi^2)\, u \quad = v\, R_{cd} \frac{dU_o}{d\xi} \qquad (5.3)$$

$$(D^2 - \Phi^2)\, T \quad = v\, c\, P_r \frac{dT_1}{d\xi}$$

where $\Phi = cA$, $R_{cd} = c\, R_d$, $K_c = cK$ and $Gr_c = c^3\, G_r$.

The revised boundary conditions are

$$\xi = 0 \;, \quad u,v,T, \quad D\,v = 0$$

$$\xi = 1 \;, \quad u,v,T, \quad D^2 v = 0$$

where D now means $\equiv \frac{d}{d\xi}$. Following Rintel (1971), the perturbation velocity components are now expanded in a series of independent functions satisfying the boundary conditions.

We therefore write

$$u = \sum_{n=1}^{\infty} B_n\, x_n$$

$$v = \sum_{n=1}^{\infty} A_n\, z_n \qquad (5.4)$$

$$T = \sum_{n=1}^{\infty} C_n\, x_n$$

where we choose

$$\lambda_n\, x_n = \mathrm{Sin}\; n\,\pi\,\xi$$

$$\lambda_n^2\, z_n = \lambda_n\, x_n + \frac{2n\pi}{\mathrm{Sinh}2\Phi - 2\Phi}\{\mathrm{Sinh}\Phi\xi - \xi\;\mathrm{Sinh}\Phi\;\mathrm{Cosh}(\Phi\xi - \Phi)\}$$

$$\lambda_n = n^2\pi^2 + \Phi^2$$

where the last relation is chosen so that

$$(D^2 - \Phi^2)\, x_n = -\,\lambda_n\, x_n \;.$$

The reason for this choice will become clear in the subsequent analysis. We also note that

$$(D^2 - \Phi^2)^2 z_n = \lambda_n\, x_n .$$

On substitution of the expressions for u, v and T into the set (5.3) there results

$$(D^2 - \Phi^2)^2 \sum_{n=1}^{\infty} A_n z_n = \Phi^2 (2K_c \; R_{cd} \; U_o \sum_{n=1}^{\infty} B_n x_n - \frac{Gr_c}{C} \sum_{n=1}^{\infty} C_n \; x_n)$$

or

$$\sum_{n=1}^{\infty} A_n \; {}_n x_n = \Phi^2 (2K_c \; R_{cd} \; U_o \sum_{n=1}^{\infty} B_n x_n - \frac{1}{c} \; Gr_c \sum_{n=1}^{\infty} C_n x_n) \; . \quad (5.5)$$

Since the functions Sin $n \; \pi\xi$, Sin $m \; \pi\xi$ are orthonormal over the range 0 to 1 we multiply equation (5.5) by Sin $m\pi\xi$ and integrate over the range $\xi = 0$ to 1 . One then obtains:

$$\sum_{n=1}^{\infty} A_n \frac{1}{2} \; \delta_{nm} = \Phi^2 [2K_c R_{cd} \sum_{n=1}^{\infty} \frac{B_n}{\lambda_n} \; \lambda_n \lambda_m \int_o^1 U_o \; x_m x_n d\xi$$

$$- \frac{1}{C} \; Gr_c \sum_{n=1}^{\infty} C_n \frac{1}{2} \, \phi_{nm} \; \frac{1}{\lambda_n} \;]$$

where δ_{nm} is the kronecker delta

$$\frac{A_m}{2} = \Phi^2 [2K_c \; R_{cd} \sum_{n=1}^{\infty} \frac{B_n X'_{nm}}{\lambda_n} - \frac{1}{2c\lambda_m} \; Gr_c \; C_m]$$

where $X'_{nm} = \lambda_n \lambda_m \int_o^1 U_o \; x_m x_n d\xi$

interchanging n and m we have

$$A_n = \Phi^2 [4K_c \; R_{cd} \sum_{m=1}^{\infty} \frac{B_m X'_{mn}}{\lambda_m} - \frac{1}{c\lambda_n} \; Gr_c \; C_n] \quad . \quad (5.6)$$

From the second equation of (5.3) we obtain

$$(D^2 - \Phi^2) \sum_{n=1}^{\infty} B_n x_n = \sum_{n=1}^{\infty} A_n z_n \; R_{cd} \frac{dU_o}{d\xi}$$

$$\sum_{n=1}^{\infty} - \lambda_n \; B_n x_n = R_{cd} \sum_{n=1}^{\infty} A_n z_n \frac{dU_o}{d\xi}$$

multiplying throughout by $\lambda_m x_m$ and integrating from 0 to 1

$$-\frac{B_m}{2} = R_{cd} \sum_{n=1}^{\infty} \frac{A_n}{n} Y'_{nm}$$

where $Y'_{nm} = \lambda_n \lambda_m \int_o^1 \frac{dU_o}{d\xi} Z_n X_m \, d\xi$

$$B_n = -2 R_{cd} \sum_{m=1}^{\infty} \frac{A_m}{\lambda_m} Y'_{mn} \qquad (5.7)$$

and finally from the last equation of (5.3) the result is

$$C_n = - 2cPr \sum_{n=1}^{\infty} \frac{A_m}{\lambda_m} Y^o_{mn} \qquad (5.8)$$

where $Y^o_{mn} = \lambda_n \lambda_m \int_o^1 z_m x_n \frac{dT_1}{d\xi} d\xi$.

Substituting the values of the coefficients B_n and C_n from (5.7) and (5.8) into (5.6) we obtain

$$A_n = \Phi^2[- 8 N_{Gc}^2 \sum_{m=1}^{\infty} \frac{X'_{mn}}{\lambda_m} \sum_{\ell=1}^{\infty} \frac{A_\ell Y'_{\ell m}}{\lambda_\ell}$$

$$+ \frac{1}{\lambda_n} 2 \, Ra_c \sum_{m=1}^{\infty} \frac{A_m}{\lambda_m} Y^o_{mn}] \qquad (5.9)$$

where $N_{Gc} = R_{cd} \sqrt{K_c}$ the Goertler number based on the penetrated height $d = c\delta$ and $Ra_c = P_r \, Gr_c$ the Rayleigh number also based on the height d . We may extract the quantity c , the penetration coefficient from Eq. (5.9) and rewrite it as

$$A_n = c^3\Phi^2[8 N_G^2 \sum_{m=1}^{\infty} \frac{X'_{nm}}{\lambda_m} \sum_{\ell=1}^{\infty} \frac{A_\ell Y'_{\ell m}}{\lambda_\ell} + \frac{1}{\lambda_n} 2Ra \sum_{m=1}^{\infty} \frac{A_m}{\lambda_m} Y^o_{mn}]$$

$$(5.10)$$

where we have also taken the sign convention that concave curvature corresponds to a positive Goertler number. Equation (5.10) may be further rewritten as

$$A_n = c^3\Phi^2 \sum_{\ell=1}^{\infty} A_\ell\{8N_G^2P_{\ell n} + 2\ Ra_\ell Q_{\ell n}\} = c^3\Phi^2 \sum_{\ell=1}^{\infty} A_\ell R_{\ell n} \tag{5.11}$$

where $Q_{\ell n} = \dfrac{Y^o{}_{\ell n}}{\lambda_\ell \lambda_n}$, $P_{\ell n} = \sum\limits_{m=1}^{\infty} \dfrac{X'{}_{nm}\ Y'{}_{\ell m}}{\lambda_\ell \lambda_m}$

and $R_{\ell n} = 8N_G^2P_{\ell n} + 2Ra\ Q_{\ell n}$. In matrix notation we have the familiar eigenvalue problem

$$[A] = \Phi^2 c^3[R][A]$$

and for a non-trivial solution we must have $|\delta_{nm} - c^3\Phi^2\ R_{nm}| = 0$ which is the relation for the neutral stability curve. To simplify numerical evaluation of equation (5.11) it is written in the form

$$A_n = c^3\Phi^2\ N_G^2 \sum_{\ell=1}^{\infty} A_\ell\ \{8P_{\ell n} + 2R_n\ Q_{\ell n}\} \tag{5.12}$$

where $R_n = R_a/N_G{}^2$. Equation (5.12) is then solved, treating R_n as a variable parameter. Several cases of parallel as well as stationary flows were studied using this method. For purposes of numerical evaluation, the infinite series expansion in equations (5.4) was truncated after thirty terms and the matrices were limited to ninth order. For some cases fifth order matrices provided satisfactory convergence.

The results obtained, indicated that nonlinear mean temperature profiles in stationary fluid layers were more unstable and penetrative than linear ones. Furthermore, it was found that for parallel layers of fluid along curved heated walls, a unique stability curve for neutral disturbances could be obtained if the quantity plotted along the abscissa was $R_a + K N_G^2$ where K is a constant which expresses the relative importance of the mean temperature and velocity profiles.

A complete description of the various cases studied together with a discussion of the results obtained is included in Kahawita and Meroney (1972).

A Convergence Proof - This section is devoted to proving that the functional representations of the disturbance components in equations (5.4) converge in the limit to the true eigenfunction solutions.

We have
$$u = \sum_{n=1}^{\infty} B_n x_n$$

$$v = \sum_{n=1}^{\infty} A_n z_n$$

$$T = \sum_{n=1}^{\infty} C_n x_n$$

with
$$\lambda_n x_n = \sin n\pi\xi$$

$$\lambda_n^2 z_n = \lambda_n x_n + \frac{2n\pi}{\text{Sinh}2\Phi - 2\Phi}\{\text{Sinh}\Phi\xi - \xi\ \text{Sinh}\Phi\ \text{Cosh}(\Phi\xi - \Phi)\}$$

$$\lambda_n = n^2\pi^2 + \Phi^2 .$$

Evidently the functions x_n and z_n form a convergent sequence and are twice continuously differentiable in the interval 0 to 1 . Differentiating z_n twice does not introduce any powers of n . Therefore $|z_n|$, $|z'_n|$, $|z''_n| \leq \frac{M}{n^3}$ where M is the greatest absolute value of z_n .

$$x_n'' \text{ goes as } -\frac{n^2\pi^2 \text{ Sin } n\ \pi\ \xi}{n^2\pi^2 + \Phi^2} \leq M_1$$

$$x_n\ , \leq \frac{1}{n^2\pi^2} \quad \text{and} \quad x_n' \leq \frac{M_2}{n\pi} .$$

For all reasonable choices of the functions

V_o , $\frac{d V_o}{d\xi}$, $\frac{d T_1}{d\xi}$, consistent with physical reality, the quantities

$$X'_{nm} = \lambda_n \lambda_m \int_o^1 U_o \, x_m x_n d\xi$$

$$Y^o_{mn} = \lambda_n \lambda_m \int_o^1 \frac{d T_1}{d\xi} z_m x_n d\xi$$

$$Y'_{mn} = \lambda_n \lambda_m \int_o^1 z_n x_m \frac{d U_o}{d\xi} \, d\xi$$

are bounded.

Let the maximum absolute value of X'_{nm} , Y^o_{mn} , $Y'_{mn} \leq M_3$ say. Then from equation (5.10) we have

$$A_n = c^3\Phi^2[8N_G{}^2 \sum_{m=1}^{\infty} \frac{X'_{nm}}{\lambda_m} \sum_{\ell=1}^{\infty} \frac{A_\ell Y'_{\ell m}}{\lambda_\ell} + \frac{2R_a}{\lambda n} \sum_{m=1}^{\infty} \frac{A_m}{\lambda_m} Y^o_{mn}]$$

Noting that λ_n is of the order of n^2 we see that

$$A_n \leq c^3\Phi^2[8N_G{}^2 \sum_{m=1}^{\infty} \frac{M_3}{O(n^2)} \sum_{\ell=1}^{\infty} \frac{A_\ell M_3}{O(\ell^2)} + \frac{2 \, Ra}{O(n^2)} \sum_{m=1}^{\infty} \frac{A_m M_3}{O(m^2)}]$$

where O( ) means "order of magnitude." Clearly, all the A_n's are bounded in the range $\xi = 0$ to 1 . Similarly we may show that the B_n's and C_n's are also bounded for all n .

Hence the series for u, v and T

$$u = B_1 x_1 + B_2 x_2 + \ldots\ldots$$
$$v = A_1 x_1 + A_2 x_2 + \ldots\ldots$$
$$T = C_1 x_1 + C_2 x_2 + \ldots\ldots$$

are dominated term by term by a series of the type $\sum_{n=1}^{\infty} \frac{M_4}{x_n{}^2}$ which is absolutely convergent. Therefore, the series for u, v and T form a uniformly convergent sequence by the Weirstrass 'M' Test for uniform convergence. Furthermore, Theorem 4.1 guarantees that the limit of the sequences just mentioned are the eigenfunction solutions u, v and T of the differential equation.

Chapter 6

GOERTLER INSTABILITY IN BOUNDARY LAYERS ON CURVED HEATED WALLS

This chapter is concerned with obtaining solutions to the system of differential equations derived in Chapter 3. They have been applied to a study of the Hydrodynamic Stability of the following flows:

(a) The stability of a Blasius Boundary Layer on a concave heated wall;

(b) The stability of the "Asymptotic Suction Profile" Boundary Layer on a concave plate;

(c) The stability of a Wall Jet on a concave as well as convex surface;

(d) The spin up of a Two-Dimensional Cylinder in an infinite medium.

The equations of interest (3.6) from Chapter 3 are reproduced here:

$$\frac{d^2u}{d\eta^2} - [V_oR_d + K]\frac{du}{d\eta} + [B^2 - A^2 - R_d(BU_o - \frac{dV_o}{d\eta}) + K\eta B(2B - U_oR_d)]u$$
$$- [R_d\frac{dU_o}{d\eta} + K(2B - U_oR_d)]v = \frac{B}{2}\ C_p\ (1 + K\eta)$$

$$\frac{d^2v}{d\eta^2} - [V_oR_d + K]\frac{dv}{d\eta} + [B^2 - A^2 + 2K\eta B^2 - B\ R_dU_o(1 + K\eta) - R_d\frac{dV_o}{d\eta}]v$$
$$- [2KR_dU_o - 2KB]u = \frac{1}{2}\frac{dC_p}{d\eta} - Gr\ T \qquad (3.6)$$

$$\frac{d^2w}{d\eta^2} - [V_oR_d + K]\frac{dw}{d\eta} + [B^2 - A^2 + 2KB^2\eta - B\ R_dU_o(1 + K\eta)]w$$
$$= -\frac{A}{2}C_p$$

$$Bu + K\ Bu\eta + \frac{dv}{d\eta} + Aw - Kv = 0$$

$$\frac{d^2T}{d\eta^2} - [V_o\ Pr\ R_d + K]\frac{dT}{d\eta} + [B^2 - A^2 + 2KB^2\eta - BU_o\ Pr\ R_d(1 + K\eta)]T$$
$$= Pr\ v\frac{dT_1}{d\eta}$$

Defining

$$y_1 = u$$

$$y_2 = \frac{du}{d\eta}$$

$$y_3 = v$$

$$y_4 = \frac{dv}{d\eta}$$

$$y_5 = w$$

$$y_6 = \frac{dw}{d\eta}$$

$$y_7 = C_p$$

$$y_8 = T$$

$$y_9 = \frac{dT}{d\eta}$$

we rewrite the equations as a first order system obtaining

$$\begin{aligned}
y'_1 &= y_2 \\
y'_2 &= (a_1+K)y_2 - (a_2+Ka_3)y_1 + (a_4+Ka_5)y_3 + \frac{B}{2}(1+K\eta)y_7 \\
y'_3 &= y_4 \\
y'_4 &= Ky_4 - Ay_6 - B(1+K\eta)y_2 - KBy_1 \\
y'_5 &= y_6 \\
y'_6 &= (c_1+K)y_6 - (c_2+Kc_3)y_5 - \frac{A}{2}y_7 \\
y'_7 &= 2[-Ay_6 - B(1+K\eta)y_2 - b_1y_4 - K(B+b_4)y_1 + (b_2+Kb_3)y_3 + Gry_8] \\
y'_8 &= y_9 \\
y'_9 &= (d_1+K)y_9 - (d_2+Kd_3)y_8 + d_4y_3
\end{aligned} \tag{6.1}$$

where primes denote differentiation with respect to η and

$$a_1 = V_o R_d$$

$$a_2 = B^2 - A^2 - R_d\left(BU_o - \frac{dV_o}{d\eta}\right)$$

$$a_3 = \eta\, B(2B - U_o R_d)$$

$$a_4 = R_d \frac{dU_o}{d\eta}$$

$$a_5 = 2B - U_o R_d$$

$$b_1 = V_o R_d$$

$$b_2 = B^2 - A^2 - R_d\left(BU_o + \frac{dV_o}{d\eta}\right)$$

$$b_3 = \eta\, B(2B - U_o R_d)$$

$$b_4 = 2(R_d U_o - B)$$

$$c_1 = V_o R_d$$

$$c_2 = B^2 - A^2 - B\, R_d U_o$$

$$c_3 = 2B^2\eta - B\, R_d U_o \eta$$

$$d_1 = V_o\, Pr\, R_d$$

$$d_2 = B^2 - A^2 - B\, U_o\, Pr\, R_d$$

$$d_3 = 2B^2\eta - B\, U_o\, Pr\, R_d \eta$$

$$d_4 = Pr \frac{dT_1}{d\eta}$$

In vector form we have

$$\underset{\sim}{y}' = \underset{\sim}{F}(X)$$

with the boundary conditions

$$\eta = 0, \quad y_1 = y_3 = y_4 = y_5 = y_8 = 0$$

$$\eta \to \infty, \quad y_1 , y_3 , y_5 , y_8 \to 0 .$$

The system (6.1) has a set of four linearly independent solution vectors denoted by

$$\underset{\sim}{y}^{(1)} , \underset{\sim}{y}^{(2)} , \underset{\sim}{y}^{(3)} \text{ and } \underset{\sim}{y}^{(4)}$$

At $\eta = 0$ we have

$$\begin{aligned} \underset{\sim}{y}^{(1)}(0) &= (0, 1, 0, 0, 0, 0, 0, 0, 0) \\ \underset{\sim}{y}^{(2)}(0) &= (0, 0, 0, 0, 0, 1, 0, 0, 0) \\ \underset{\sim}{y}^{(3)}(0) &= (0, 0, 0, 0, 0, 0, 1, 0, 0) \\ \underset{\sim}{y}^{(4)}(0) &= (0, 0, 0, 0, 0, 0, 0, 0, 1) \end{aligned} \tag{6.2}$$

Any combination of the general solution as written will satisfy the initial conditions. If it is to satisfy the boundary conditions at $\eta = \eta_\infty$ (where η_∞ is a satisfactory representation of infinity,) we must have the following relations:

$$\begin{aligned} \beta_1 y_1^{(1)}(\eta_\infty) + \beta_2 y_1^{(2)}(\eta_\infty) + \beta_3 y_1^{(3)}(\eta_\infty) + \beta_4 y_1^{(4)}(\eta_\infty) &= 0 \\ \beta_1 y_3^{(1)}(\eta_\infty) + \beta_2 y_3^{(2)}(\eta_\infty) + \beta_3 y_3^{(3)}(\eta_\infty) + \beta_4 y_3^{(4)}(\eta_\infty) &= 0 \\ \beta_1 y_5^{(1)}(\eta_\infty) + \beta_2 y_5^{(2)}(\eta_\infty) + \beta_3 y_5^{(3)}(\eta_\infty) + \beta_4 y_5^{(4)}(\eta_\infty) &= 0 \\ \beta_1 y_8^{(1)}(\eta_\infty) + \beta_2 y_8^{(2)}(\eta_\infty) + \beta_3 y_8^{(3)}(\eta_\infty) + \beta_4 y_8^{(4)}(\eta_\infty) &= 0 \end{aligned} \tag{6.3}$$

The homogeneous linear system (6.3) will have a non trivial solution only if the determinant of the coefficient matrix vanishes. In general, this occurs only if the eigenvalue has been chosen correctly. When the root of the determinant is found, β_1, β_2, β_3 and β_4 may be found (one of them is of course arbitrary), and the solution $\underset{\sim}{y}(x) = \beta_1 \underset{\sim}{y}^{(1)}(x) + \beta_2 \underset{\sim}{y}^{(2)}(x) + \beta_3 \underset{\sim}{y}^{(3)}(x) + \beta_4 \underset{\sim}{y}^{(4)}(x)$ easily constructed. This mathematically exact procedure is ideally suited for the use of shooting methods and only iteration on the eigenvalue is required. The procedure then, is to numerically integrate the four linearly independent solution vectors from $\eta = 0$ to $\eta = \eta_\infty$ and then combine them to construct the total solution after convergence to the eigenvalue is obtained.

However, a direct shooting method proves useless for the reasons mentioned briefly in Chapter 4, Section (b). Due to the rapidly increasing parasitic solutions, the independent solutions $\underset{\sim}{y}^{(i)}$ rapidly become dependent upon each other. In other words, small errors introduced at any step of the integration are magnified by the exponential components and eventually dominate the solution. For this reason, whenever the magnitude of one of the solution vectors $M = \left(\sum_{j=1}^{9} (y_j^{(i)})^2 \right)^{1/2}$ exceeds a certain preassigned constant, the four vectors are orthonormalized by the Gram-Schmidt process. This restores their independency as well as scaling them down to unity so that exponential overflow does not occur. Integration is then resumed using the normalized solution vectors as initial values at the intermediate points.

Iteration methods used for convergence to the eigenvalue - Three rootfinder techniques were employed, the Muller iterative method, Wegstein's method and a variation of the Newton method. Muller's method requires two initial guesses bracketing the eigenvalue while Wegstein's iteration is slightly more convenient to use since it requires only an initial guess to the eigenvalue. Both methods are adequately described in Carnahan, Luther, and Wilkes (1969). In most cases however, a third method described below was used, which proved the fastest and most efficient in terms of computer time. A brief description follows:

Let λ be the eigenvalue, then the determinant of the coefficient matrix at $\eta = \eta_\infty$ is denoted by $f(\lambda)$. Hence we require $\lambda = \lambda_r$ such that $f(\lambda_r) = 0$. Newton's Algorithm is $\lambda^{n+1} = \lambda^n - \frac{f(\lambda^n)}{f'(\lambda^n)}$ where the superscript denotes iteration number. The major difficulty in applying Newton's Algorithm is of course, evaluation of $f'(\lambda^n)$. This was overcome by evaluating $f'(\lambda^n)$ by numerical differentiation. λ^n was perturbed by a small value $\delta\lambda$ and the new $f(\lambda^n + \delta\lambda)$ evaluated. Hence $f'(\lambda^n) \simeq \frac{f(\lambda^n + \delta\lambda) - f(\lambda^n)}{\delta\lambda}$. The technique worked very well for the majority of cases, since Newton's method is quadratically convergent. Most of the difficulty with the method occurred with the case of the Blasius Boundary Layer when the normal flow terms were retained. In these cases, the Muller Iteration method was used.

Results - This section is devoted to a presentation and discussion of the results obtained for the various cases of instability that were examined. As stated earlier, the flow fields studied were

(a) The Blasius Boundary Layer on a concave heated wall;

(b) The "Asymptotic Suction Profile" on a concave plate;

(c) The Wall Jet on concave as well as convex surfaces;

(d) The Spin Up of a Two Dimensional Cylinder in an infinite medium.

(a) The Stability of the Blasius Boundary Layer on a Concave Heated Wall

The results presented in this section include the case where the wall is unheated. Solutions have also been obtained, in which the normal flow terms have been neglected in the analysis, in order to assess their effect on the stability. The analysis requires the pre-specification of the mean flow velocity and temperature components in analytical form. The "similar" solutions of the Blasius Velocity Profile were approximated by seventh order polynomials. To increase the accuracy of the representation, the derivatives of the profiles were approximated separately by different polynomials. [Some idea of the accuracy obtained may be inferred from figs. (3a) to (3c).]

The scaling length chosen for the calculations was the one conventionally used in the similarity calculations (Schlichting 1968). The interval of numerical integration was restricted to the thickness of the boundary layer, here taken as $\eta(=y/\delta) = 6$. Analytical solutions to the differential equations were obtained in the free stream and the solutions matched at the boundary layer edge. The outer 'free stream' solutions are derived in Appendix B. Numerical experimentation with $\eta = 5$ and $\eta = 7$ taken as the boundary layer edge did not result in a significant variation in the results obtained. It was concluded therefore that the choice of $\eta = 6$ as the edge of the boundary layer should provide sufficient accuracy in the computations. All results were obtained at a Reynold's number of 2000 based on the characteristic length. The results are presented in terms of the momentum thickness in order to facilitate comparison with the results of Smith (1955) and of Hammerlin (1955).

Figures (2a) to (2c) have been presented to indicate the accuracy with which the mean profiles in a Blasius Boundary Layer were approximated by the seventh order polynomials. Figure (4) is a plot of the neutral stability curve obtained with and without the inclusion of the normal flow terms. The results of the stability calculations of Smith (1955) and of Hammerlin (1955) also performed on Blasius Boundary Layers has been plotted in comparison. Above a dimensionless wavenumber of about 0.6, the present results with the normal flow terms included are in close agreement with those of Smith (1955). At the lower wavenumbers however, the curve deviates from Smith's and appears to reach a limiting wavenumber of about 0.3 at a critical Goertler number of zero. Several calculations in the vicinity of a wavenumber of 0.29 failed to converge to a solution, leading to the conclusion that no solutions exist for wavenumbers below about 0.3. The discrepancy between the present results and that of Smith (1955) is probably due to his use of Galerkin's method, criticized by Chang and Sartory (1968). Smith assumed the solution to have the form of a polynomial times an exponential factor which decayed far from the wall. The coefficients of the polynomial were calculated in solving the problem, but the exponential decay rate was assumed mainly on the basis of numerical experimentation. Chang and Sartory (1968) indicate that Smith's answers at the lower wavenumbers could be incorrect by over an order of magnitude. Their results for a Blasius Boundary Layer indicate critical conditions of zero Goertler number at zero wavenumber. This peculiarity in the solutions at small wavenumbers has also been observed in the analogous case of stationary convection in a fluid with a lower stress-free boundary and unconfined vertically by Ogura and Kondo (1970). They too obtained marginal conditions indicating a critical Rayleigh number of zero at a critical wavenumber of zero. Chang and Sartory (1968) anticipated that retention of the finite curvature terms should somehow serve to limit the size of the disturbance to a finite wavenumber. The present results bear this out; however the physically strange behavior of zero Goertler number remains unexplained. It is believed that the present results are solutions to the mathematical problem but that, somehow, the mathematical description of the physical situation is inaccurate at the lower wavenumbers.

The inclusion of the critical stability curve with the normal flow terms omitted in the same fig. (4) permit some assessment of their effect on the stability. The destabilizing influence of the normal velocity component is clearly evident since the critical curve now passes through a minimum. The critical value of the Goertler number agrees well with those of Smith (1955) and Hammerlin (1955), however the critical wavenumbers are different. This discrepancy between the parallel flow analysis of the present work and that of Hammerlin is probably due to the retention in the present study, of the finite curvature terms. The results so far indicate that the normal flow component of the base flow tends to destabilize the flow. If this is true, then it is reasonable to expect that suction at the wall should improve the stability of the flow to three dimensional disturbances. Accordingly, the results obtained with the Asymptotic Suction Profile have been plotted in comparison with the other results on fig. (4). It is immediately evident that suction does indeed improve the stability

It appears therefore, that the parallel flow approximation to quasi-parallel flows may yield results incorrect by as much as an order of magnitude in critical Goertler numbers. The normal velocity component if directed away from the wall, tends to destabilize the flow by encouraging penetration into the free stream where viscous dissipation is small. The application of suction results in the disturbance being restrained to a region closer to the wall where viscous dissipation is larger thereby increasing the stability of the flow.

Figure (5) is a plot of the various amplification curves obtained for the Blasius Boundary Layer, together with some data taken from the experiments of Tani (1962). Insertion of a finite amplification rate into the equations results in all the curves passing through a minimum. Hence, a finite value of the Goertler number is required, before amplification of a disturbance will occur. The finite amplification curves of Hammerlin (1955) also possess minima which indicate a trend to larger wavenumbers at higher amplification rates.

(ii) Unstably Stratified Flow (Heated Wall Conditions)

The earliest known work on the Goertler instability under heated wall conditions is that of DiPrima and Dunn (1956). They restricted their analysis to an investigation of variable property effects on the stability of liquids along concave heated walls. The present analysis differs in that the thermal buoyancy effect of heating at the wall is considered rather than variable property effects. The results disagree considerably in that the stability of a boundary layer is <u>increased</u> by wall heating if only variable property effects are considered while a consideration of the thermal buoyancy force within the framework of the Boussinesqu approximation results in a decrease in stability.

Figure (6) is a presentation of the neutral stability curves at two values of the Grashof number for a fluid of Prandtl number = 0.72. It is interesting to note that the curves intersect on the line of zero Goertler number at a wavenumber of 0.31. To the left of this intersection point, heating at the wall appears to stabilize the flow. The reason for this may be an interaction between the thermal and centrifugal instability mechanisms so that at the lower wavenumbers, an increasing Grashof number increases the stability of the flow. Another possible explanation on the other hand may be a peculiarity in the mathematical behavior of the solutions which are of no physical significance.

The results of a parallel flow analysis in which neutral stability curves are obtained using the Goertler number as a parameter and for two values of the Prandtl number are presented in figs. (7) and (8). The curves now display well-defined minima which reduce as expected with increasing Goertler number. This indicates that retention of the normal flow terms in the analysis somehow causes the appearance of the strange solutions at the low wavenumbers provided of course, that the direction of the normal flow is away from the wall. Figure (9) has been constructed to indicate the amplification of the disturbance at various Rayleigh numbers for a fixed value of the Goertler number.

The amplitudes of the disturbance functions obtained for two different Prandtl number fluids at critical conditions and a Goertler number of 3 are displayed in Fig. (10). They have been drawn scaled to the boundary layer thickness so that $\eta = 1$ indicates the edge of the boundary layer. Although the temperature fluctuations are confined close to the wall, the vertical velocities indicate strong penetration into the free stream. The disturbances induce pressure fluctuations which are largest at the wall.

(b) The Stability of the "Asymptotic Suction Profile" is examined in this section. The characteristic length chosen for the calculations was the momentum thickness δ_1 given in Schlichting (1968) as $\frac{\nu}{-v_o}$ where v_o is the suction (negative) vertical velocity, constant throughout the boundary layer. The equation of the mean velocity profile is $f(\equiv \frac{U}{U_\infty}) = 1 - e^{-\eta}$. $\eta \equiv \frac{y}{\delta_1}$ where y is the vertical coordinate.

The results were computed using a matching point of $\eta = 6$ where $\frac{U}{U_\infty} = 0.9975$. The results are displayed in figs. (11) and (12). Suction in the boundary layer increases it's stability to three dimensional perturbations. Bussmann and Muenz (1942) as well as Chen and Huang (1972) among others, have noted a corresponding increase in stability to two-dimensional disturbances when surface suction is applied. The reason for the improved stability is probably twofold. First, increasing suction decreases the thickness of the boundary layer and second, the disturbances remain confined within the boundary layer where dissipative action is strong. Figure (11) which is a plot of the eigenfunctions at critical conditions appears to confirm the latter. The peak of the perturbations are confined to a region well within the boundary layer.

(c) Stability of Wall Jets on Curved Walls - The study of the stability of a wall jet on a curved surface yielded some interesting results. It appears that a wall jet can be unstable to three-dimensional disturbances on a convex as well as concave wall. The reason for this may be explained quite simply in physical terms. Consider a wall jet on a concave as well as convex wall as depicted in fig. (13). If the region between the wall and the maximum in the profile is termed the 'inner' layer, then this layer is unstable with respect to a concave wall. The condition for instability is that the direction of increasing velocity must point towards the center of curvature of the streamlines. With this criterion, it becomes immediately evident that the outer layer is unstable with respect to a convex wall. In a penetrative convection sense, the first case corresponds to an unstable ('inner') layer of fluid bounded above by a stable layer; the second case corresponds to an unstable layer bounded below by a stable layer and a wall. The two types of instability have been denoted as Type I and Type II respectively.

For purposes of calculation, the wall jet profile was approximated by a parabola in the inner region and a Gaussian function in the outer layer with matching first derivatives. The more accurate similarity solutions derived by Glauert (1956) could also have been easily incorporated into the analysis by using approximating polynomials as was done for the Blasius Profile. The intent here however, has been to treat the problem as a pentrative convective instability in the centrifugal sense. Accordingly the profiles used were

$$f(\eta) \equiv \frac{U}{U_m} = \eta(2-\eta) \qquad 0 \leq \eta \leq 1$$

and

$$f(\eta) = e^{-\lambda(1-\eta)^2} \qquad \eta \geq 1 \quad .$$

The scaling length chosen was the thickness of the inner layer. The constant λ is a free parameter used to adjust the decay rate in the outer flow. This is analogous to adjusting the 'stability' of the upper layer in Chapter 7. Calculations were performed for three values of

$$\lambda = 0 \;,\; 0.01 \quad \text{and} \quad 0.2$$

for a Reynold's number of 7070.

The existence of the outer flow required a direct numerical integration of the equations to be performed to some distant point in the outer layer. This point was chosen as a satisfactory representation of "infinity" when an increase of twenty percent in the integration interval produced less than a one percent change in the calculated eigenvalue. The flow was assumed parallel, i.e. the normal velocity component was taken as zero.

The neutral stability curves for the Type I and Type II instabilities are presented in fig. (14). Generally, the Type II instability occurs at a lower value of the Goertler number than the Type I instability. This is simply because the outer mean flow is in general several times the thickness of the inner layer. The scaling of the Goertler number in terms of the inner layer thickness appears to make it artificially small. The disturbance amplitudes presented in fig. (15) reveal that for slowly decaying outer flows, a double vortex structure is observed in the Type II instability. This is due perhaps to the instability in the outer flow driving an inner vortex by viscous action. Such secondary vortices have been observed by Taylor (1923) in the analogous flow between counter rotating cylinders. In his case, the fluid layer adjoining the inner cylinder is unstable since the velocity decreases with increasing radial distance. Since the outer cylinder rotates in a direction opposite to that of the inner cylinder, the velocity profile in the annular space passes through zero and reverses direction. The fluid adjoining the outer cylinder is therefore stable. Taylor observed that the inner layer formed a vortex structure which generated a secondary system in the outer flow due to a non-vanishing of the tangential stresses at the interphase.

Figure (15) also indicates that the Type I disturbances are fairly closely confined to a region near the surface, although they succeed to some extent in driving weak vortices in the outer flow. This type of penetrative action by viscous stresses at the boundary of stable and unstable fluid has been discussed by Rintel (1967).

The principle value of the present results are in demonstrating the type and form of disturbances that may be obtained in wall jets along curved walls. In practice, most wall jets are turbulent or become so at a short distance from the exit nozzle. Nevertheless, this type of instability can form even under turbulent conditions as noted by Tani (1962), who observed Goertler instability in turbulent boundary layers along concave walls.

(d) The Spin Up of a Cylinder in an Infinite Medium - The stability of the spin up of a cylinder within an annulus has been experimentally and theoretically investigated by Kirchner and Chen (1970) and Chen and Kirchner (1971). Their theoretical investigation consisted of two different analyses; the first was an initial value method in which random disturbances are artificially introduced at a given instant and their evolution with time followed, the second was a quasi-steady approach. In an unsteady disturbed system the basic profile is evolving with time as are the perturbations. The quasi-steady approximation neglects this and examines the stability of the instantaneous basic profile. This approximation is good if the disturbances are amplifying at a rate much faster than the growth of the basic profile. The quasi-steady approach was adopted here. This study was performed in order to gauge the quality of results that could be obtained with a simple approach and trivial changes in the computer program developed during the course of this research.

The mean (time dependent) velocity profiles were calculated from the theory of Mallick (1957). In order to remove the time dependence of the mean profile, it was necessary to artificially construct a scaling parameter so that all the curves of mean profiles may be represented by a single line. By using logarithmic plots, it was discovered that the dimensionless quantity $[\frac{\nu t}{a^2}]^{0.411}$ provided suitable scaling. Here

ν is the kinematic viscosity

t is time

a is the cylinder radius.

The quasi-steady profile could now be approximated from a curve fit by the relation

$$f\ (\equiv \frac{U}{U_s}) = e^{-1.2625\eta}$$

where U_s is the cylinder surface speed

$$\eta = \frac{(r/a - 1)}{(\frac{\nu t}{a^2})^{0.411}}$$

r is the radial coordinate.

The mean velocity profiles calculated from Mallick (1957) are presented in fig. (16) for different values of the dimensionless time $\frac{\nu t}{a^2}$. Figure (17) provides some indication of the success obtained by using $(\frac{\nu t}{a^2})^{0.411}$ as a scaling parameter. The solid line is the curve $f = e^{-1.2625\eta}$. The points have been taken from the different curves in fig. (16) and scaled with the dimensionless parameter mentioned above.

The curve of neutral stability is presented in fig. (18) with the eigenfunction disturbances being displayed in fig. (19). The critical Goertler number obtained is about 9.8. Based on this result, a curve of critical Reynolds number R_d versus critical dimensionless time $\tau(= \frac{\nu t}{a^2})$ has been constructed in fig. (20) with the experimental points of Kirchner and Chen (1970) plotted in comparison. The Reynold's number is based on the cylinder radius a.

The quasi-steady analysis underestimates the critical times by a factor of from 10 to 15. This discrepancy is probably due to three reasons: the first is neglecting the time growth of the mean profile; the second is the impossibility in observing the point of first instability in the flow; and the third is the fact that comparison is being made with experiments performed in a confined flow. Most of the discrepancy is due to the first two reasons. Chen and Kirchner (1971) observe that by the time the instabilities become visible, they have grown to perhaps a thousand times their initial size. They base this conclusion on a comparison between their initial value approach and experimental observation. The initial value calculation appears to underestimate the critical time by a factor of from three to nine.

Considering the simplicity of the present approach compared to theirs, the present calculation has some merit.

Chapter 7

THE STABILITY OF THERMALLY STRATIFIED STATIONARY FLOWS

This chapter deals with the stability of stationary flows having nonlinear basic temperature profiles. The examples chosen have been taken as being indicative of examples of penetrative convection in the atmosphere. The set of equations (3.7) have been solved for different values of the amplification parameter σ .

(a) The Quasi-Steady Analysis of a Time Dependent Profile - In this section, the results of a stability analysis of a layer of fluid suddenly heated from below are presented. The scaling length δ is defined as

$$\delta = 2\sqrt{\kappa t}$$

where κ is the thermal diffusivity of the fluid and t is time. Use of this scaling length produces similarity solutions for the basic temperature profile whose shape thereby becomes independent of time. With the dimensionless vertical coordinate η defined as y/δ the dimensionless temperature profile is

$$T_o = \frac{T-T_\infty}{T_w-T_\infty} = 1 - \frac{2}{\sqrt{\pi}} \int_o^\eta e^{-\eta^2} d\eta$$

where T_∞ is the temperature of the undisturbed fluid and T_w is the temperature of the wall. In terms of the dimensionless quantities, the temperature gradient is $\frac{dT_o}{d\eta} = \frac{2}{\sqrt{\pi}} e^{-\eta^2}$. This gradient was specified in the solution of equations (3.7) with the following boundary conditions

$$\eta = 0 \qquad T = v = v' = w = 0$$

$$\eta \rightarrow \infty \qquad T, v, w \rightarrow 0 .$$

Currie (1967) used a two segment linear profile as an approximation to the actual non-linear profile. He defined an "effective thermal depth" ℓ constructed as in fig. (21) such that the area under the actual and approximate mean temperature distribution was the same.

$$\text{i.e.} \qquad \int_0^\infty \eta \frac{2}{\sqrt{\pi}} e^{-\eta^2} d\eta = \int_0^\ell - \frac{\eta}{\ell} d\eta$$

$$\text{i.e.} \qquad \frac{1}{\sqrt{\pi}} = \frac{\ell}{2} \quad \text{from which } \ell = \frac{2}{\sqrt{\pi}} \quad .$$

The amplification curves obtained in the present study are presented in fig. (22). The neutral amplification curve exhibits a minimum at a Rayleigh number of 22.9 and a wavenumber of 0.28. Currie (1967) obtained a limiting critical Rayleigh number of 32 as the ratio of his thermal depth to total fluid depth approached zero. To compare the present results to Currie's, it is necessary to express the critical Rayleigh number obtained in terms of ℓ . This is readily done by multiplication of the Rayleigh number by $(\frac{2}{\sqrt{\pi}})^3$. Hence

$$22.9 \times (\frac{2}{\sqrt{\pi}})^3 = 32.89.$$

Since the values obtained are in good agreement the conclusion may be drawn that the two segment linear approximation made by Currie does indeed provide satisfactory results.

The comparison with Lick's (1970) work is less satisfactory. He obtained a critical Rayleigh number of 225 at a wavenumber of 1.25. To convert the present result into a form which permits comparison, the δ used in this study must be increased by a factor of two. This merely defines a "thermal thickness" beyond which the temperature is more than 99% of the free stream. The present critical wavenumber must therefore be multiplied by a factor of two and the Rayleigh number by a factor of 2^3.

This results in a critical wavenumber of 0.56 and a critical Rayleigh number of 183.2. The values obtained are lower than Lick's due to the nonlinearity of the basic temperature profile in the present calculation and the different boundary conditions assumed by him. His model consisted of an unstable layer with linear stratification bounded above by fluid of neutral stratification but infinite thermal diffusivity. Hence, his temperature perturbations were forced to vanish at the interface although the vertical velocity of the disturbance was permitted penetration into the neutral layer. The lower boundary was assumed as a free surface whereas the present calculation assumes it to be a rigid conducting plane.

(b) The Onset of Convection in Unstable Fluid Layers Adjacent to Stable Fluid

This section is devoted to a presentation of the results obtained when a layer of fluid which is bounded above by fluid of differing stability is heated from below. The example has been taken to represent a possible situation in the atmosphere. The results are of mainly qualitative value in simulating dry convection in the atmosphere. The model is limited by it's two dimensionality and use of a constant viscosity and thermal diffusivity contained in the parameterization of the Rayleigh number.

The lower mean temperature profile is assumed to have the same shape as the time dependent profile analysed in the previous section.

The temperature profile of the upper layer is considered linear with stable stratification, corresponding to an elevated inversion. Results are presented for the cases where the inversion height is varied keeping the stability γ constant and the stability is varied at a fixed height above ground level. Figure (23) is a sketch of the temperature stratification under study. It is representative of inversions found over urban areas in the winter months.

Figure (24) denotes the variation of the critical Rayleigh number with inversion height at constant stability, while in fig. (25) the dependence of the critical Rayleigh number with inversion stability at fixed height is presented. The scaling length used in the calculations is identical to the one used in the previous section. To a high degree of accuracy it is approximately half the thickness of the unstable layer.

Some idea of the penetrative action of the disturbances may be obtained from a plot of the critical wavenumbers displayed in fig. (26). Decreasing wavenumbers with raising of the inversion indicates increased penetration as would be expected.

To obtain some information on the role of the disturbances in transporting heat into the inversion, the normalized correlation between the vertical velocity and temperature fluctuation has been calculated and is presented in fig. (27). The convective transfer displayed is inaccurate near the ground since it indicated a zero heat transfer. In the actual atmosphere, almost all the heat in the lowest layer would be transferred by small scale turbulence. The model however gives good qualitative results above the level of the 'peak' in the correlation curve, that is to say, the shape of the calculated curve resembles actual vertical profiles of heat flux measured in the atmosphere.

Chapter 8

THE VORTEX MODE OF INSTABILITY IN NATURAL CONVECTION FLOW ALONG INCLINED PLATES

This chapter deals with the formation of longitudinal rolls in Inclined Plate Natural Convection. The motivation for this study was twofold: the first was to analytically study the convective instability mechanism of the flow; the second was to investigate the applicability of the solution methods described earlier in solving a non parallel entraining flow. Since the situation under consideration here does not closely resemble the material in the main body of this thesis, this chapter is to be treated as a separate self-contained part.

Recent observations (Sparrow et al. 1969, 1970, 1972) of natural convection flow along inclined plates have indicated that the flow exhibits an instability in the form of streamwise oriented vortices whenever the inclination angle of the flow with the vertical exceeds a certain critical value. These references have already been cited in Chapter 2. For smaller angles of inclination, it appears that the two dimensional Tollmein Schlichting wave-type disturbances are the dominant mode of instability.

The occurrence of streamwise oriented vortices in other stratified flows is by no means uncommon. Gage and Reid (1968), Kuo (1963) and more recently Kahawita and Meroney (1972) have indicated that unstable stratification in various shear flows can cause the appearance of three-dimensional disturbances. Furthermore, Gage and Reid (1968) have shown that for thermally stratified plane Poiseille flow, Squire's Theorem is inapplicable when the Richardson Number (defined by them as Ra/64Rd, where Ra , Rd are the Rayleigh and Reynolds numbers, respectively) goes below a certain small negative value. This implies that when the Rayleigh number of the flow is greater than some critical value, three dimensional rolls will form regardless of the magnitude of the shear.

For the case of inclined plate natural convection, it appears reasonable to suggest therefore that whenever the component of the body force at right angles to the plate exceeds a certain critical value, streamwise oriented vortices are generated. For smaller inclination angles, the body force component along the plate serves to accelerate the flow streamwise, until the critical Reynold's number which is unstable to two dimensional waves is exceeded. The dominant instability mechanism for the transition process is therefore dependent on two competing factors, the first being the critical Reynold's number for wave disturbances, while the second is the critical Rayleigh number for longitudinal rolls.

The stability of natural convection flow to wave-type disturbances has been analytically investigated by Nachsteim (1963) and Gebhart (1969) among others. In this chapter, some results of a linearized stability analysis of the three dimensional instability are presented.

8.1 Formulation

Consider an isothermal plate inclined at some angle ϕ to the vertical as depicted in fig. (28). The coordinate axes and velocities are assumed conventionally as x, y, z and u, v, w respectively, with x being measured in the streamwise direction from the leading edge of the plate. The equations of motion may be written as

$$\frac{\partial u}{\partial t} + u\,\frac{\partial u}{\partial x} + v\,\frac{\partial u}{\partial y} + w\,\frac{\partial u}{\partial z} = g\,\hat{\beta}\,\theta\,\mathrm{Cos}\phi + \nu\nabla^2 u - \frac{1}{\rho}\,\frac{\partial p}{\partial x}$$

$$\frac{\partial v}{\partial t} + u\,\frac{\partial v}{\partial x} + v\,\frac{\partial v}{\partial y} + w\,\frac{\partial v}{\partial z} = g\,\hat{\beta}\,\theta\,\mathrm{Sin}\phi + \nu\nabla^2 v - \frac{1}{\rho}\,\frac{\partial p}{\partial y}$$

$$\frac{\partial w}{\partial t} + u\,\frac{\partial w}{\partial x} + v\,\frac{\partial w}{\partial y} + w\,\frac{\partial w}{\partial z} = \nu\,\nabla^2 w - \frac{1}{\rho}\,\frac{\partial p}{\partial z}$$

$$\frac{\partial u}{\partial x} + \frac{\partial v}{\partial y} + \frac{\partial w}{\partial z} = 0 \qquad (8.1)$$

while the energy equation is

$$\frac{\partial \theta}{\partial t} + u\,\frac{\partial \theta}{\partial x} + v\,\frac{\partial \theta}{\partial y} + w\,\frac{\partial \theta}{\partial z} = \alpha\,\nabla^2\,\theta$$

where ν = kinematic viscosity

$$\hat{\alpha} = \frac{k}{\rho\hat{c}}\ , \qquad \hat{\beta} = -\frac{1}{\rho}\,\left(\frac{\partial \rho}{\partial \theta}\right)_p$$

t = time and $\theta = T - T_\infty$. In writing the above equations, the assumption of an incompressible, Boussinesq fluid has been made. The instantaneous velocity, temperature and pressure are now perturbed by small fluctuating components so that we may write

$$u = \overline{u} + \tilde{u} \qquad p = \overline{p} + \tilde{p}$$

$$v = \overline{v} + \tilde{v} \qquad \theta = \overline{\theta} + \tilde{\theta}$$

$$w = \overline{w} + \tilde{w}$$

where overbars signify the mean (base flow) quantites and $\tilde{}$ the fluctuations. The base flow is assumed two-dimensional so that $\overline{w}$ and variations with respect to z are zero. The equations for the base flow are then

$$\overline{u}\,\frac{\partial\overline{u}}{\partial x} + \overline{v}\,\frac{\partial\overline{u}}{\partial y} = g\,\hat{\beta}\;\;\overline{\theta}\;\mathrm{Cos}\phi + \nu\nabla_h^2\,\overline{u} - \frac{1}{\rho}\,\frac{\partial\overline{p}}{\partial x}$$

$$\overline{u}\,\frac{\partial\overline{v}}{\partial x} + \overline{v}\,\frac{\partial\overline{v}}{\partial y} = g\;\;\hat{\beta}\;\overline{\theta}\;\mathrm{Sin}\phi + \nu\nabla_h^2\,\overline{v} - \frac{1}{\rho}\,\frac{\partial\overline{p}}{\partial y}$$

$$\frac{\partial\overline{u}}{\partial x} + \frac{\partial\overline{v}}{\partial y} = 0$$

$$\overline{u}\,\frac{\partial\overline{\theta}}{\partial x} + \overline{v}\,\frac{\partial\overline{\theta}}{\partial y} = \hat{\alpha}\;\nabla_h^2\;\overline{\theta} \tag{8.2}$$

where

$$\nabla_h^2 \equiv \frac{\partial^2}{\partial x^2} + \frac{\partial^2}{\partial y^2}\;.$$

On substitution of the instantaneous velocity components into equations (8.1) and subtraction of the mean flow velocities in equations (8.2) we obtain the differential equations of the perturbation components. As is usual in the linearized theory only first order perturbation terms are retained. In addition, although the base flow is assumed two dimensional, $\frac{\partial\overline{v}}{\partial x}$ and $\frac{\partial\overline{\theta}}{\partial x}$ are neglected in this approximation. This is certainly justifiable within the framework of boundary layer theory as far as $\frac{\partial\overline{v}}{\partial x}$ is concerned. It would be possible to incorporate $\frac{\partial\overline{\theta}}{\partial x}$ into the analysis if some analytical representation is available. In the present analysis, it is excluded (although it provides weak coupling between the temperature and velocity fluctuations) since it's variation through the boundary layer is small. The term $\frac{\partial\overline{u}}{\partial x}$ is conveniently replaced by $-\frac{\partial\overline{v}}{\partial y}$ from the continuity equation thus providing an easily specified analytic representation as a function of y . The approximations for the base flow are then $\overline{\theta} = \overline{\theta}(y)$, $\overline{v} = \overline{v}(y)$, $\overline{u} = \overline{u}(y)$. The base flow is therefore not assumed to be parallel.

The differential equations governing the motion of the perturbations may then be written as

$$\frac{\partial \tilde{u}}{\partial t} - \tilde{u}\frac{\partial \bar{v}}{\partial y} + \bar{u}\frac{\partial \tilde{u}}{\partial x} + \tilde{v}\frac{\partial \bar{u}}{\partial y} + \bar{v}\frac{\partial \tilde{u}}{\partial y} = g\,\hat{\beta}\,\tilde{\theta}\,\mathrm{Cos}\phi + \nu\,\nabla^2\,\tilde{u} - \frac{1}{\rho}\frac{\partial \tilde{p}}{\partial x}$$

$$\frac{\partial \tilde{v}}{\partial t} + \bar{u}\frac{\partial \tilde{v}}{\partial x} + \bar{v}\frac{\partial \tilde{v}}{\partial y} + \tilde{v}\frac{\partial \bar{v}}{\partial y} = g\,\hat{\beta}\,\tilde{\theta}\,\mathrm{Sin}\phi + \nu\,\nabla^2\,\tilde{v} - \frac{1}{\rho}\frac{\partial \tilde{p}}{\partial y}$$

$$\frac{\partial \tilde{w}}{\partial t} + \bar{u}\frac{\partial \tilde{w}}{\partial x} + \bar{v}\frac{\partial \tilde{w}}{\partial y} = \nu\,\nabla^2\,\tilde{w} - \frac{1}{\rho}\frac{\partial \tilde{p}}{\partial z}$$

$$\frac{\partial \tilde{u}}{\partial x} + \frac{\partial \tilde{v}}{\partial y} + \frac{\partial \tilde{w}}{\partial z} = 0\ . \tag{8.3}$$

$$\frac{\partial \tilde{\theta}}{\partial t} + \bar{u}\frac{\partial \tilde{\theta}}{\partial x} + \tilde{v}\frac{\partial \bar{\theta}}{\partial y} + \bar{v}\frac{\partial \tilde{\theta}}{\partial y} = \hat{\alpha}\,\nabla^2\,\tilde{\theta}\ .$$

Since the scope of the present investigation is confined to three-dimensional disturbances, and in particular longitudinal vortices, the following representation of the perturbations are postulated.

$$\tilde{u} = u_p(y)e^{\beta x}\mathrm{Cos}\alpha z$$

$$\tilde{v} = v_p(y)e^{\beta x}\mathrm{Cos}\alpha z$$

$$\tilde{w} = w_p(y)e^{\beta x}\mathrm{Sin}\alpha z \tag{8.4}$$

$$\tilde{p} = p_p(y)e^{\beta x}\mathrm{Cos}\alpha z$$

$$\tilde{\theta} = T_p(y)e^{\beta x}\mathrm{Cos}\alpha z$$

Equations (8.4) assume a spacewise growth of disturbances because physically a representation of this nature is more accurate than time varying disturbances. In experiments, the vortices appear at some distance from the leading edge of the plate and amplify with increasing distance downstream. At any given x the vortices appear stationary, with lateral wavenumber α .

Substitution of equations (4) into the set (3) results in

$$- u_p \frac{d\bar{v}}{dy} + \bar{u}\, u_p \beta + \bar{v}\, u_p' + v_p \frac{d\bar{u}}{dy} = - \frac{1}{\rho} \beta\, p_p$$

$$+ g\, \hat{\beta}\, T_p \operatorname{Cos}\phi + \nu[u_p'' - (\alpha^2 - \beta^2) u_p]$$

$$\bar{u}\, v_p \beta + \bar{v}\, v_p' + v_p \frac{d\bar{v}}{dy} = g\, \hat{\beta}\, T_p \operatorname{Sin}\phi - \frac{1}{\rho} p_p'$$

$$+ \nu[v_p'' - (\alpha^2 - \beta^2) v_p]$$

$$\bar{u}\, \beta\, w_p + \bar{v}\, w_p' = \alpha \frac{p_p}{\rho} + \nu[w_p'' - (\alpha^2 - \beta^2) w_p]$$

$$\beta u_p + v_p' + \alpha w_p = 0$$

$$\bar{u}\, \beta\, T_p + v_p \frac{\partial\bar{\theta}}{\partial y} + \bar{v}\, T_p' = \hat{\alpha}[T_p'' - (\alpha^2 - \beta^2) T_p] \ .$$

The temperatures and velocities are now generalized and made dimensionless in the manner usually employed in boundary layer and stability theory. In accordance with Gebhart (1969), the following scaling lengths and velocities are defined:

Grashof number $Gr_x = \dfrac{g\, \hat{\beta}\, x^3\, \Delta T}{\nu^2}$

$$\Delta T = T_w - T_\infty$$

$$G = 4\left(\frac{Gr_x}{4}\right)^{1/4}$$

$$\eta = \frac{y}{x}\left(\frac{Gr_x}{4}\right)^{1/4}$$

$$\delta = \sqrt{2}\, x/(Gr_x)^{1/4}$$

$$V^* = \frac{2\nu}{x}(Gr_x)^{1/2}$$

$$B = \beta\delta$$

$$A = \alpha\delta$$

$$C_p = \frac{p_p}{\rho U^{*2}} \quad .$$

Temperatures are scaled with ΔT .

The following system of differential equations results

$$\frac{d^2u}{d\eta^2} - GV\frac{du}{d\eta} + [B^2 - A^2 - G(BU - \frac{dV}{d\eta})]u - G\frac{dU}{d\eta} v$$

$$= GBC_p - T \,\mathrm{Cos}\phi$$

$$\frac{d^2v}{d\eta^2} - GV\frac{dv}{d\eta} + [B^2 - A^2 - G(BU + \frac{dV}{d\eta})]\; v = G\frac{dC_p}{d\eta} - T \,\mathrm{Sin}\phi$$

$$\frac{d^2w}{d\eta^2} - GV\frac{dw}{d\eta} + [B^2 - A^2 - BGV]\; w = -\,GAC_p$$

$$Bu + Aw + v' = 0 \tag{8.5}$$

and finally

$$\frac{d^2T}{d\eta^2} - Pr\; GV\frac{dT}{d\eta} + [B^2 - A^2 - Pr\; BGU]T = Pr\; G\; v\; \frac{dT_o}{d\eta}$$

Here $Pr = \frac{\nu}{\hat{\alpha}}$ is the Prandtl number, U, V and T_o refer to the dimensionless base flow quantities. The boundary conditions for the perturbations are:

$$\eta = 0\;, \quad u = v = w = T = \frac{dv}{d\eta} = 0$$

$$\eta \to \infty\;, \; u,\; v,\; w,\; T \to 0\;.$$

The equations are homogeneous and linear with homogeneous boundary conditions with their coefficients containing the parameters A, B, G, and ϕ. They therefore constitute an eigenvalue problem. The information sought in solving the system (5) is the variation of G with the remaining three parameters A, B, and ϕ.

The linearized theory presented here, requires an analytical representation of the mean flow (also referred to as the "base flow") components. In this analysis, the similarity solutions of Ostrach (1953) for the natural convection flow along a vertical heated plate were approximated by high order polynominals. Seventh degree polynominals were used to represent the base flow profiles for Pr = 0.72 while thirteenth degree polynominals were employed for Pr = 10.0. Figures (29a to 29c) provide some illustration of the accuracy of representation of the mean profiles by the polynominals. Calculations were made for Prandtl numbers of 0.72 and 10.0 at five different plate inclination angles.

A refinement in the analysis would be utilization of the base flow profiles obtained for inclined plates from perturbation solutions such as those of Kierkus (1968). The presentation followed herein is equivalent to using the boundary layer ("similarity") solutions for the base flow profiles. This approximation is expected to be adequate however, since Kierkus' results indicate that the profile shapes of the mean flow components are not strongly affected by inclination angle, at least up to 45° for which angle his results are presented. Furthermore, the shape of the temperature profile is almost completely independent of inclination angle. What does change with inclination angle however, is the destabilizing component of the body force at right angles to the plate. This change far outweighs the effect of minor variations in the profile shapes.

8.2 Method of Solution

At this stage, several choices for solving the system of equations (5) are available. Approximate analytic techniques such as the Galerkin Method (described in Kantorovich and Krylov (1958)) could be employed. However, due to the complexity and number of dependent variables in the equations, Galerkin's procedure would involve an excessive amount of algebra resulting from the several analytical integrations required. The problems encountered by other researchers in using Galerkin's method to obtain accurate solutions has been pointed out in earlier chapters of this thesis. In the present problem, all mean flow quantities except the velocity component perpendicular to the wall are zero in the region outside the boundary layer. The differential equations in the free stream therefore simplify to the constant coefficient type, which are readily solved in terms of elementary functions. This permits application of the method detailed in Chapter 4, Section 3. The method of solution then, is to integrate the equations numerically from the edge of the boundary layer to the wall, using the exponentially decaying far field solutions to provide initial conditions at the boundary layer edge (taken as $\eta = 6$ for $Pr = 0.72$ and $\eta = 8$ for $Pr = 10.0$). The far field solutions are derived in Appendix C. The method just described results in a considerable saving in computer time without any sacrifice of accuracy.

Results were obtained for inclination angles from the vertical of 15, 30, 45, 60 and 75° at Prandtl numbers of 0.72 and 10.0. In addition, amplification curves were computed for a fixed angle of inclination of 45° for different values of the amplification parameter B G .

8.3 Results and Discussion

The results obtained are presented in figs. (30) to (36). Figures (30) and (31) are the neutral amplification curves for the Prandtl numbers 0.72 and 10 respectively. Both figures have been plotted, using for the abscissca the quantity G , which Nachstein (1963) interprets as a characteristic Reynolds number of the flow. As expected, the flow is increasingly susceptible to the vortex instability at the higher inclination angles. It is interesting that the critical dimensionless wavenumbers appear unaffected by inclination angle, in agreement with the experiments of Sparrow and Husar (1969). At the higher Prandtl number, the critical wavenumber is increased to about 1.15 which is a factor of two over its value at the lower Prandtl number of 0.72. The value of G is consistently lower at the higher Prandtl number as would be expected, since increasing Prandtl numbers result in steeper mean temperature gradients.

A comparison of the neutral amplification curve from the present theory for $\phi = 45°$, and the corresponding curves for the two dimensional wave instability on a vertical heated plate calculated by Nachsteim (1963) have been drawn in fig. (32). The two curves from Nachsteim's work are the result of two different stability calculations, with and without velocity-temperature coupling effects. When temperature fluctuations are taken into consideration, the critical values of G and the wavenumber is sharply reduced. However, both neutral amplification curves of the wave instability have critical G values above that of the vortex instability.

Using Nachsteim's (1963) results for the wave disturbances, a curve has been constructed of critical Rayleigh number (calculated from $Ra = 4\ Pr([\frac{G}{4}]^4)$ versus inclination angle ϕ. His results were extrapolated to non zero inclination angles by dividing his calculated critical Rayleigh number by the cosine of the inclination angle. For angles up to about 30° this is probably a good approximation since intuitively, one would expect a higher value of the critical Rayleigh number for two dimensional instability due to a reduction in the streamwise body force component. This of course ignores the effect of the normal body force component on the stability of the flow.

The curve obtained is shown in fig. (33) together with similar curves of the critical Rayleigh number for the vortex mode of instability. Nachsteim's results were evaluated for a Prandtl number of 0.733. The intersection point of his curve with the $Pr = 0.72$ curve of the present calculation should mark the inclination angle at which transition between the wave and vortex modes of instability occurs. The value of 19.5° obtained agrees fairly well with the experimental values of 14° to 17° reported by Lloyd and Sparrow (1970).

Figure (33) also contains the experimental results of Lloyd and Sparrow (1970) together with some data of other researchers in the field. The data of Lock, Gort and Pond (1967) as well as that of Tritton (1963) and Kierkus (1968) plotted in comparison contain a large amount of uncertainty as pointed out by Lloyd and Sparrow. For this reason, although their data are in closer agreement with the present calculations than the experiments of Lloyd and Sparrow the agreement must be considered fortuitous. By far the most reliable data at the present time is Lloyd and Sparrow's and even they obtained standard deviations of 50% in their measurements. The difference between their experimental and the theoretically predicted values is about two orders of magnitude.

Some of the possible reasons for the discrepancy are:

(i) The inability of linear theory to predict eventual finite disturbance growth as opposed to initial instability. By the time the vortices are visible, the fluctuations may have amplified a thousand times. Since we have considered perturbations that grow in the streamwise direction and the value of the Rayleigh number has a third power dependence on x, the actual point of first instability corresponds to a much lower value of the Rayleigh number.

(ii) The experimental value of the Rayleigh number is very sensitive to errors made in measuring x. The experiments of Lloyd and Sparrow seem to be consistent and reliable; therefore most of the discrepancy is probably due to (i).

(iii) The use here of the natural convection boundary layer solutions for a vertical plate as input to the calculation rather than the solutions for an inclined plate.

The amplification curves for the case $Pr = 0.72$ and $\phi = 45°$ are drawn in fig. (34). A cross plot of the amplification versus wavenumber for given values of G was prepared and is displayed in fig. (35). Cross plots of this type, indicate the wavenumbers subject to maximum amplification, and therefore provide some indication of the spanwise vortex spacing most likely to be observed. In actual fact, the dominant wavenumber will more likely be influenced by non linear effects.

Unfortunately, sufficient data on experimentally observed wavenumbers is unavailable at this time to permit a comparison between theory and experiment.

Figure (36) is a sample of the eigenfunctions obtained, arbitrarily normalised to unity. They indicate that the fluctuations do not penetrate beyond the base flow region for that particular case, and are more or less confined to the boundary layer.

8.4 Conclusions

A linearized stability analysis of the natural convection flow along inclined plates has been performed, considering three dimensional spatially growing disturbances.

The results are in qualitative agreement with experiment. Quantitative discrepancies may be attributed to the limitations of linear theory in predicting transition, and the uncertainties involved in experimentally determining the first point of instability.

Chapter 9

SUMMARY AND CONCLUSIONS

9.1 Summary

This report presents some results of a theoretical investigation into the stability of Parallel, Quasi-Parallel and Stationary Flows. The analyses were confined to three dimensional disturbances that evolve either with distance or with time, as a result of the action of unstable body forces. The body forces considered herein were due to thermal stratification and centrifugal action. Similar analyses may be performed when the body forces are due to say Coriolis or magnetic effects.

Linearized Perturbation Theory was used to obtain the stability equations for the following flows:

(i) Parallel as well as Quasi-Parallel flows along Curved Heated Walls;

(ii) Stationary (Stagnant) Layers of Fluid with arbitrary temperature stratification;

(iii) Natural Convection along Inclined Plates.

The resulting system of coupled ordinary differential equations was solved mainly numerically using two different computing schemes. For a particular case, approximate analytical methods were also used. The computer program developed, was able to handle the wide variety of flows examined. The results obtained were that:

(a) For Quasi Parallel Flows along Curved, Unheated Walls the critical curve of Goertler number versus Wavenumber did not display a minimum but extrapolated to a critical Goertler number of zero at a finite value of Wavenumber. At higher wall temperatures, or at finite amplification rates, the critical curve displayed a minimum.

(b) For stagnant layers of fluid with arbitrary temperature stratification, the onset of convective activity was influenced by the nonlinearity of the profile and imposition of the semi-infinite boundary condition which tends to reduce the critical limit.

(c) For Natural Convection Flow along an Inclined Plate, the vortex instability becomes the dominant mode at angles of inclination from the vertical, greater than about 20°. At lower angles of inclination, the two dimensional wave-type oscillation dominates the transition process.

9.2 Conclusions

The results of the analyses presented herein provide lower bounds on the stability of the various flows to infinitesimal disturbances. This has been confirmed by experiment in most cases, where linear theory has been found to consistently underestimate experimental results. In the light of this experience, the theoretical results obtained are in as good agreement with experimental data (where available) as may be expected. The computer programs developed during this study have been successful in solving the large number of "stiff" differential equations describing the stability of the various flows investigated. A further step in the analysis, would be the incorporation of variable property effects which should provide results approaching the limit possible with linearized perturbation theory. Beyond this lies the domain of nonlinear analyses and numerical simulation, -- an expensive and time-consuming process.

REFERENCES

Avsec, D. (1939). "Thermoconvective Eddies in Air; Application to Meteorology." Scientific and Technical Publications of the Air Ministry (France) No. 155.

Bernard, H. (1900). "Tourbillions Cellulaires dan un Nappe Liquide." Revue Generale des Sciences Pures et Appliques, Vol. 11, p. 1261-1271 and 1309 - 1328.

Berg, T. C., Bourdart, M., and Acrivos, A. (1966). "Natural Convection in Pools of Evaporating Liquids." Jour. of Fluid Mech., Vol. 24, Part 4.

Bradshaw, P. (1969). "The Analogy between Streamline Curvature and Buoyancy in Turbulent Shear Flow." Jour. of Fluid Mech., Vol. 36, Part 1, p. 177.

Bussmann, K. and H. Munz (1942). "Die Stabilität der Laminaren Reibungsschicht mit Absaugung." Jb. dt. Luftfahrtforschung I, p. 36-39.

Chandra, K. (1938). "Instability of Fluids Heated from Below." Proc. of Roy. Soc. of London Ser. A., Vol. 164, p. 231 - 242.

Chandrasekhar, S. (1961). "Hydrodynamic and Hydromagnetic Stability." Oxford University Press.

Chang, T. S. and Sartory, W. K. (1968). "Hydromagnetic Goertler Instability in a Boundary Layer on a Concave Wall." Developments in Theoretical and Applied Mechanics, Vol. 4 Ed. by Daniel Frederick, Published by Pergammon Press.

Chen, C. F. and Kirchner, R. P. (1971). "Stability of Time Dependent Rotational Couette Flow, Part II Stability Analysis." Jour. of Fluid Mech., Vol. 48, Part 2, July 1971, p. 365.

Chen, T. S. and Huang, L. M. (1972). "Hydrodynamic Stability of Boundary Layers with Surface Suction." AIAA Journal, Vol. 10, No. 10, p. 1366, October 1972.

Clauser, F. H. and M. U. Clauser (1937). "The Effect of Curvature on the Transition from Laminar to Turbulent Boundary Layer." NACA Tech. Note 613.

Coles, D. (1965). "Transition in Circular Couette Flow." Jour. of Fluid Mech., Vol. 21, p. 385.

Currie, I. G. (1957). "The Effect of Heating Rate on the Stability of Stationary Fluids." Jour. of Fluid Mech., Vol. 29, p. 337-347.

Di Prima, R. C. and D. W. Dunn (1956). "The Effect of Heating and Cooling on the Stability of the Boundary-Layer Flow of a Liquid over a Curved Surface." Jour. of the Aeronautical Sciences, Vol. 23, No. 10, p. 913, October 1956.

Donnelly, R. J. and Schwartz, K. W. (1965). "Experiments on the Stability of Viscous Flow between Rotating Cylinders." Proc. of Roy. Soc. Ser. A., Vol. 283, p. 531.

Faller, A. J. (1965). "Large Eddies in the Atmospheric Boundary Layer and Their Possible Role in the Formation of Cloud Rows." Jour. of Atm. Science, Vol. 22, p. 176-184.

Faller, A. J. (1969). "The Generation of Longitudinal Vortices in Rotating, Stratified and Turbulent Boundary Layer Flows." Paper presented at the conference on Boundary Layer Concepts in Fluid Mechanics, held at the University of Massachusetts, School of Engineering, Amherst, Massachusetts, July 30-31, 1969.

Faller, A. J. and Kaylor, R. E. (1966). "A Numerical Study of the Instability of the Laminar Ekman Boundary Layer." Jour. of Atm. Science, Vol. 23, p. 466.

Fox, L. (1960). "Some Numerical Experiments with Eigenvalue Problems in Ordinary Differential Equations." Boundary Problems in Differential Equations, University of Wisconsin Press, Madison, Wisconsin, p. 243.

Gage, K. and W. H. Reid (1968). "The Stability of Thermally Stratified Plane Poiseuille Flow." Jour. of Fluid Mech., Vol. 33, Part 1, p. 21.

Gebhart, B. (1969). "Natural Convection Flow, Instability and Transition." Transaction of ASME, Jour. of Heat Transfer, Vol. 91, Series C, No. 3, p. 293.

Glauert, M. B. (1956). "The Wall Jet." Jour. of Fluid Mech., Vol. 1, Part 6, p. 625.

Goertler, H. (1940). "Uber eine dreidimensionale Instabilität Laminarer Grenzschichten an Konkaven Wanden." Nachr. Akad. Wiss., Goettingen Math-Physik Kl. IIa, Math-Physik-Chem. Abt. 2, 1-26 (Translated "On the Three-Dimensional Instability of Laminar Boundary Layers on Concave Walls: NACA Tech. Memo. 1375, June 1954).

Goertler, H. (1959). "Uber eine Analogie Zwischen den Instabilitaten Laminarer Grenzschichtstromungen an Konkaven Wanden und an Erwarmten Wanden." Ingenieur-Archiv, Vol. 28.

Goldstein, A. W. (1959). "Stability of a Horizontal Fluid Layer with Unsteady Heating from Below and Time Dependent Body Forces." NASA Tech. Report No. R-4.

Graham, A. (1933). "Shear Patterns in an Unstable Layer of Air." Phil. Trans. of Roy. Soc. of London Ser. A., Vol. 232, p. 285-296.

Gribov, V. N. and Gurevich, L. E. (1957). "On the Theory of the Stability of a Layer Located at a Superadiabatic Temperature Gradient in a Gravitational Field." Sov. Phys. JETP, Vol. 4, p. 720-729.

Hammerlin, G. (1955). "Uber das Eigenwertproblem der driedimensionalen Instabilitat Laminarer Grenzschichten an Konkaven Wanden." Jour. of Rational Mechanics and Analysis, Vol. 4, p. 279-321.

Hammerlin, G. (1961). "Uber die Stabilität einer Kompressiblen Stromumg langs einer Konkaven Wand bei Verschiedenen Wandtemperatureverhaltnissen." Bericht der Deutschen Versuchsanstalt für Luftfart E. V. Nr. 176, 1961.

Heikes, K. E. (1971). "Steady Convection in Stratified Fluid." M. Sc. Thesis Dept. of Atmos. Science, Colorado State University.

Idrac, P. (1920). "On Convective Currents in the Atmosphere with Respect to Their Relation to Planing Flight and to Certain Cloud Formations." Comptes Rendus de l'Academie des Sciences, Paris t.171, p. 42.

Jeffreys, H. (1926). "The Stability of a Layer of Fluid Heated Below." Phil. Magazine, Vol. 2, p. 833.

Jeffreys, H. (1928). "Some Cases of Instability in Fluid Motion." Proc. of the Royal Soc. of London, Series A., Vol. 118, p. 195.

Kahawita, R. A. and R. N. Meroney (1972). "Penetrative Convective Instabilities in Parallel Flows." Fluid Dynamics and Diffusion Laboratory Themis Report No. 13, Colorado State University.

King, L. G. (1961). "The Generation of Orthogonal Functions." M. Sc. Dissertation, Dept. of Mathematics, Colorado State University.

Kirchner, R. P. and Chen, C. F. (1970). "Stability of Time Dependent Rotational Couette Flow, Part I Experimental Investigation." Jour. of Fluid Mech., Vol. 40, Part I, p. 39.

Krueger, A. and Fritz, S. (1961). "Cellular Cloud Patterns Revealed by TIROS I." Tellus, Vol. 13, p. 1-7.

Kuettner, J. (1959). "The Band Structure of the Atmosphere." Tellus, Vol. 11, No. 3, p. 267.

Kuo, H. L. (1963). "Perturbations of Plane Couette Flow in Stratified Fluid and Origin of Cloud Streets." Physics of Fluids, Vol. 6, No. 2, p. 195.

Lebovitz, N. R. (1965). "Convective Instability in Stars." in 'Non Equilibrium Thermodynamics, Variational Techniques and Stability' ed. by Donnelly, Herman and Prigogine, University of Chicago Press.

Lick, W. (1965). "The Stability of a Fluid Layer with Time-Dependent Heating." Jour. of Fluid Mech. Vol. 21, p. 565-576.

Liepmann, H. W. (1943). "Investigation of Laminar Boundary Layer Stability and Transition on Curved Boundaries." NACA Adv. Conference Report No. 31730.

Lilly, D. K. (1966). "On the Stability of Ekman Boundary Flow." Jour. of Atm. Sc., Vol. 23, p. 481.

Lindberg, W. (1970). "Theoretical Aspects of Thermohaline Convection." Ph.D. Thesis Mech. Eng. Department, Colorado State University, Fort Collins.

Lloyd, J. M. and Sparrow, E. M. (1970). "On the Instability of Natural Convection Flow on Inclined Plates." Jour. of Fluid Mech., Vol. 42, Part 3, p. 465.

Lloyd, J. R., E. M. Sparrow and E. R. G. Eckert (1972). "Laminar, Transition and Turbulent Natural Convection Adjacent to Inclined and Vertical Surfaces." Int. Jour. of Heat and Mass Transfer, Vol. 15, No. 3, March 1972, p. 457.

Lock, G. S. H., C. Gort and G. R. Pond (1967). "A Study of Instability in Free Convection from an Inclined Plate." Applied Science Res., Vol. 18, p. 171.

Low, A. R. (1929). "On the Criterion for Stability of a Layer of Viscous Fluid Heated from Below." Proc. of Roy. Soc. of London, Ser. A., Vol. 125, p. 180-195.

Lumley, J. L. and Panofsky, H. A. (1964). "The Structure of Atmospheric Turbulence." Published by Interscience.

McCormack, P. D., Welker, H. and Kelleher, M. (1969). "Taylor-Goertler Vortices and Their Effect on Heat Transfer." ASME-AIChE Heat Transfer Conference, Minneapolis, Minnesota. Paper No. 69-HT-3.

Meksyn, D. (1950). "Stability of Viscous Flow over Concave Cylindrical Surfaces." Proc. of Roy. Soc. of London, Vol. 203, Ser. A., p. 253.

Nachsteim, P. (1963). "Stability of Free-Convection Boundary-Layer Flows." NASA TN D-2809.

Ogura, Y., and Kondo, H. (1970). "The Linear Stability of Convective Motion in a Thermally Unstable Layer Below a Stable Region." Jour. of Meteor. Soc. of Japan, Vol. 48, p. 204-215.

Orgill, M. M., (1971). "Laboratory Simulation and Field Estimates of Transport-Dispersion in Mountainous Terrain." Ph.D. Thesis, Department of Civil Engineering, Fluid Mechanics, Colorado State University, Fort Collins, Colorado.

Ostrach, S. (1953). "An Analysis of Laminar Free-Convection Flow and Heat Transfer about a Flat Plate Parallel to the Direction of the Generating Body Force." NACA TN 2635.

Ostrach, S. (1957). "Convection Phenomena in Fluids Heated from Below." Trans. ASME, Jour. of Heat Transfer, Vol. 79, p. 299.

Pretsch, J. (1941). "Über die Stabilitat der Laminarströmung in einem geraden Rohr mit Kreisförmigem Querschnitt." Ziet. fur Ang. Math. und Mech. (ZAMM) Vol. 21, p. 204.

Rayleigh, (1916). "On Convection Currents in a Horizontal Layer of Fluid When the Higher Temperature is on the Underside." Philosophical Mag. and Jour. of Science, Vol. 32, No. 192, p. 529.

Rayleigh, Lord (1917). "On the Dynamics of Revolving Fluids." Proc. Roy. Soc. of London, Ser. A93, p. 148.

Rintel, L. (1967). "Penetrative Convective Instabilities." Physics of Fluids, Vol. 10, No. 4, p. 848.

Rintel, L. (1971). "Goertler Instability of Boundary Layers." Phys. of Fluids, Vol. 14, No. 4, p. 753.

Sandmayr, G. (1966). "Über das Auftreten von Laengswirkein in Turbulenten Grenzschichten an Konkaven Wanden." Deutsche Luft und Raumfahrt. June 1966 DLR FB-66-41. Also NASA TT F-14120, February 1972.

Schmidt, R. J. and Milverton, S. W. (1935). "On the Instability of a Fluid When Heated from Below." Proc. of Roy. Soc. (London). Ser. A., Vol. 152, p. 586.

Schmidt, R. J. and Saunders, O. A. (1938). "On the Motion of a Fluid Heated from Below." Proc. of Roy. Soc. (London), Vol. 165, p. 216-218.

Schwarzschild, K. (1906). Gottinger Nachrichten, Vol. 41.

Segal, L. A. (1965). "Non Linear Problems in Hydrodynamic Stability." in 'Non Equilibrium Thermodynamics Variational Techniques and Stability' ed. by Donnelly, Herman and Prigogine, University of Chicago Press.

Sexl, Th. and K. Spielberg (1958). "Zum Stabilitätsproblem der Poiseuille-Stromung." Acta Phys. Austriaca, Vol. 12, p. 9-28.

Silveston, P. L. (1958). "Warmedurchgang in Waagerechtan Flussegkeitsschickten." Part 1. Forsch. Ing. Wes. Vol. 24, p. 29-32 and 59-69.

Smith, A. M. O. (1955). "On the Growth of Taylor Goertler Vortices Along Highly Concave Walls." Quarterly of Appl. Math. Vol. 13, p. 223-262.

Snyder, H. and Lambert, R. (1965). "Harmonic Generation in Taylor Vortices Between Rotating Cylinders." Unpublished Report Brown University, Providence, R.I.

Sparrow, E. M., R. J. Goldstein and V. K. Johnson (1964). "Thermal Instability in a Horizontal Fluid Layer: Effect of Boundary Conditions and Nonlinear Temperature Profiles." Jour. of Fluid Mech., Vol. 18, Part 4, p. 513.

Sparrow, E. M. and Husar, R. B. (1969). "Longitudinal Vortices in Natural Convection Flow on Inclined Plates." Jour. of Fluid Mech., Vol. 37, Part 2, p. 251-255.

Taylor, G. I. (1923). "Stability of a Viscous Liquid Contained Between Two Rotating Cylinders." Phil. Trans. of Roy. Soc. of London, Ser. A223, p. 289-243.

Terada, et al. (1928). "Some Experiments on Periodic Columnar Forms of Vortices Caused by Convection." Tokyo Imperial University Research Report No. 31, January 1928.

Terada and Tamano (1929). "Further Researches on Periodic Columnar Vortices Produced by Convection." Tokyo Imperial University Aeronautical Research Report No. 53, December 1929.

Tritton, D. J. (1963). "Transition to Turbulence in the Free Convection Boundary Layers on an Inclined Heated Plate." J.F.M. Vol. 16, p. 417.

Wazzan, A. R., T. Okamura and A. M. O. Smith (1966). "Spatial Stability Study of Some Falkner-Skan Similarity Profiles." Proc. of Fifth U.S. National Congress of Appl. Mech., p. 836, A.S.M.E., University of Minnesota.

Whitehead, J. A., (1971). "Cellular Convection." American Scientist, Vol. 59, p. 444.

Witting, H. (1958). "Über den Einfluss der Strönlinienkrümmung auf die Stabilität Laminarer Strömungen." Arch. Ratl. Mech. and Anal., Vol. 2, p. 243-283.

Yamada, T. and R. N. Meroney (1971). "Numerical and Wind Tunnel Simulation of Response of Stratified Shear Layers to Nonhomogeneous Surface Features." ERC Fluid Mechanics Project Themis Technical Report No. 9, Colorado State University, Fort Collins, Colorado.

Appendix A

DERIVATION OF THE EQUATIONS DESCRIBING THE ONSET OF CONVECTIVE OVERTURNING IN STATIONARY LAYERS OF FLUID

The Navier Stokes Equations in vector form for an incompressible, constant property fluid with the Boussinesq approximation are:

$$\frac{\partial \utilde{V}}{\partial t} + \utilde{V}\cdot\nabla\, \utilde{V} = o\, \frac{1}{\rho}\, \nabla p + \utilde{\lambda j}\; g\gamma\; (T - T_{\infty}) + \nu\nabla^{2}\utilde{V} \tag{A.1}$$

$$\nabla\cdot\utilde{V} = 0 \tag{A.2}$$

and the energy equation is

$$\frac{\partial T}{\partial t} + \utilde{V}\cdot\nabla T = \frac{\nu}{Pr}\; \nabla^{2}T \tag{A.3}$$

where $\utilde{V}$ is the velocity vector with components u, v, w in the x, y, and z directions respectively. Here the y direction is taken as coincident with the direction of gravity;

$\utilde{\lambda j}$ is the unit vector in the vertical direction;

ν, ρ and γ are the kinematic viscosity, density and temperature expansion coefficient respectively;

k is the thermal diffusivity;

$Pr(= \frac{\nu}{k})$ is the Prandtl number;

∇ is the standard del operator.

Using the standard perturbation method, the velocity, pressure and temperature are represented by a mean and a fluctuating component. Thus we write

$$\begin{aligned} \utilde{V} &= \utilde{\overline{V}} + \utilde{\tilde{v}} \\ p &= \overline{p} + \tilde{p} \\ T &= \overline{T} + \tilde{T}\ . \end{aligned} \tag{A.4}$$

Since the base flow is truly stationary, we have

$$\underset{\sim}{\overline{V}} = 0 \ , \quad \overline{T} = \overline{T}(y) \ .$$

The perturbations are assumed two dimensional for representation of columnar convection. Substituting the set (A.4) into equations (A.1) to (A.3) and neglecting all terms higher than first order in the perturbations there results the following system in component form:

$$\frac{\partial \tilde{v}}{\partial t} = g\gamma\tilde{T} - \frac{1}{\rho}\frac{\partial \tilde{p}}{\partial y} + \nu\left\{\frac{\partial^2 \tilde{v}}{\partial y^2} + \frac{\partial^2 \tilde{v}}{\partial z^2}\right\}$$

$$\frac{\partial \tilde{w}}{\partial t} = -\frac{1}{\rho}\frac{\partial \tilde{p}}{\partial z} + \nu\left\{\frac{\partial^2 \tilde{w}}{\partial y^2} + \frac{\partial^2 \tilde{w}}{\partial z^2}\right\}$$

$$\frac{\partial \tilde{v}}{\partial y} + \frac{\partial \tilde{w}}{\partial z} = 0 \qquad \text{(A.5)}$$

$$\frac{\partial \tilde{T}}{\partial t} + \tilde{v}\frac{d\overline{T}}{dy} = \frac{\nu}{P_r}\left\{\frac{\partial^2 \tilde{T}}{\partial y^2} + \frac{\partial^2 \tilde{T}}{\partial z^2}\right\} \ .$$

An arbitrary two dimensional disturbance may be represented as

$$\begin{aligned} \tilde{v} &= v_p(y)\ \mathrm{Cos}\alpha z\ e^{\beta t} \\ \tilde{w} &= w_p(y)\ \mathrm{Sin}\alpha z\ e^{\beta t} \\ \tilde{p} &= p_p(y)\ \mathrm{Cos}\alpha z\ e^{\beta t} \\ \tilde{T} &= T_p(y)\ \mathrm{Cos}\alpha z\ e^{\beta t} \end{aligned} \qquad \text{(A.6)}$$

where β is the amplification rate of the disturbance and α is a horizontal wavenumber.

Substitution of the set (A.6) into the equations (A.5) results in

$$-\ g\theta\ T_p = -\frac{p_p'}{\rho} + \nu\left\{v_p'' - \left(\alpha^2 + \frac{\beta}{\nu}\right) v_p\right\}$$

$$0 = \alpha \frac{p_p}{\rho} + \nu\{ w_p'' - (\alpha^2 + \frac{\beta}{\nu}) w_p \}$$

$$v_p' + \alpha w_p = 0 \qquad \text{(A.7)}$$

$$v_p \frac{d\overline{T}}{dy} = \frac{\nu}{P_r} \{ T_p'' - (\alpha^2 + \frac{\beta}{\nu}) T_p \} .$$

The equations (A.7) are now made dimensionless using the following scaling lengths, velocities and temperature.

δ - scaling length, characteristic thickness of layer;

$U_m = \frac{\nu}{\delta}$ - characteristic velocity;

ΔT - temperature difference between lower boundary T_w and free stream T_∞ .

Use of these scaling quantities results in

$$\begin{aligned} v'' - (\phi^2 + \sigma)v &= C_p' - G_r T \\ w'' - (\phi^2 + \sigma)w &= - \phi C_p \\ v' + \phi w &= 0 \\ T'' - (\phi^2 + \sigma)T &= P_r v \frac{dT_1}{d\eta} \end{aligned} \qquad \text{(A.8)}$$

which are equations (A.7) in dimensionless form. Here primes denote differentiation with respect to η the independent vertical coordinate $(= \frac{y}{\delta})$

$C_p = \frac{p_p}{\rho U_m^2}$ - dimensionless pressure;

T_1 = basic dimensionless temperature profile;

$\phi = \alpha\delta$

$\sigma = \frac{\beta\delta^2}{\nu}$.

These equations are presented as equations (3.7) in Chapter 3.

Note:

The derivation outlined here is equivalent to the conventional analysis that assumes a disturbance of the form

$$\tilde{v} = v_p(y)\ \mathrm{Exp}\ \{i(k_x x + k_z z) + \beta t\} \quad \text{etc.}$$

where k_x and k_z are the longitudinal and transverse wavenumbers. The alternative analysis equates $k_x{}^2 + k_z{}^2$ to a 'horizontal' wavenumber ϕ^2. Reduction of equations (A.8) to a single sixth order equation results in

$$v^{VI} - (3\phi^2 + 2\sigma)v^{IV} + (\phi^2 + \sigma)(3\phi^2 + \sigma)v'' - \phi^2(\phi^2 + \sigma)^2 v$$
$$= Ra\ \phi^2\ v\ \frac{dT_1}{d\eta}$$

which is the same result obtained with the alternative analysis where $Ra = Pr\ Gr$ is the Rayleigh number.

Appendix B

DERIVATION OF THE OUTER SOLUTIONS FOR THE CASE OF GOERTLER INSTABILITY IN A HEATED BOUNDARY LAYER ON A CURVED WALL

[Note: Some of the temporary symbols used here may be identical to those used in other sections of this thesis. They are however completely unrelated and should not be confused.]

Let η_m be the boundary layer edge which is used as the matching point between the 'outer' and 'inner' numerical solutions.

In the outer flow we have $V_o = V_\infty$ = constant.

$$U_o = U_\infty = \text{constant and } \frac{dV_o}{d\eta} = \frac{dU_o}{d\eta} = 0 .$$

We may also assume terms like $K\eta$ small at the matching point (since K is of the order of 10^{-5}) and treat them as constants. Then equations (3.6) may then be written as

$$u'' - \alpha u' + \gamma u - \theta v = \beta\, C_p \tag{B1.1}$$

$$v'' - \alpha v' + \gamma v - \theta_1 u = \frac{1}{2}\, C_p' - \mathrm{Gr}\, T \tag{B1.2}$$

$$w'' - \alpha w' + \gamma w = -\frac{A}{2}\, C_p \tag{B1.3}$$

$$2\beta u + v' + Kv + Aw = 0 \tag{B1.4}$$

$$T'' - \alpha_1\, T' + \gamma_1\, T = 0 \tag{B1.5}$$

in the free stream where

$$\alpha = V_\infty R_d + K$$

$$\gamma = B^2 - A^2 - B\, R_d\, U_\infty + \eta_m\, KB(2B - U_\infty R_d)$$

$$\theta = K(2B - U_\infty\, R_d)$$

$$\theta_1 = 2K(R_d U_\infty - B)$$

$$\beta = \frac{B}{2}(1 + K\eta_m)$$

$$\alpha_1 = V_\infty P_r R_d + K$$

$$\gamma_1 = B^2 - A^2 - B R_d P_r U_\infty + \eta_m KB(2B - U_\infty P_r R_d).$$

In general the terms A^2 and $B R_d U_\infty$ dominate γ and γ_1 so that they are always negative. Equation (B1.5) may be solved for the temperature fluctuation in the free stream since it is completely uncoupled.

The solution may be written as

$T = A_1 e^{t\eta}$ where the decaying solution

$t = \frac{1}{2}(\alpha_1 - \sqrt{\alpha_1^2 - 4\gamma_1})$ is chosen.

A_1 is an arbitrary constant of integration.

From (B1.2) and (B1.3), C_p may be eliminated giving

$$\begin{aligned} v'''' - (\alpha + K) v''' + (\alpha K + \gamma - A^2) v'' + (\alpha A^2 - \gamma K) v' \\ - \gamma A^2 v = A^2 Gr\, T - 2\beta(u''' - \alpha u'' + \gamma u') \\ - \theta_1 A^2 u \end{aligned} \tag{B1.6}$$

where (B1.4) has been used to eliminate w. From equations (B1.1) and (B1.3) C_p may be again eliminated.

There

$$\begin{aligned} (u'' - \alpha u' + \gamma u)(4\beta^2 - A^2) = -A^2\theta v - 2\beta(v''' - (\alpha+K)v'' \\ + (\alpha K+\gamma)v' - \gamma K v) \quad . \end{aligned} \tag{B1.7}$$

Differentiating (B1.7) and substituting for $u''' - \alpha u'' + \gamma u'$ into (B1.6) we obtain

$$u = \frac{Gr}{\theta_1} T - D_1 v'''' + D_2 v''' - D_3 v'' - D_4 v' + \frac{\gamma}{\theta_1} v \tag{B2}$$

where

$$D_1 = \frac{1}{\theta_1(A^2 - 4\beta^2)}$$

$$D_2 = \frac{\alpha + K}{\theta_1(A^2 - r\beta^2)}$$

$$D_3 = [\frac{\alpha K + \gamma}{A^2 - 4\beta^2} - 1]/\theta_1$$

$$D_4 = [\alpha + \frac{(2\beta\theta - \gamma K)}{(A^2 - 4\beta^2)}]/\theta_1 .$$

Use of equation (B2) in equation (B1.7) results in the following sixth order equation for v

$$C_7\, v^{VI} + C_6\, v^{V} + C_5\, v'''' + C_4\, v''' + C_3\, v''$$

$$+ C_2\, v' + C_1\, v = (A^2 - 4\beta^2)\, \frac{Gr}{\theta_1}\, (T'' - \alpha T' + \gamma T)$$

$$= (A^2 - 4\beta^2)\, \frac{Gr}{\theta_1}\, A_1(t^2 - \alpha t + \gamma)\, e^{t\eta}$$

$$= D_5\, e^{t\eta} \tag{B3}$$

where

$$D_5 = (A^2 - 4\beta^2)\, \frac{Gr}{\theta_1}\, A_1(t^2 - \alpha t + \gamma)$$

The particular solution is

$v = X\, e^{t\eta}$ where

$$X = \frac{D_5}{(C_7 t + C_6 t + C_5 t + C_4 t + C_3 t + C_2 t + C_1)}$$

The coefficients of the sixth order equation are given by

$$C_1 = -\ (A^2 - 4\beta^2)\ \frac{\gamma^2}{\theta_1} - (2\beta\gamma K - A^2\theta)$$

$$C_2 = (A^2 - 4\beta^2)(\ \frac{\alpha\gamma}{\theta_1} + \gamma\ D_4) + 2\beta(\alpha K + \beta)$$

$$C_3 = (A^2 - 4\beta^2)\ \frac{\gamma^2}{\theta_1} - (2\beta\gamma K - A^2\theta)$$

$$C_4 = (A^2 - 4\beta^2)(D_4 - \alpha D_3 - \gamma D_2) + 2\beta$$

$$C_5 = (A^2 - 4\beta^2)(D_3 + \alpha D_2 + \gamma D_1)$$

$$C_6 = -\ (A^2 - 4\beta^2)(D_2 + \alpha D_1)$$

$$C_7 = D_1(A^2 - 4\beta^2)\ .$$

The roots of (B3) were examined for a variety of values of A , K and B. In practice only three roots with negative real parts are obtained. The other roots do not of course satisfy the boundary conditions and are therefore rejected on that basis.

The useable roots may be real or complex. Let the roots be designated as S_1 , S_2 and S_3 . Then

$$v = A_2\ e^{S_1\eta} + A_3\ e^{S_2\eta} + A_4 e^{S_3\eta} + X\ e^{t\eta}$$

or

$$v = A_2\ e^{S_1\eta} + A_3 e^{S_2\eta}\ \mathrm{Sin}\ S_3\eta + A_4 e^{S_2\eta}\ \mathrm{Cos}\ S_3\eta$$
$$+ X\ e^{t\eta} \quad \text{for complex conjugates.}$$

Once v is established, u, w, T, C_p are known in principle although the algebra required to obtain them is tedious. We now generate four linearly independent vectors of

u - y_1

u' - y_2

v - y_3

v' - y_4

w - y_5

w' - y_6

C_p - y_7

T - y_8

T' - y_9

by setting the arbitrary constants A_1 , A_2 , A_3 , and A_4 to unity in turn, with the others zero, i.e.

$$A_1 = 1, \quad A_2 = A_3 = A_4 = 0$$
$$A_2 = 1, \quad A_1 = A_3 = A_4 = 0$$
$$A_3 = 1, \quad A_1 = A_2 = A_4 = 0$$
$$A_4 = 1, \quad A_1 = A_2 = A_3 = 0 .$$

Because of the way in which we obtained the four vectors $\underset{\sim}{y}^{(1)}$, $\underset{\sim}{y}^{(2)}$, $\underset{\sim}{y}^{(3)}$ and $\underset{\sim}{y}^{(4)}$ there is no question about their independence. η is set equal to η_m to obtain the numerical starting values at the edge of the boundary layer. The four vectors are then integrated numerically to the wall from the boundary layer edge. At the wall we must have the conditions

$$\begin{aligned}
\beta_1 y_1^{(1)} + \beta_2 y_1^{(2)} + \beta_3 y_1^{(3)} + \beta_4 y_1^{(4)} &= 0 \\
\beta_1 y_3^{(1)} + \beta_2 y_3^{(2)} + \beta_3 y_3^{(3)} + \beta_4 y_3^{(4)} &= 0 \\
\beta_1 y_4^{(1)} + \beta_2 y_4^{(2)} + \beta_3 y_4^{(3)} + \beta_4 y_4^{(4)} &= 0 \\
\beta_1 y_8^{(1)} + \beta_2 y_8^{(2)} + \beta_3 y_8^{(3)} + \beta_4 y_8^{(4)} &= 0
\end{aligned} \qquad \text{(B4)}$$

which expresses the fact that u, v, v' and T must be zero there. For a non trivial solution of the above homogeneous algebraic system of equations we must have that the determinant of the coefficients vanishes. This is only achieved when the correct eigenvalue is chosen. The problem reduces to that of finding the zero of the determinant. Once this is achieved, the system (B4) may be solved for the β's (one of them is of course arbitrary) and the solution reconstructed within the boundary layer. At the boundary layer edge, the coefficients A_1, A_2, A_3 and A_4 may be determined from the matching conditions which in this case is a question of only obtaining the correct scaling between the four vectors. The eigenfunctions are then completely determined throughout the entire flow field.

Appendix C

DERIVATION OF THE ANALYTIC SOLUTIONS VALID IN THE OUTER FLOW FOR NATURAL CONVECTION INSTABILITY ON INCLINED PLATES

The reasoning and method of attack is clearly similar to that used in Appendix B. Outside the boundary layer region, the component of mean velocity along the plate is zero and the component of mean velocity normal to the plate is a constant.

Hence equations reduce to

$$u'' - \alpha u' + \gamma u = BG\,C_p - T\cos\phi \tag{C1.1}$$

$$v'' - \alpha v' + \gamma v = G\,C_p' - T\sin\phi \tag{C1.2}$$

$$w'' - \alpha w' + \gamma w = -\,GA\,C_p \tag{C1.3}$$

(C1)

$$Bu + v' + Aw = 0 \tag{C1.4}$$

$$T'' - \beta T' + \gamma T = 0 \tag{C1.5}$$

where the symbols $\alpha = GV_\infty$, $\gamma = B^2 - A^2$ and $\beta = P_r\,G\,V_\infty$ are temporarily used in this section to facilitate the algebra. From equation (C1.5) we have $T = A_1\,e^{\beta_1\eta}$ where A_1 is an arbitrary constant and

$$\beta_1 = \frac{1}{2}\,[\beta - \sqrt{\beta^2 - 4\gamma}\,]$$

β_1 will of course always be negative since interest is confined only to solutions decaying at infinity. C_p' is now eliminated by multiplying equation (C1.2) by A , differentiating equation (C1.3) and adding; the result is

$$Av'' + w''' - \alpha Av' - \alpha w'' + \gamma Av + \gamma w' = - TA \sin \phi \ .$$

Substituting for w from equation (C1.4) gives

$$v'''' - \alpha v''' + (\gamma - A^2)\ v'' + \alpha A^2 v' - \gamma A^2 v$$

$$= - B(u''' - \alpha u'' + \gamma u') + TA^2 \sin \phi$$

$$= - B(GB\ C_p' - T' \cos\phi) + TA^2 \sin \phi \qquad \text{from} \qquad (C1.1)$$

$$= - B(BT \sin\phi + B(v'' - \alpha v' + \gamma v) - T' \cos\phi) + TA^2 \sin \phi$$

from equation (C1.2)

$$= - \gamma T \sin \phi + BT' \cos \phi - B^2\ (v'' - \alpha v' + \gamma v).$$

Collecting terms and simplifying we have

$$v'''' - \alpha v''' + 2\gamma v'' - \alpha\gamma v' + \gamma^2 v \ \equiv [b\beta_1 \cos\phi - \gamma \sin\phi\ ]\ A_1 e^{\beta_1 \eta} .$$

If $S \equiv (B\beta_1 \cos\phi - \gamma \sin\phi)\ A_1$ then we may write

$$v'''' - \alpha v''' + 2\gamma v'' - \alpha\gamma v' + \gamma^2 v = S\ e^{\beta_1 \eta} \ .$$

The complementary function is

$$v = B_1\ e^{r_1 \eta} + B_2\ e^{r_2 \eta}$$

where r_1 , r_2 are the negative real roots of the auxiliary equation

$$\mu^4 - \alpha\mu^3 + 2\gamma\mu^2 - \alpha\gamma\mu + \gamma^2 = 0 \ .$$

The particular solution is

$$v = X\ e^{\beta_1 \eta}$$

where

$$X = \frac{S}{(\beta_1{}^4 - \alpha\beta_1{}^3 + 2\gamma\beta_1{}^2 - \alpha\gamma\beta_1 + \gamma^2)} \ .$$

The total solution for v may then be written as

$$v = B_1 e^{r_1\eta} + B_2 e^{r_2\eta} + X e^{\beta_1\eta} \tag{C2}$$

where B_1 and B_2 are arbitrary constants of integration. We now solve for u ; multiplying equations (C1.1) by A and (C1.3) by B and adding eliminates C_p ,

$$A(u'' - \alpha u' + \gamma u) + B(w'' - \alpha w' + \gamma w) = - TA \cos \phi \quad .$$

From equation (C1.4) w may be eliminated resulting in

$$u'' - \alpha u' + \gamma u + \frac{B}{\gamma} (v''' - \alpha v'' + \gamma v') = T \frac{A^2}{\gamma} \cos \phi \quad .$$

The expression in the brackets may be rewritten in terms of elementary functions using the expression (C2) for v . After rearrangement we obtain

$$u'' - \alpha u' + \gamma u = \frac{TA^2}{\gamma} \cos\phi - \frac{B}{\gamma} (D_1 e^{r_1\eta} + D_2 e^{r_2\eta} + D_3 e^{r_3\eta}) \tag{C3}$$

where

$$D_1 = B_1(r_1{}^3 - \alpha r_1{}^2 + \gamma r_1)$$

$$D_2 = B_2(r_2{}^3 - \alpha r_2{}^2 + \gamma r_2)$$

$$D_3 = X(\beta_1{}^3 - \alpha\beta_1{}^2 = \gamma\beta_1) \quad .$$

The complementary function may be written as $u = A_2 e^{\beta_2\eta}$ where A_2 is arbitrary and $\beta_2 = \frac{1}{2} (\alpha - \sqrt{\alpha^2 - 4\gamma})$ (β_2 is negative).

The particular solution is

$$u = Z_1 e^{\beta_1\eta} + Z_2 e^{r_1\eta} + Z_3 e^{r_2\eta}$$

with

$$Z_1 = [\frac{A^2}{\gamma} \cos\phi \cdot A_1 - \frac{B}{\gamma} D_3]/[\beta_1{}^2 - \alpha\beta_1 + \gamma]$$

$$Z_2 = \frac{BD_1}{\gamma(r_1^2 - \alpha r_1 + \gamma)}$$

$$Z_3 = \frac{BD_2}{\gamma(r_2^2 - \alpha r_2 + \gamma)} .$$

The solution for the total outer region contains the four arbitrary constants A_1 , A_2 , B_1 and B_2 . A set of four linearly independent vectors may therefore be constructed setting one of the arbitrary constants to unity and the rest to zero in turn.

The values of the dependent variables w and C_p may be solved for from equations (C1.4) and (C1.1) respectively. The procedure then follows exactly the method outlined in Appendix B.

Appendix D

SOME SIMPLE EXPERIMENTS ON THE STABILITY OF A LAMINAR BOUNDARY LAYER OVER A CURVED HEATED WALL

This Appendix describes some stability experiments performed in a small wind tunnel at the Engineering Research Center of Colorado State University. The principal object of the experiments was to obtain quantitative data on the onset of instability in laminar boundary layers along curved heated walls.

The dimensions of the working section of the tunnel are 24" width by 21" height by 15 foot length. The tunnel is powered by a half horsepower variable speed motor which provides a maximum air velocity of 10 ft/sec. in the working section. A schematic of the tunnel is shown in fig. (i). Design and construction details of the tunnel are covered in the report by Yamada and Meroney (1971). An aluminum plate was mounted on shaped wood forms that gave it a longitudinal radius of 30 ft, and installed in the wind tunnel. The leading edge of the plate was mounted flush with the tunnel floor at a distance of 4' 6" from the entrance honeycomb. All discontinuities were filled in and smoothed off with modelling clay. Ten heaters, each 6" long and 2 ft wide were glued to the back of the plate. A number of thermocouples (in most cases three) were embedded with each heater in order to provide information on the magnitude and uniformness of the surface temperature distribution. The heaters were specially constructed by Chromalox Ltd. and were claimed to provide uniform heating. The thermocouple readings during the course of the experiments confirmed this, maximum temperature variation throughout a particular heater being about 1/4° F. The heaters were individually adjustable so that the plate surface could be maintained at a uniform temperature. A sketch of the plate arrangement in the tunnel together with an overall view is presented in fig. (ii). A probe traversing mechanism was designed and constructed so that a probe could be traversed at right angles to the plate at four different axial locations. In order to estimate vortex spacing from smoke visualization techniques, the surface of the plate was marked with longitudinal lines spaced laterally 1" apart.

Experimental Procedure: The tunnel was run at a free stream speed of about 1.8 ft/sec, with the upstream entrance-contraction-diffuser section replaced with a simple bellmouth and honeycomb entrance at section DD, fig. (i). This speed was low enough to make certain that the boundary layer remained laminar. (Unfortunately, this speed was also too slow to cause instability under neutral conditions.) Flow visualization using incense smoke indicated that the boundary layer as well as free stream was essentially laminar. A hot wire traverse at the boundary layer indicated a maximum turbulence level of about 4% RMS. The roof of the tunnel was adjusted so that the streamwise pressure gradient was zero.

After the tunnel was turned on, the heaters were energized and their controls adjusted until a uniform temperature distribution on the plate was achieved. This typically took about 2 hours to realize. Incense smoke was then released at several locations upstream of the honeycomb, simply by inserting the incense sticks into the perforations of the honeycomb. The smoke thus released, formed into a series of counterrotating spiral vortices at a short distance downstream of the heated edge of the plate. Their vertical extent was typically 3" with a lateral spacing of about 2". Some photographs of the smoke patterns formed are displayed in fig. (iii). Titanium Tetrachloride smoke was also used for flow visualization and some of the vortices observed with this alternate method are also presented in fig. (iii). It's use however, was discontinued, since although it provided excellent visualization, it also rapidly whitened the interior of the tunnel, making contrast photography impossible.

The velocity boundary layer was measured with a hot wire under neutral temperature conditions. Calibration of the hot wire was unnecessary, since only the thickness of the boundary layer was required, not details of it's shape. The thickness of the thermal boundary layer was similarly measured with a thermocouple mounted on the probe mechanism. Attempts were also made to employ the smokewise technique to obtain estimates of the thickness of the velocity boundary layer. The smokewise technique for measurements in low speed flows is described in detail by Orgill (1972). It consists of a Nichrome wire coated with a thin film of oil. An electric discharge or pluse instantaneously heats the wire causing vaporization of the oil into a vertical smoke line which then follows the local velocity of the flow. After an electrically set time delay, a strobelight is activated together with a camera shutter. The photograph then indicates the profile by the distortion of the smoke line. Knowledge of the time delay which is electronically measured, makes it possible to calculate the actual velocities, provided of course, that a reference distance on the photograph is known.

<u>Results</u>: Figure (iv) is an example of a smokewire photograph. Although rather faint, the height of the boundary layer may still be estimated.

Figure (v) is an example of the velocity and temperature profiles obtained with an uncalibrated hotwire and a thermocouple respectively. Estimates of dimensionless wavenumber, Rayleigh number and Goertler number were calculated utilizing the experimental information obtained. In all cases, the experimental values were about two orders of magnitude greater than the theoretically predicted critical, therefore implying that they lie in the range of amplifying wavenumbers.

The experimental values have been included on Figure (7). The Goertler numbers for both cases were 13.8; however, it should be noted that the velocity profiles and temperature profiles were not strictly speaking exactly those of Blasius.

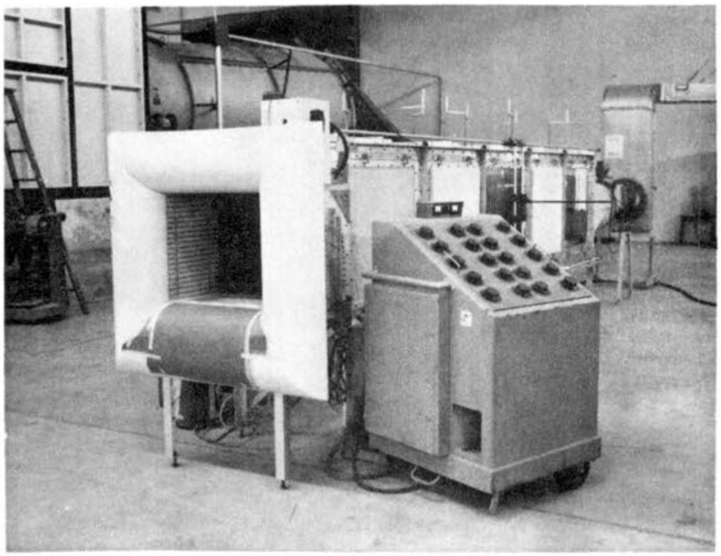

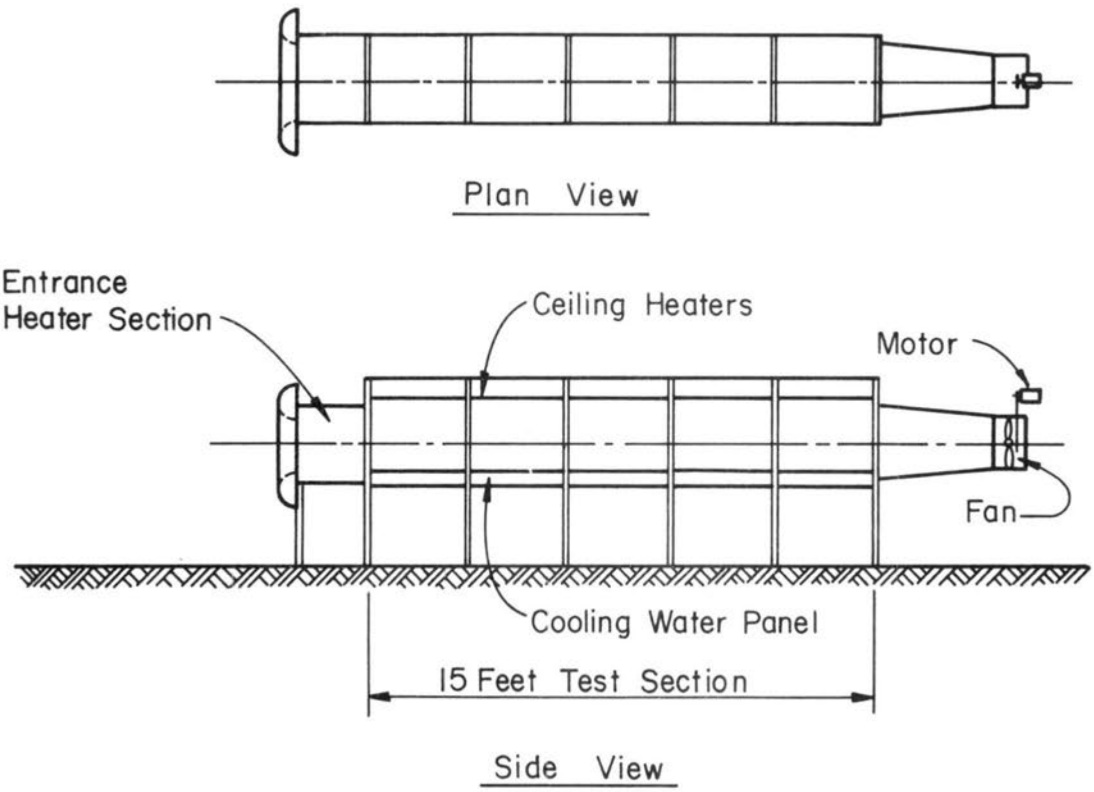

Fig. (i) Schematic of Windtunnel.

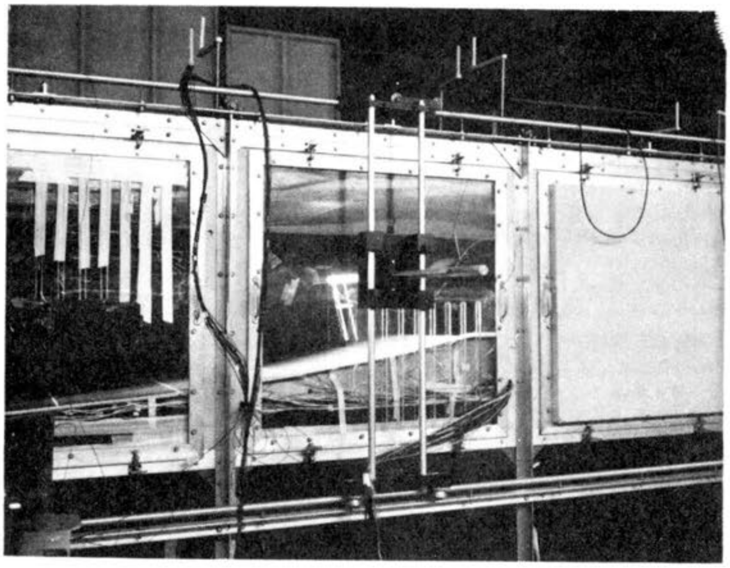

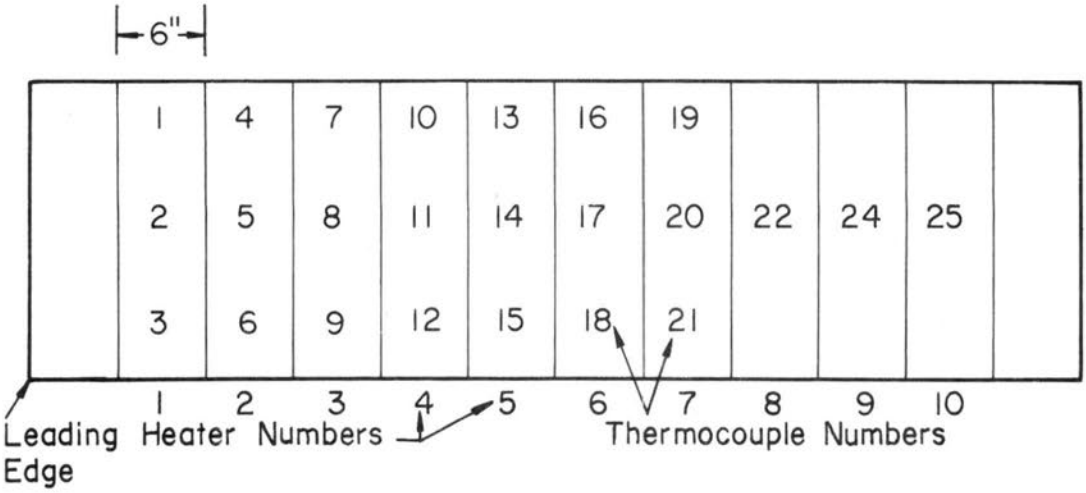

Thermocouple Number 23 Used for Measurement of Free Stream Temperature

Fig. (ii) Plate Arrangement and Overall View.

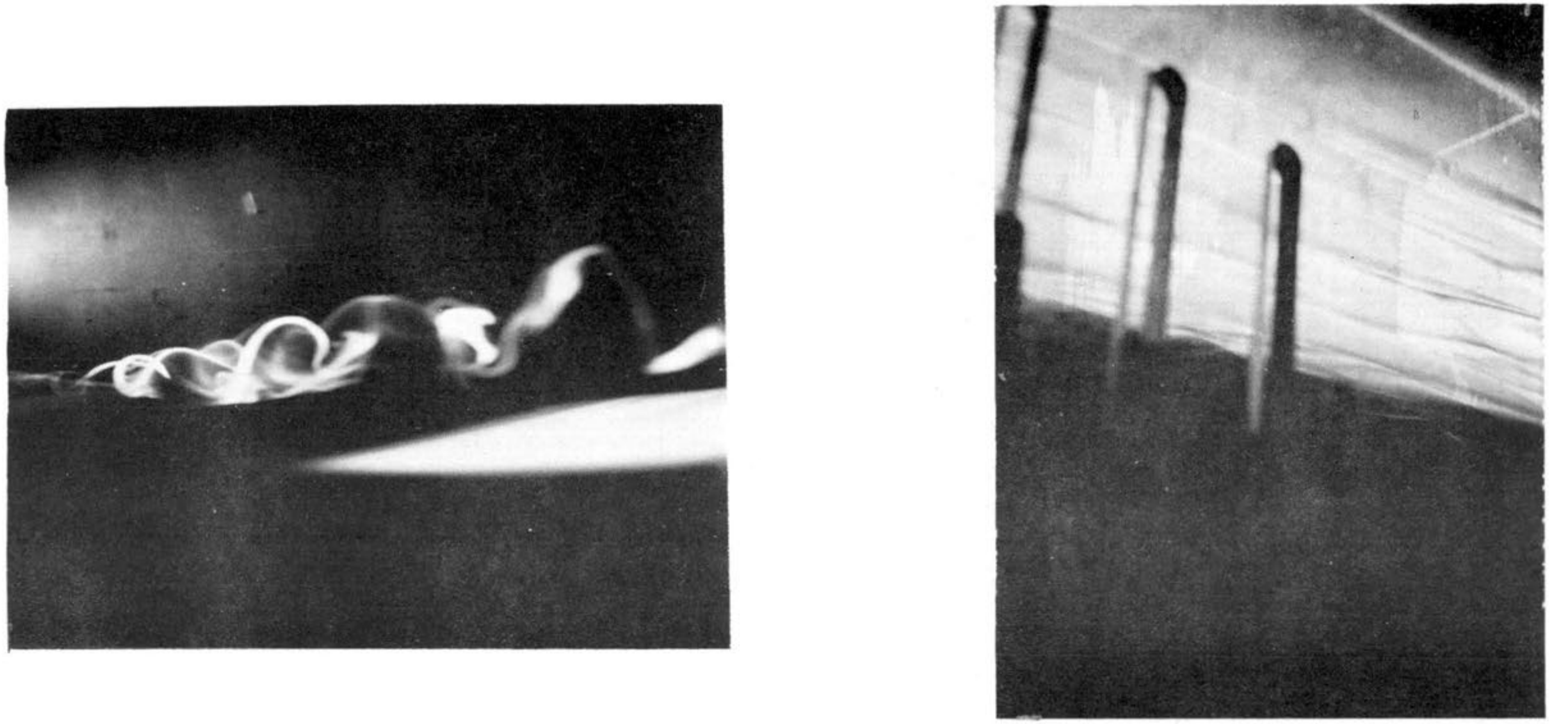

(a) Incense Smoke
Plate Temperature = 86°F
Freestream = 70°F

(b) Titanium Tetrachloride Smoke
Plate Temperature = 90°F
Freestream = 72°F

Fig. (iii) Smoke Visualization of Vortices

Fig. (iii) (c) Longitudinal Rolls

Plate Temperature = 78°F	Mean Velocity = 1.8 ft/sec
Freestream = 70°F	$\delta \sim \lambda \sim 2$ inches
	R = 30 ft

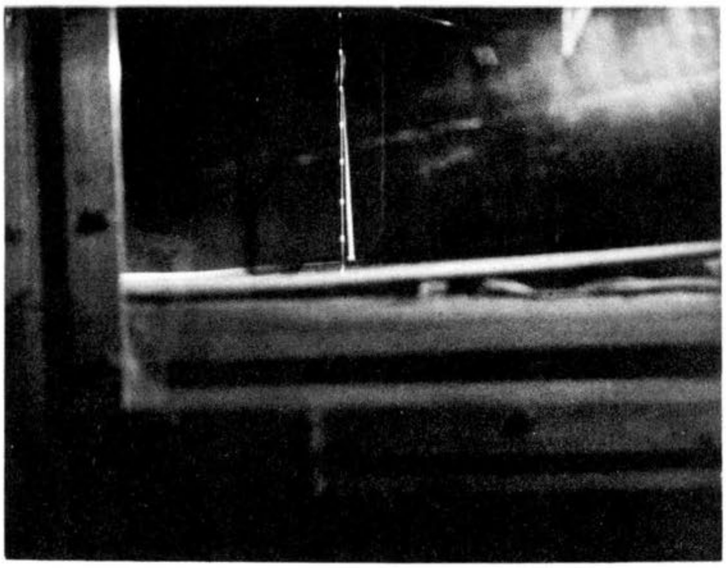

Fig. (iv) Smokewire Photograph of
Velocity Profile.

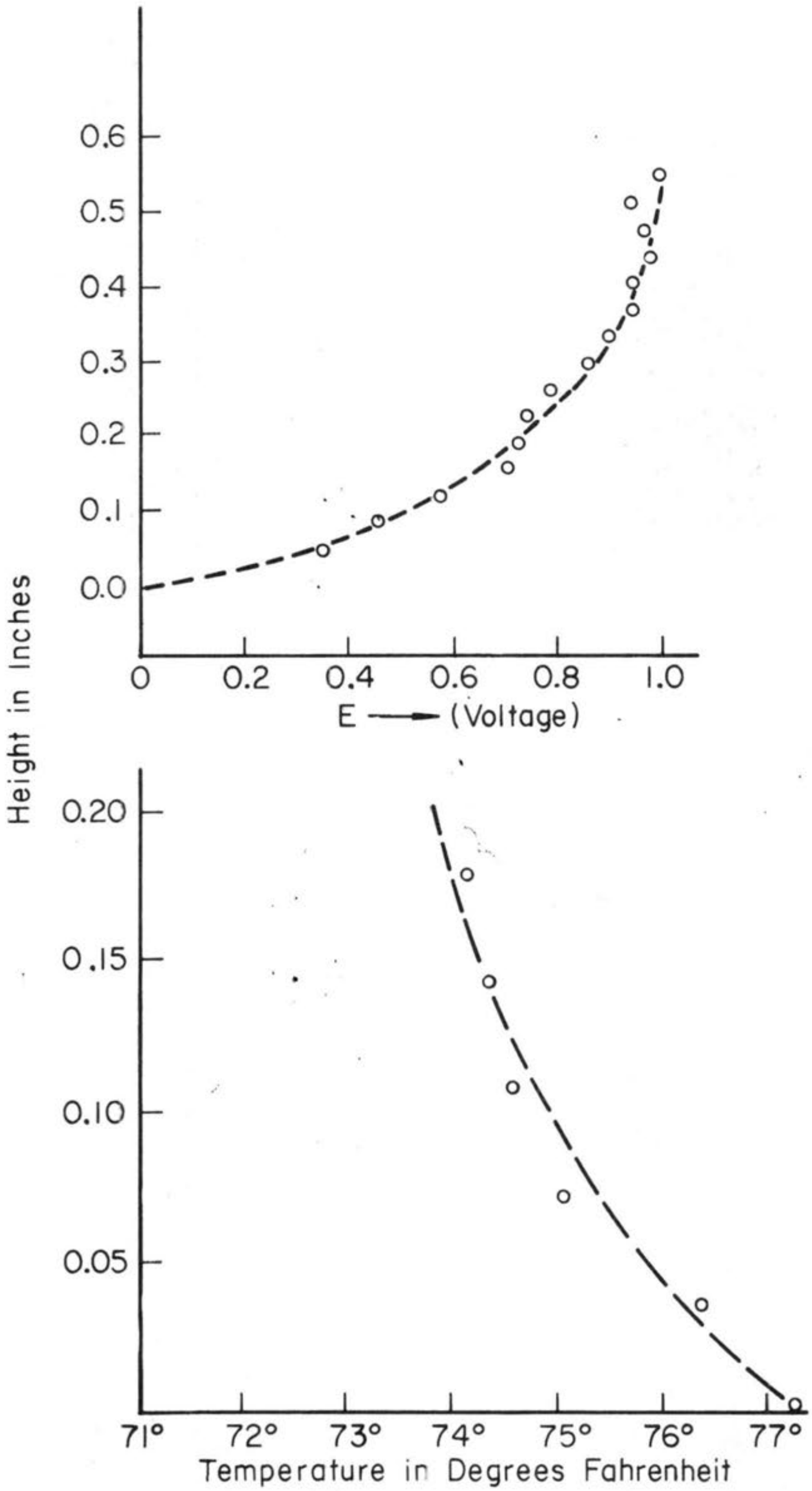

Fig. (v) Typical Velocity and Temperature Profiles.

Table I. Classification of Principal Literature on Thermoconvective Vortices - Experimental

	Type of Flow	Experimental	Theoretical	Observations
Terada et al. (1928, 1929)	Thin Alcohol Film on inclined plate	X		Longitudinal vortices observed with dye
Avsec (1930)	Plane Poiseuille Flow	X		Transverse as well as longitudinal smoke visualization
P. Idrac (1920)	Plane Poiseuille Flow	X		Longitudinal vortices
Graham (1933)	Couette Flow	X		Longitudinal vortices
Chandra (1937)	Couette Flow	X		Longitudinal as well as transverse rolls
Akiyama, Hwang and Chang (1971)	Plane Poiseuille Flow	X		Longitudinal rolls
Sparrow and Husar (1969)	Natural Convection on Inclined Plates	X		Longitudinal rolls
Lloyd and Sparrow (1970)	Natural Convection on Inclined Plates	X Quantitative measurements of instability Rayleigh number		Longitudinal rolls or wave instabilities depending on inclination angle

Table II. Stability of Thermally Stratified Fluids-Principal Theoretical Analyses

	Type of Analysis	Boundary Conditions	Type of Mean Temperature Profile	Solution Methods	Remarks
Rayleigh (1916)	Linear Perturbation Theory	Two free plane boundaries	Linear		Stationary Layers
Jeffreys (1926) (1928)	Linear Perturbation Theory	Rigid-Rigid, Rigid-Free, Free-Free	Linear	Approximate	Stationary Layers
Low (1929)	Linear Perturbation Theory	Rigid Free	Linear	Exact	Stationary Layers
Sparrow, Goldstein and Jonsson (1969)	Linear Perturbation Theory	Plane Boundaries	Non Linear	Approximate	Stationary Layers
Lick (1965)	Linear Perturbation Theory	Free Plane Boundaries	Linear Approximation to Non Linear Profile	Exact Solutions	Stationary Layers
Currie (1967)	Linear Perturbation Theory	Rigid Plane Boundaries	Linear Approximation to Non Linear Profile	Exact Solutions	Stationary Layers
Rintel (1967)	Linear Perturbation Theory	Rigid Lower Boundaries Free Upper Boundary	Two Layer Linear Profiles Approximation to Penetrative Convection	Approximate Expansion in Eigen-functions	Stationary Layers
Stix (1970)	Linear Perturbation Theory	Free Lower Boundary Upper Boundary at Infinity	Linear with Penetra-tive Convection	Exact	Stationary Layers

Table II. Stability of Thermally Stratified Fluids-Principal Theoretical Analyses (Continued)

	Type of Analysis	Boundary Conditions	Type of Mean Temperature Profile	Solution Methods	Remarks
Ogura and Kondo (1970)	Linear Perturbation Theory	Mixed Boundary Conditions	Linear	Exact	Stationary Layers
Heikes (1971)	Linear Perturbation Theory	Plane Boundaries Lower Rigid Upper Free	N-Layer Model with Linear Profiles	Exact Solutions	Stationary Layers
Gage and Reid (1967)	Linear Perturbation Theory	Plane Rigid Boundaries	Linear Temperature Profile with Plane Poiseuille Flow	Asymptotic Expansions	Unstable Stratification - Rolls Stable Stratification - Waves

Table III. Classification of Literature [Goertler Instability in Laminar Boundary Layers]

	Parallel Flow	Quasi-Parallel Flow	Small Curvature	Finite Curvature	Solution Method
Goertler (1940)	X		X		Green's Functions
Meksyn (1940)	X		X		Asymptotic Expansions
Smith (1955)		X		X	Galerkin's Method
Hammerlin (1955)	X		X		Integral Methods
Di Prima and Dunn (1956)	X (Heating at wall but no body force terms)		X		Galerkin's Method
Hammerlin (1961)					
Sandmayr (1966)	X (Turbulent)		X		Galerkin's Method
Chang and Sartory (1968)	X	X (Hydromagnetic terms included)	X		Numerical
McCormack, Welker and Kelleher (1969)	X (Experimental work included)		X		Variation of Parameters
Clauser and Clauser (1937)	Experiments in Laminar Boundary Layers				
Liepmann (1943)	Experiments in Laminar Boundary Layers				
Tani (1962)	Experiments in Laminar and Turbulent Flow Only				
Rintel (1971)	X		X		Expansion in Eigenfunctions

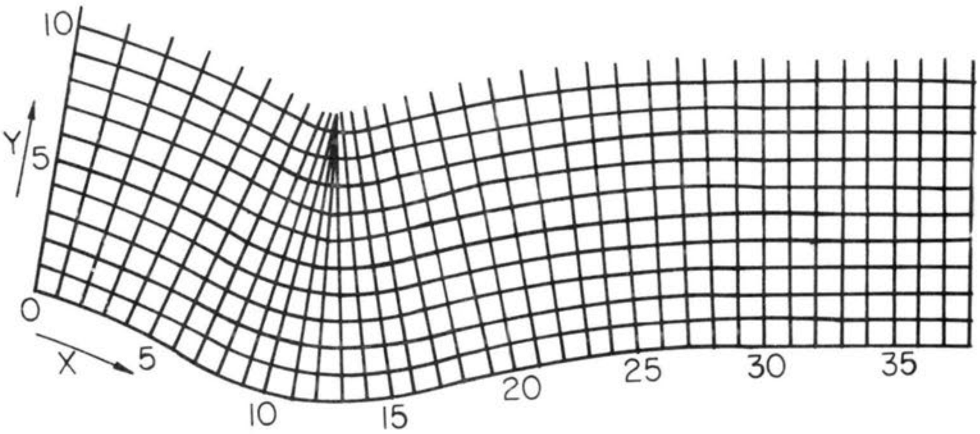

a. — A Family of Parallel Curves

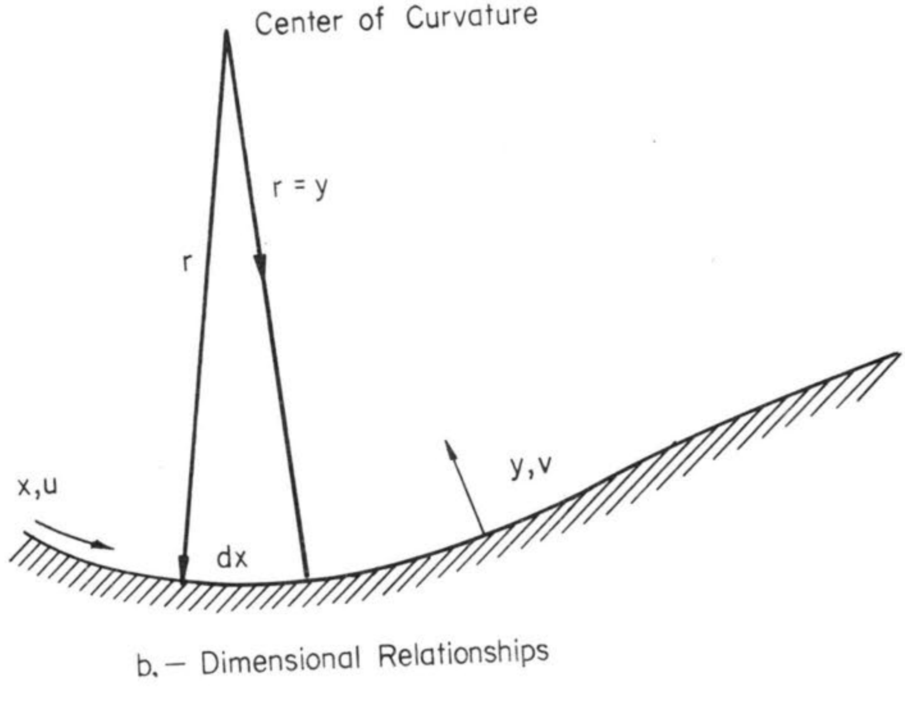

b. — Dimensional Relationships

Fig. (1) Orthogonal Curvilinear Coordinate System

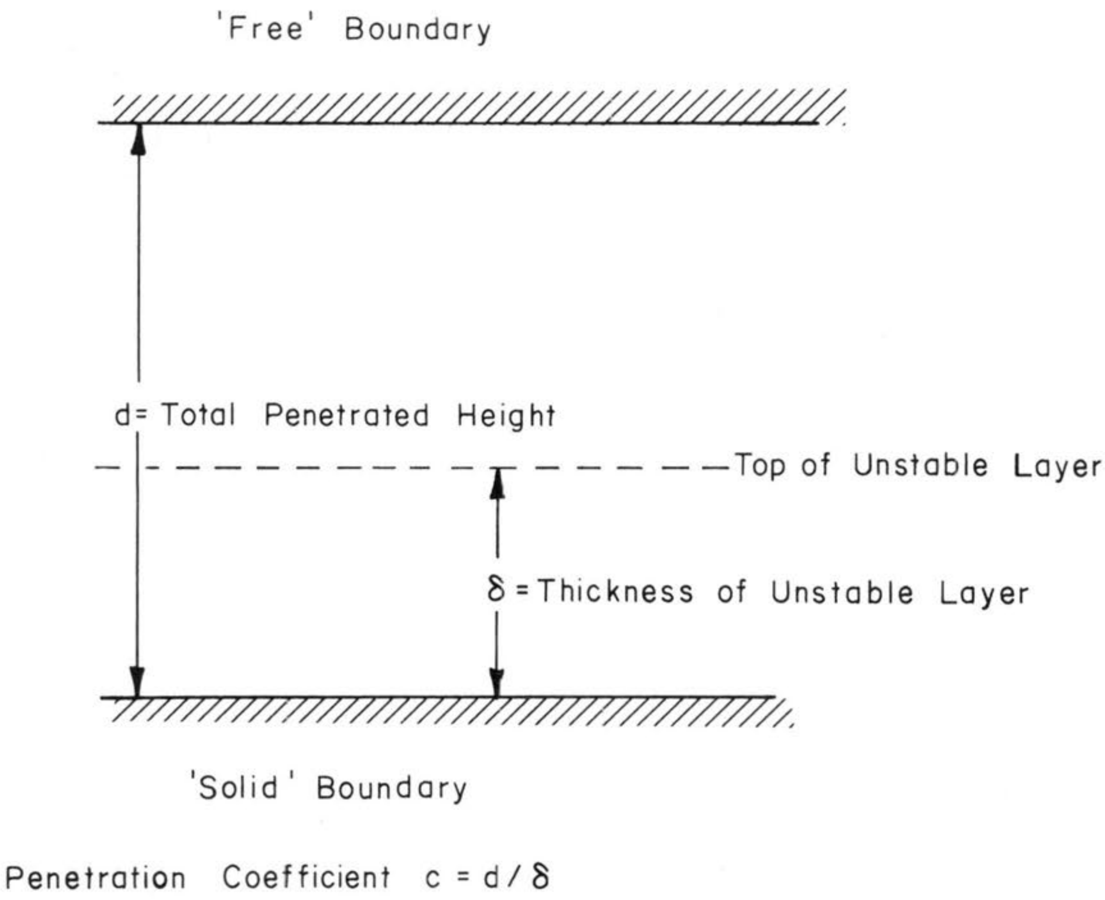

Fig. (2) Definition Sketch for the Penetration Coefficient

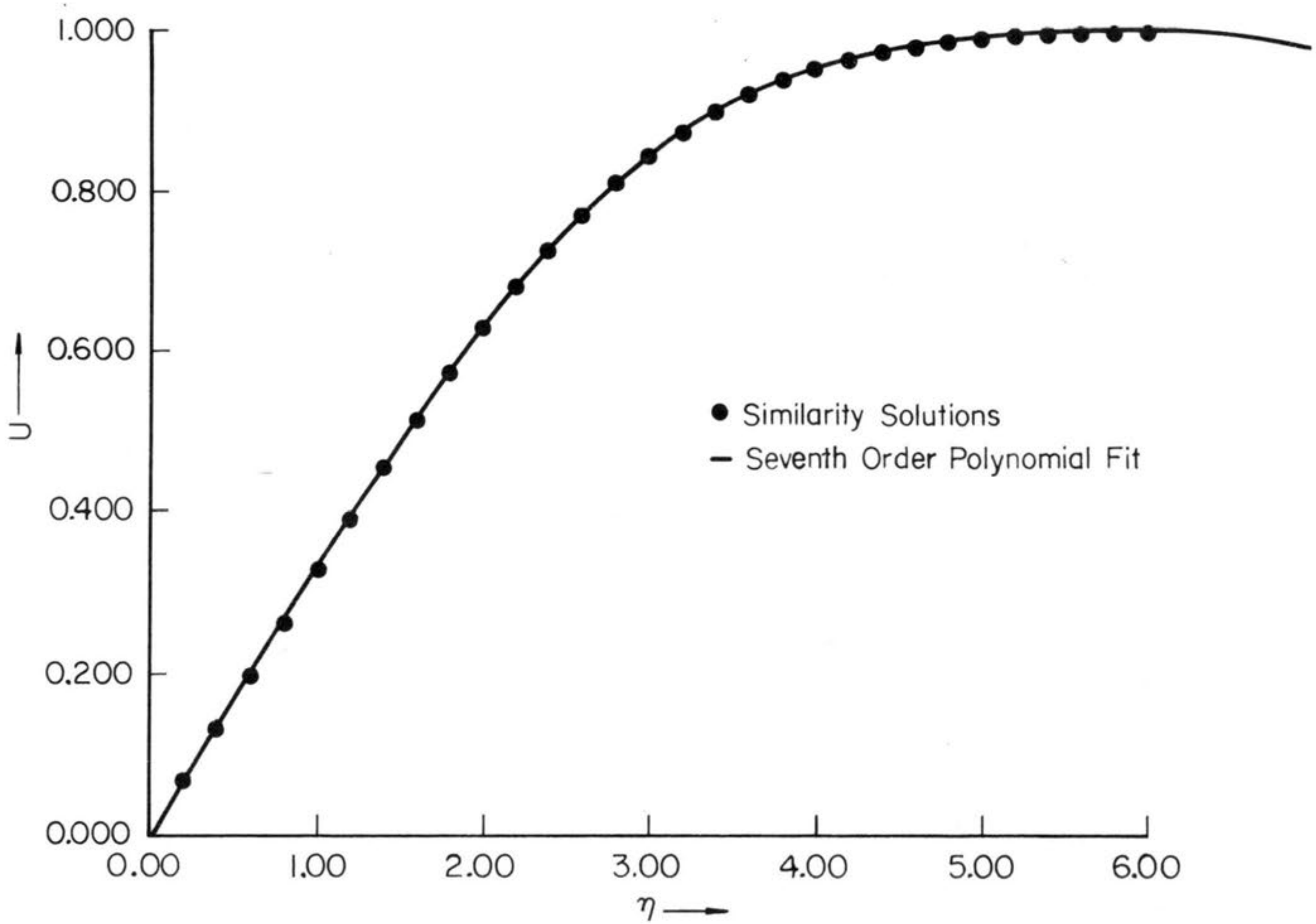

Fig. (3a) Comparison of Boundary Layer Solutions (Points) with Polynomial Approximation (line)

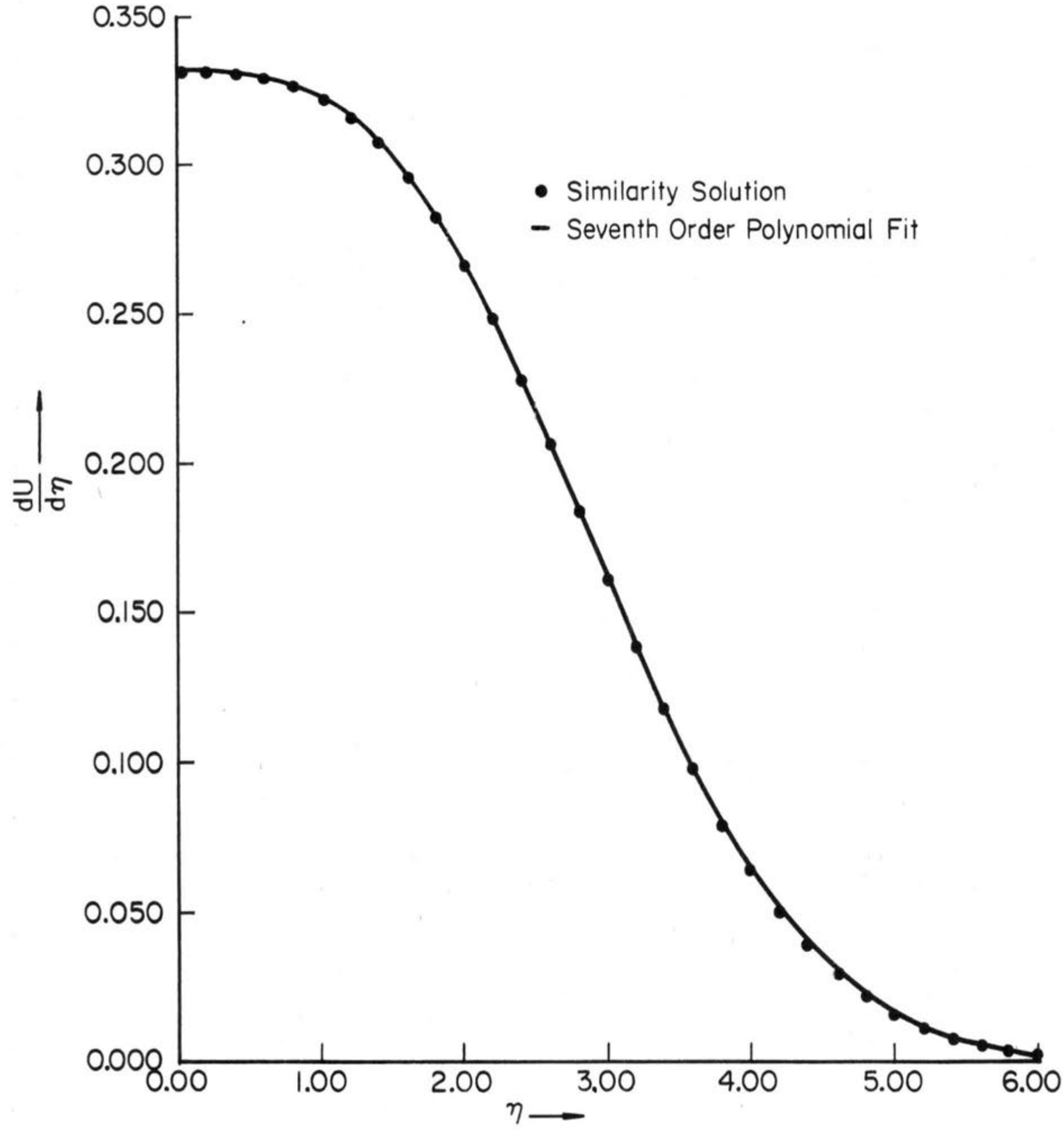
0.350
0.300
0.250
0.200
0.150
0.100
0.050
0.000
dU/dη
Similarity Solution
Seventh Order Polynomial Fit
0.00
1.00
2.00
3.00
4.00
5.00
6.00
η

Fig. (3b)

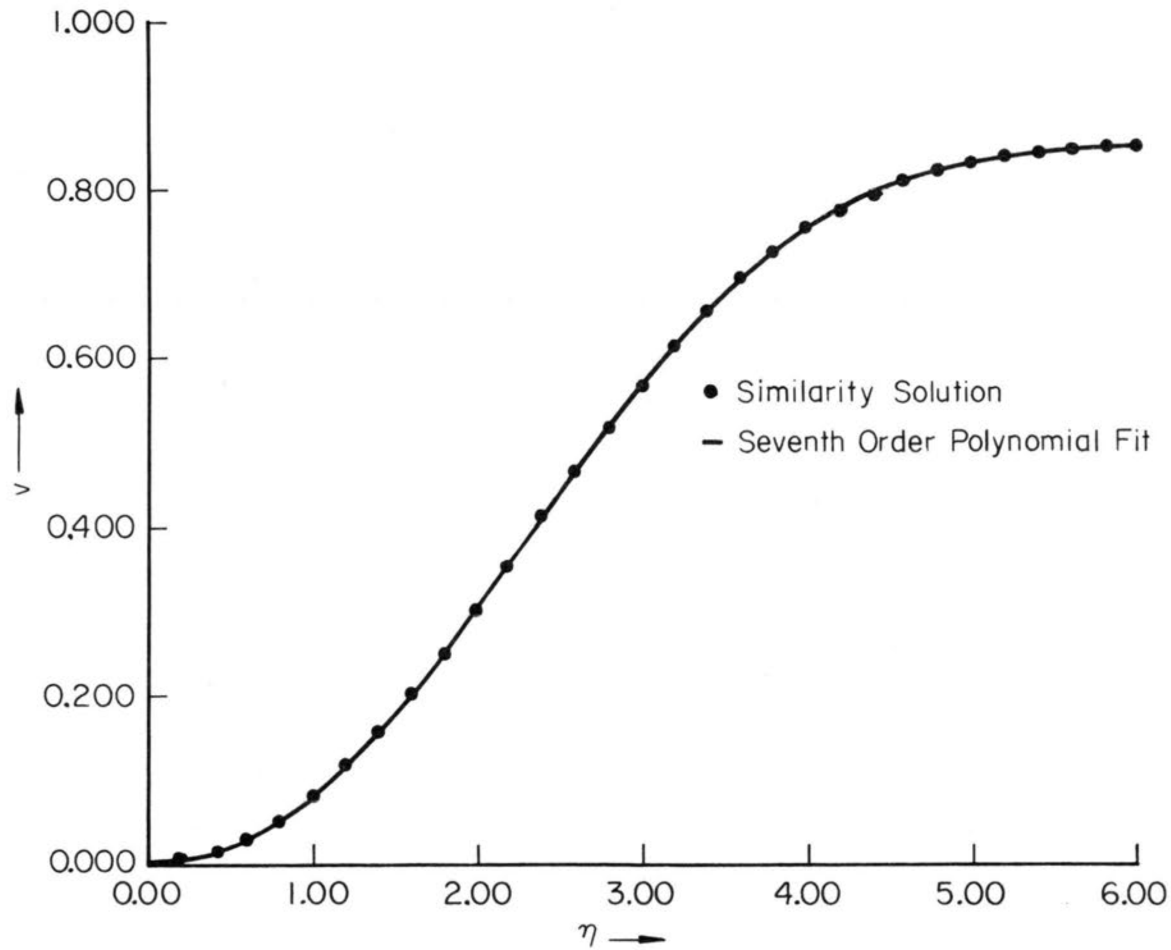

1.000
0.800
0.600
0.400
0.200
0.000
v
0.00
1.00
2.00
3.00
4.00
5.00
6.00
η
Similarity Solution
Seventh Order Polynomial Fit

Fig. (3c)

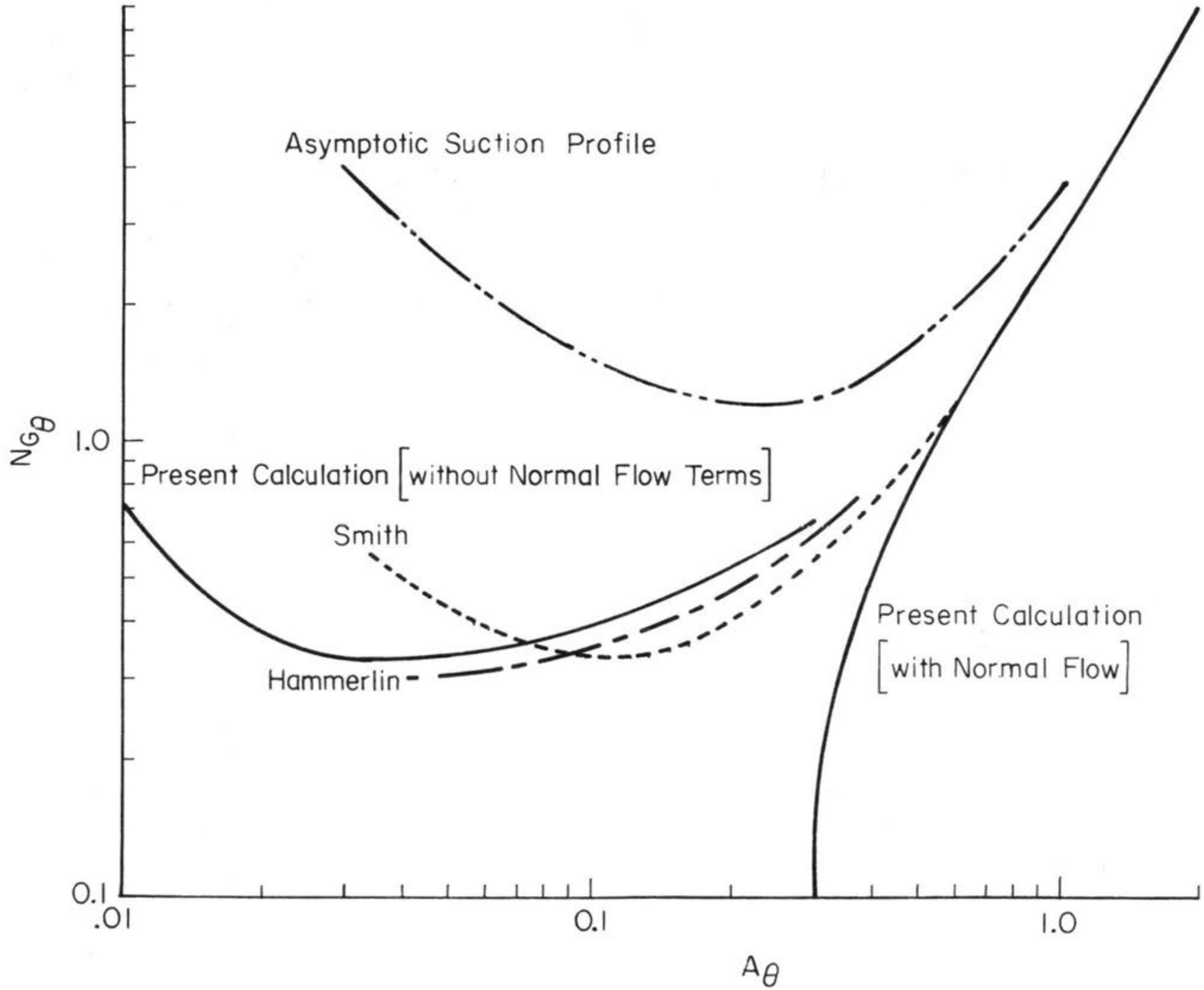

Fig. (4) Neutral Stability Curves for the Blasius and Asymptotic Suction Profiles

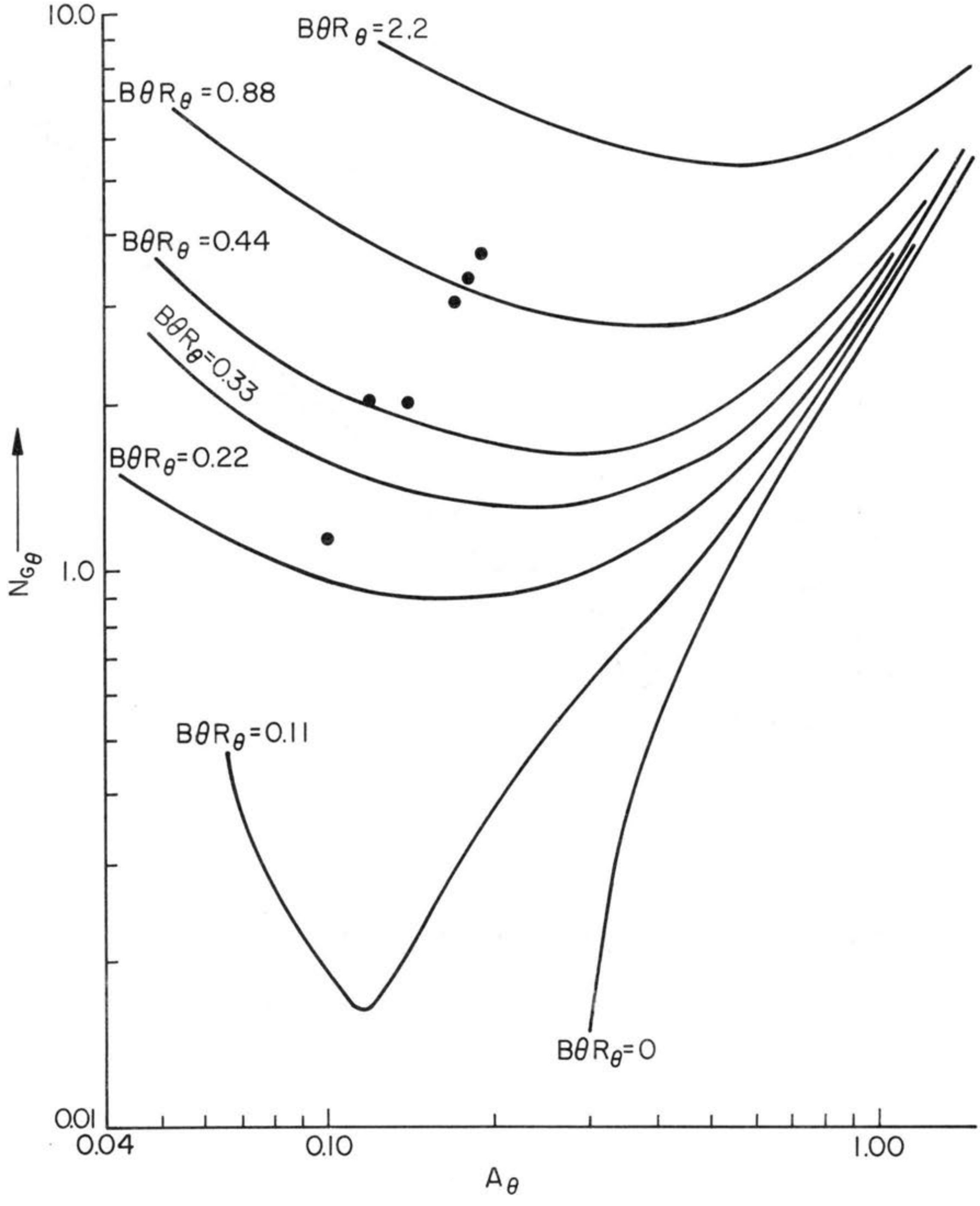

Fig. (5) Amplification Curves for Quasi-Parallel (Blasius) Flow with No Heating. The points are the data of Tani (1962).

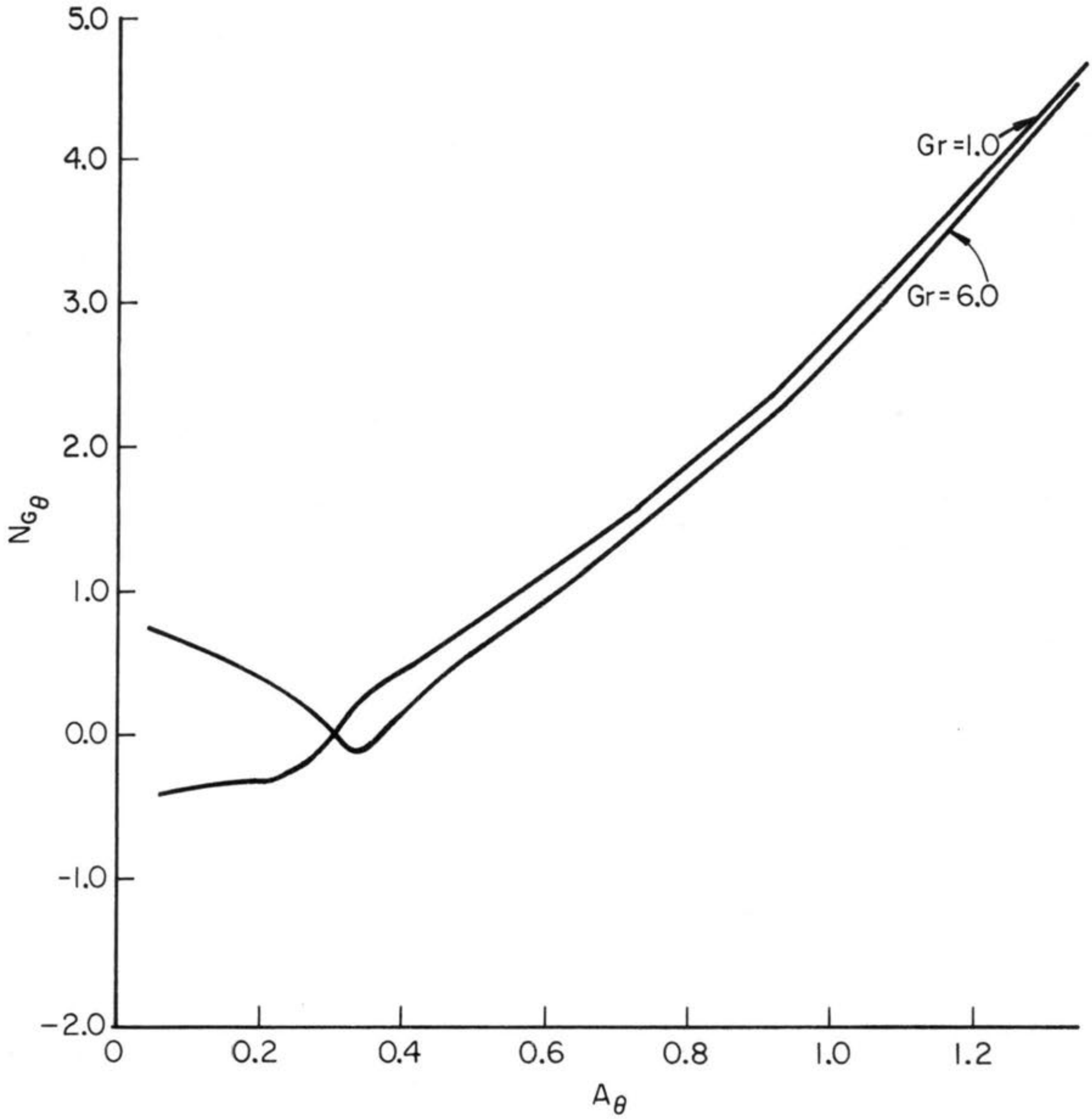

Fig. (6) Critical Stability Curves for Two Grashof Numbers (Blasius Profile, Including Normal Flow Terms)

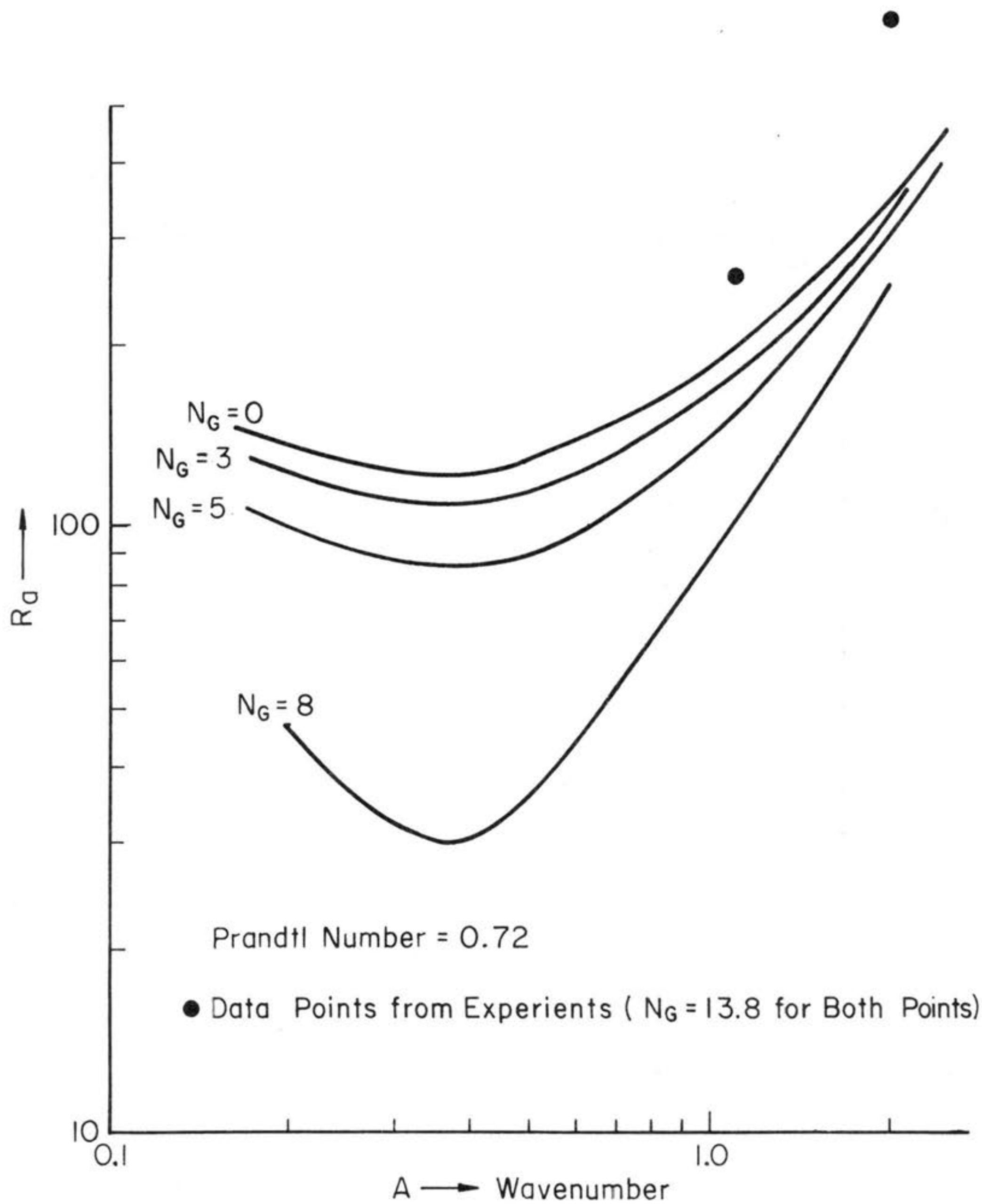

Fig. (7) Critical Stability Curves at Different Goertler Numbers.
(Blasius Profile, Normal flow terms ignored)

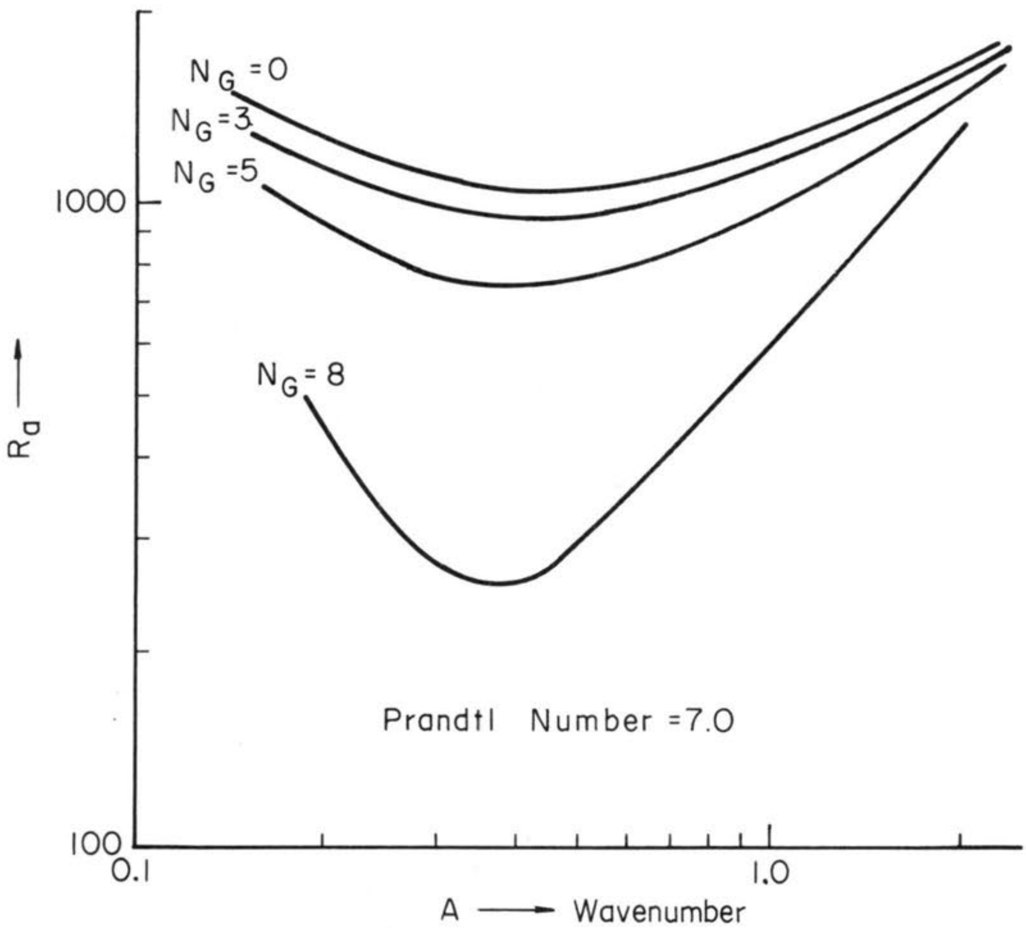

Fig. (8) Critical Stability Curves at Different Goertler Numbers.
(Blasius Profile, Normal flow terms ignored)

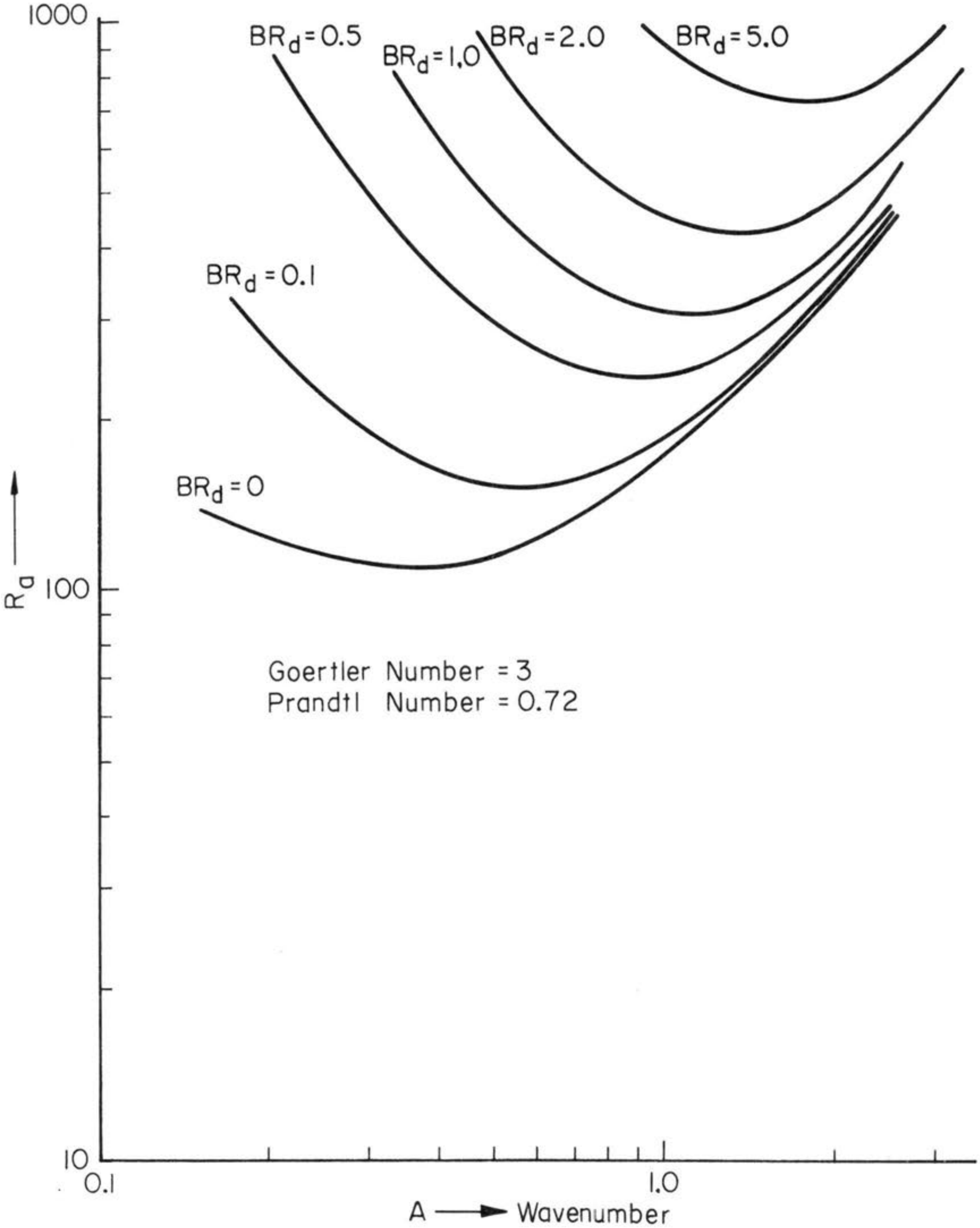

Fig. (9) Amplification Curves for Blasius Flow.
(Normal Flow Terms ignored)

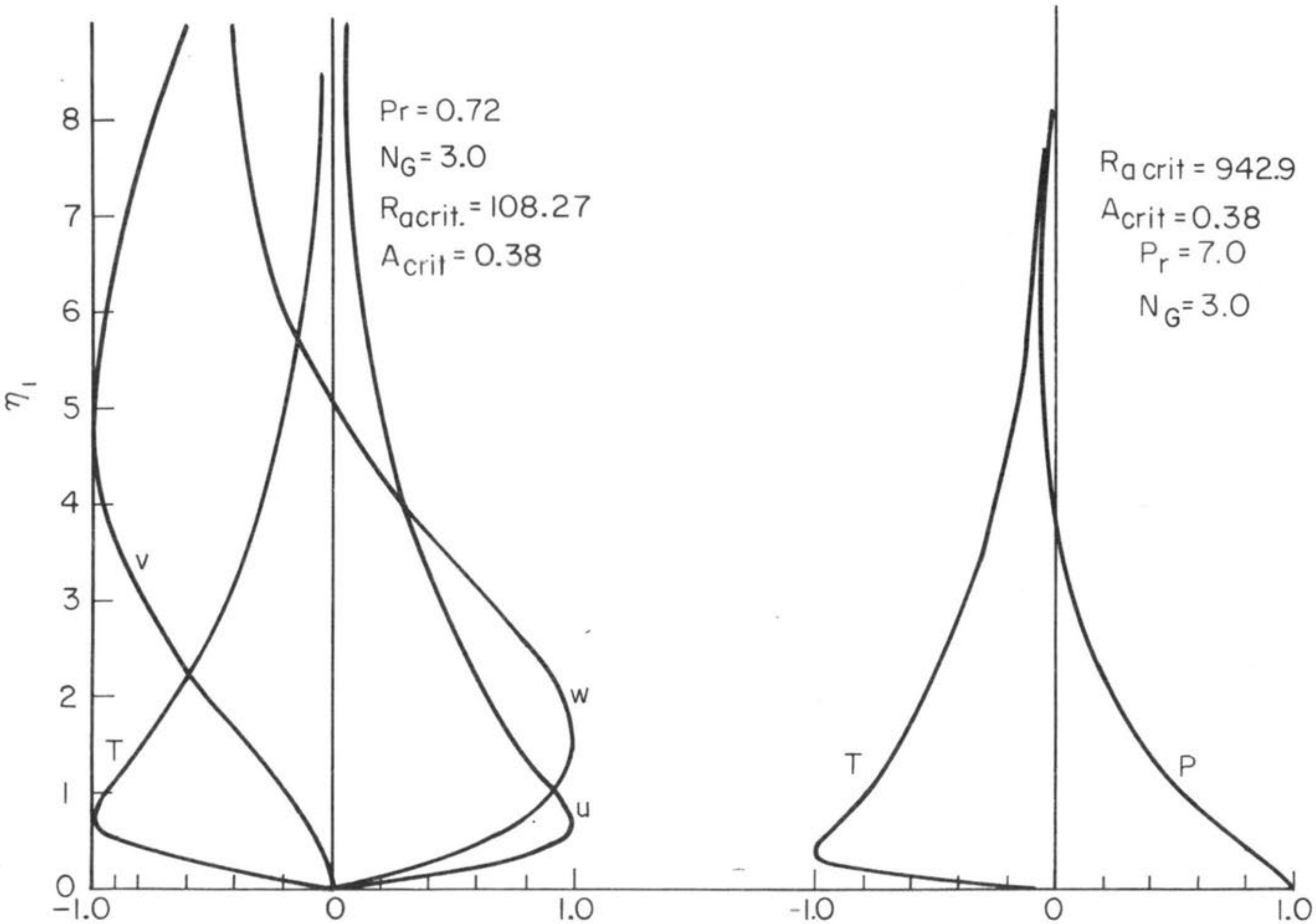

Fig. (10) Eigenfunctions of Disturbance at Critical Conditions.
(Blasius Profile, Normal flow terms ignored.
η_1 (= 6η) = 1 at boundary layer edge)

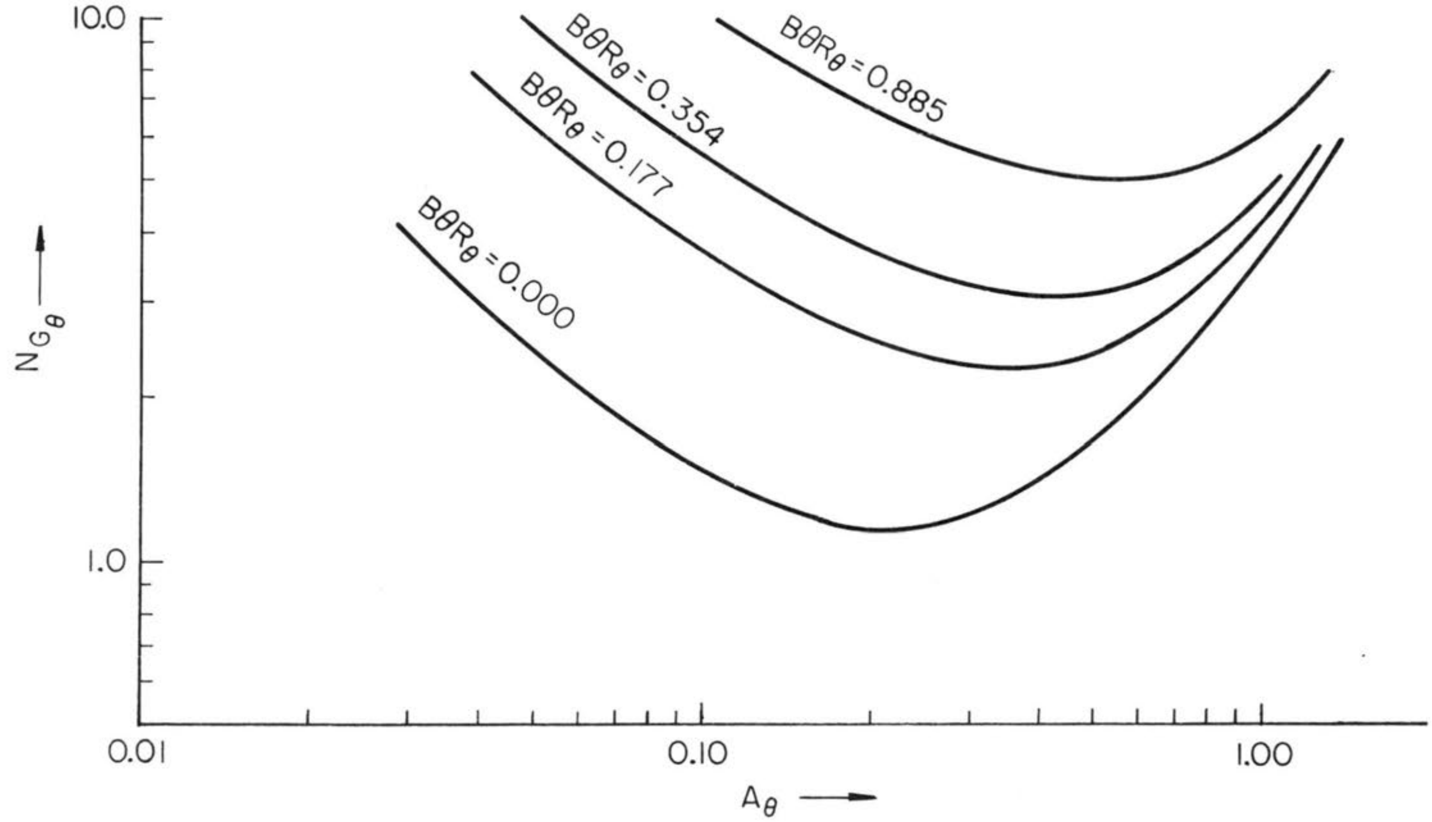

Fig. (11) Amplification Curves for the Asymptotic Suction Profile.

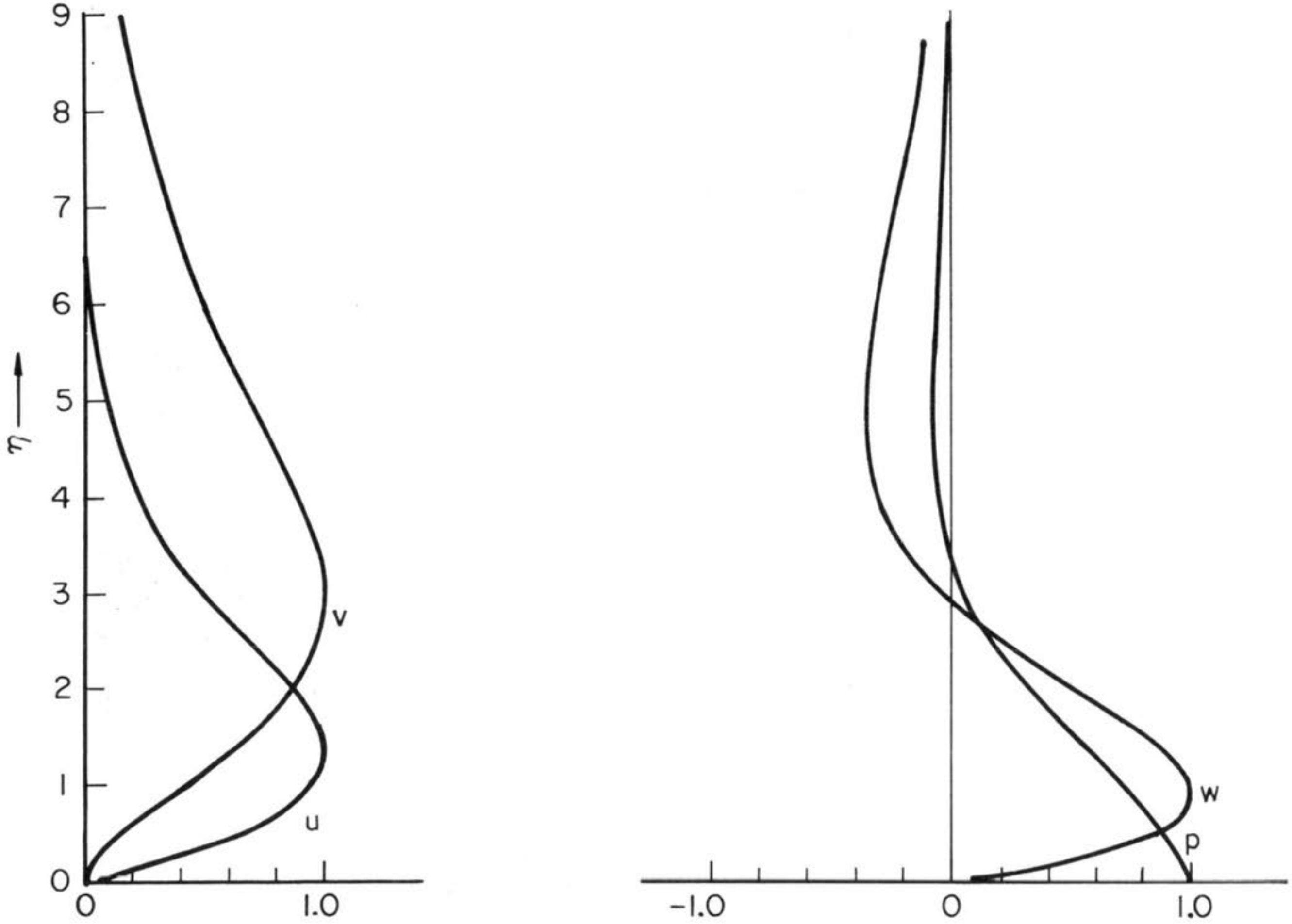

Fig. (12) Normalised Eigenfunctions at Critical Conditions for the Asymptotic Suction Profile.

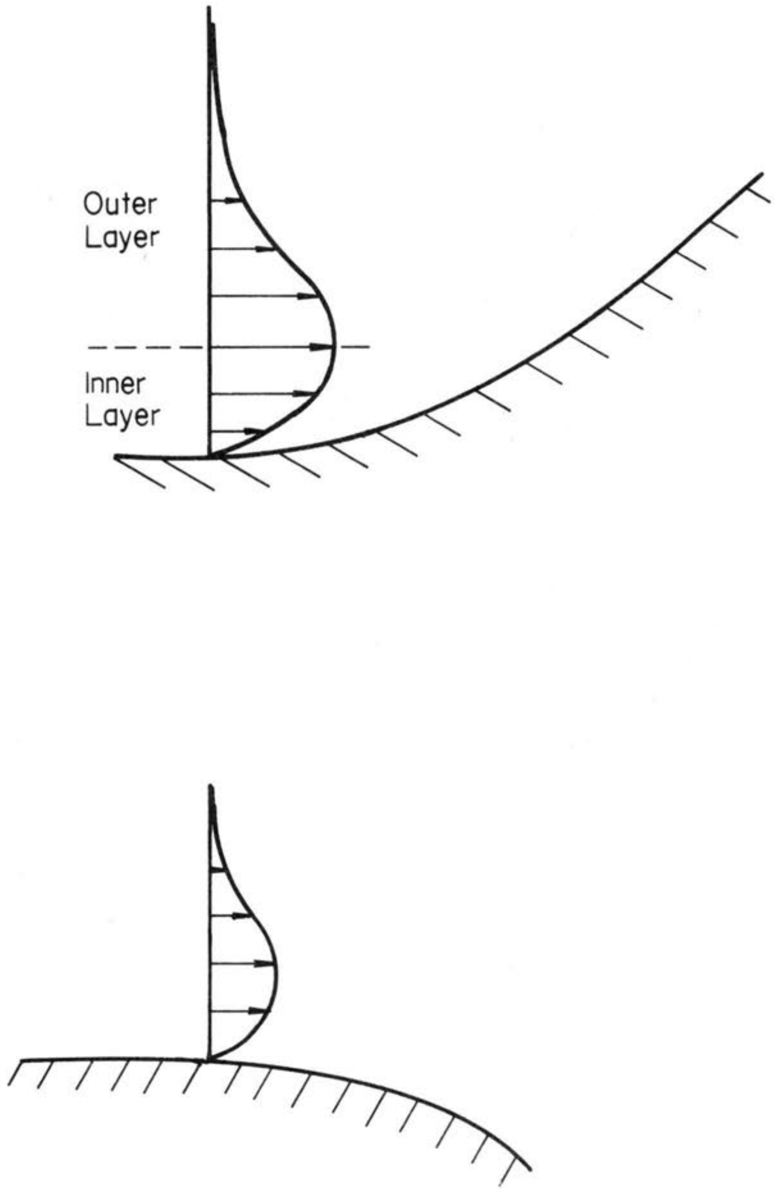

Fig. (13) Wall Jet on Curved Walls.

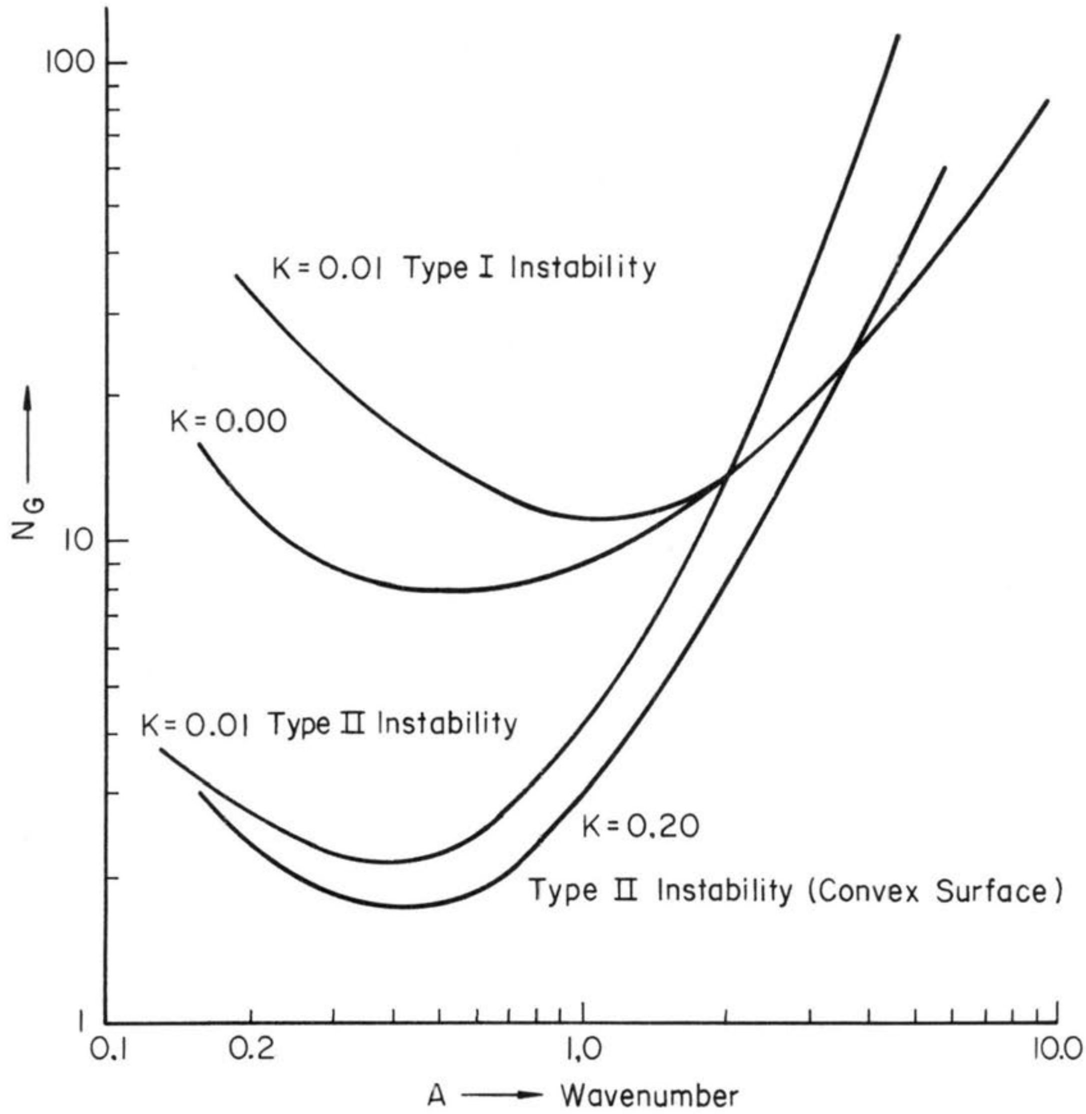

Fig. (14) Neutral Stability Curves for "Wall Jet Profiles".

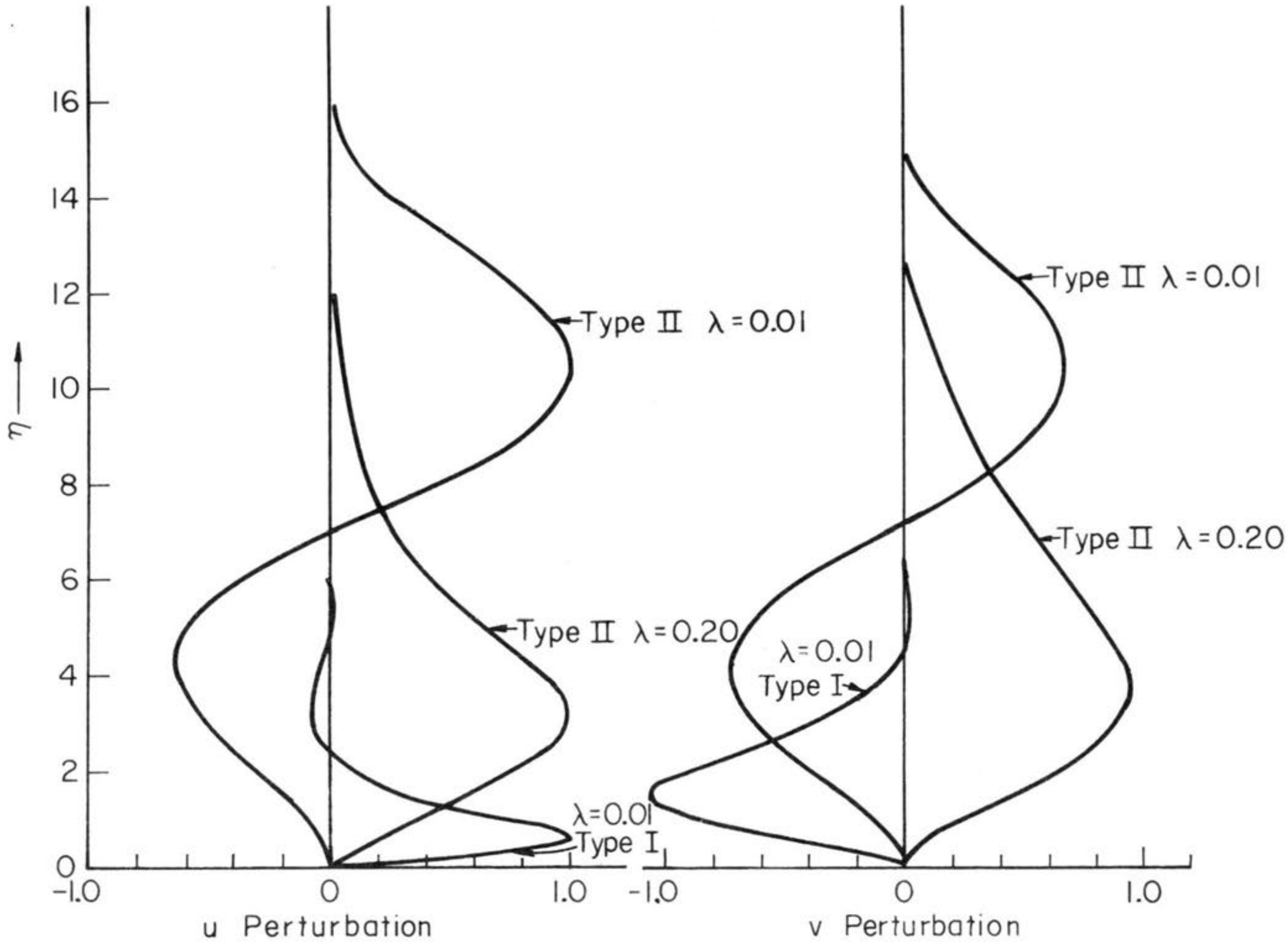

Fig. (15) Eigenfunctions for Type I and Type II Instabilities

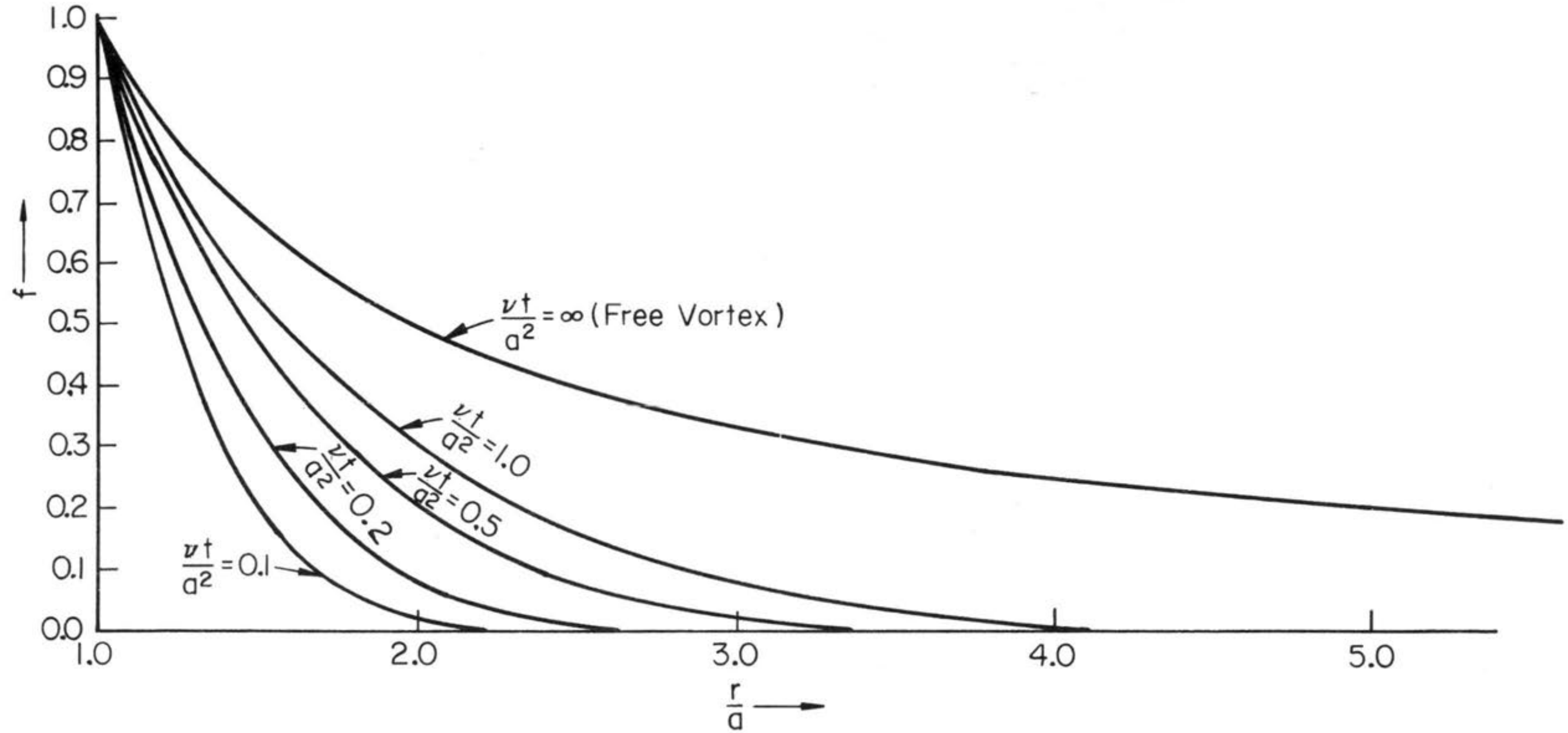

Fig. (16) Mean Velocity Profiles for Spin Up Problem (from Mallick (1957))

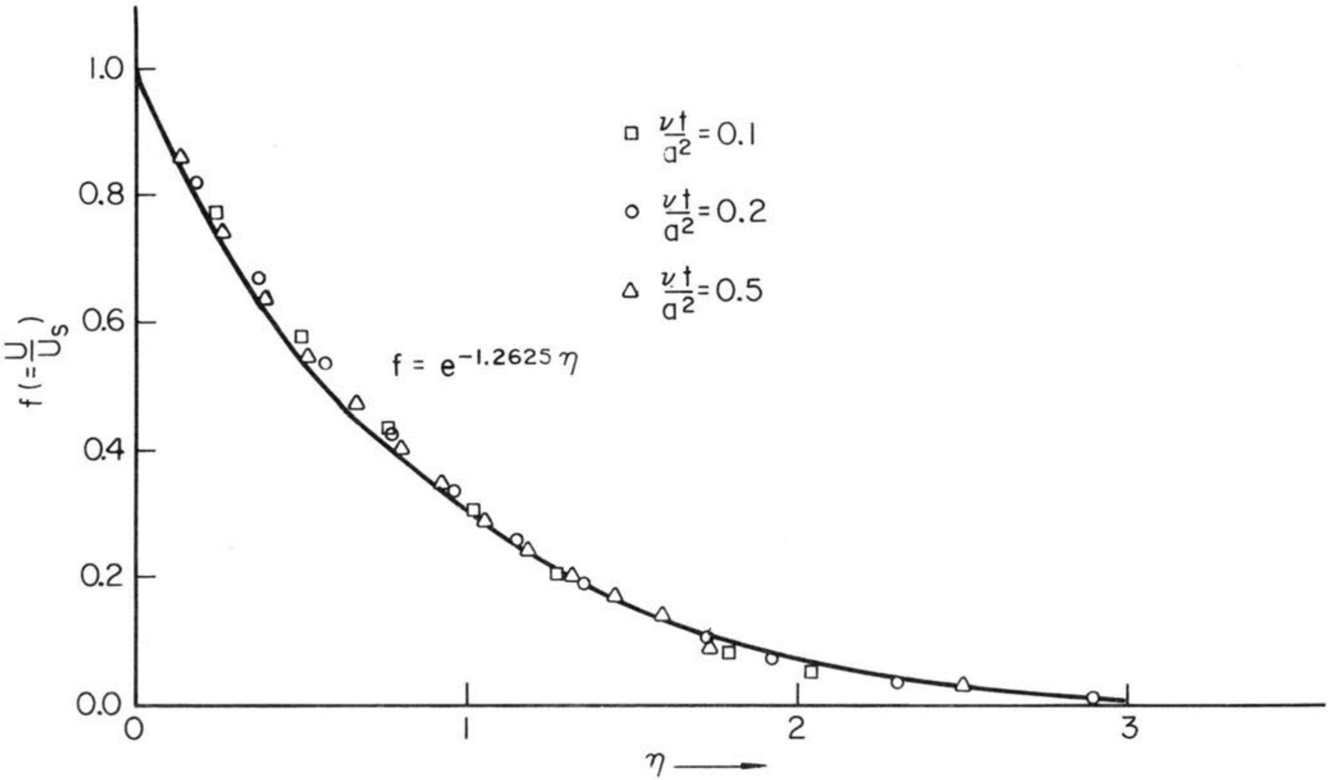

Fig. (17) Effect of Scaling the Mean Velocity Profiles with $\left(\frac{\nu t}{a^2}\right)^{0\cdot 411}$

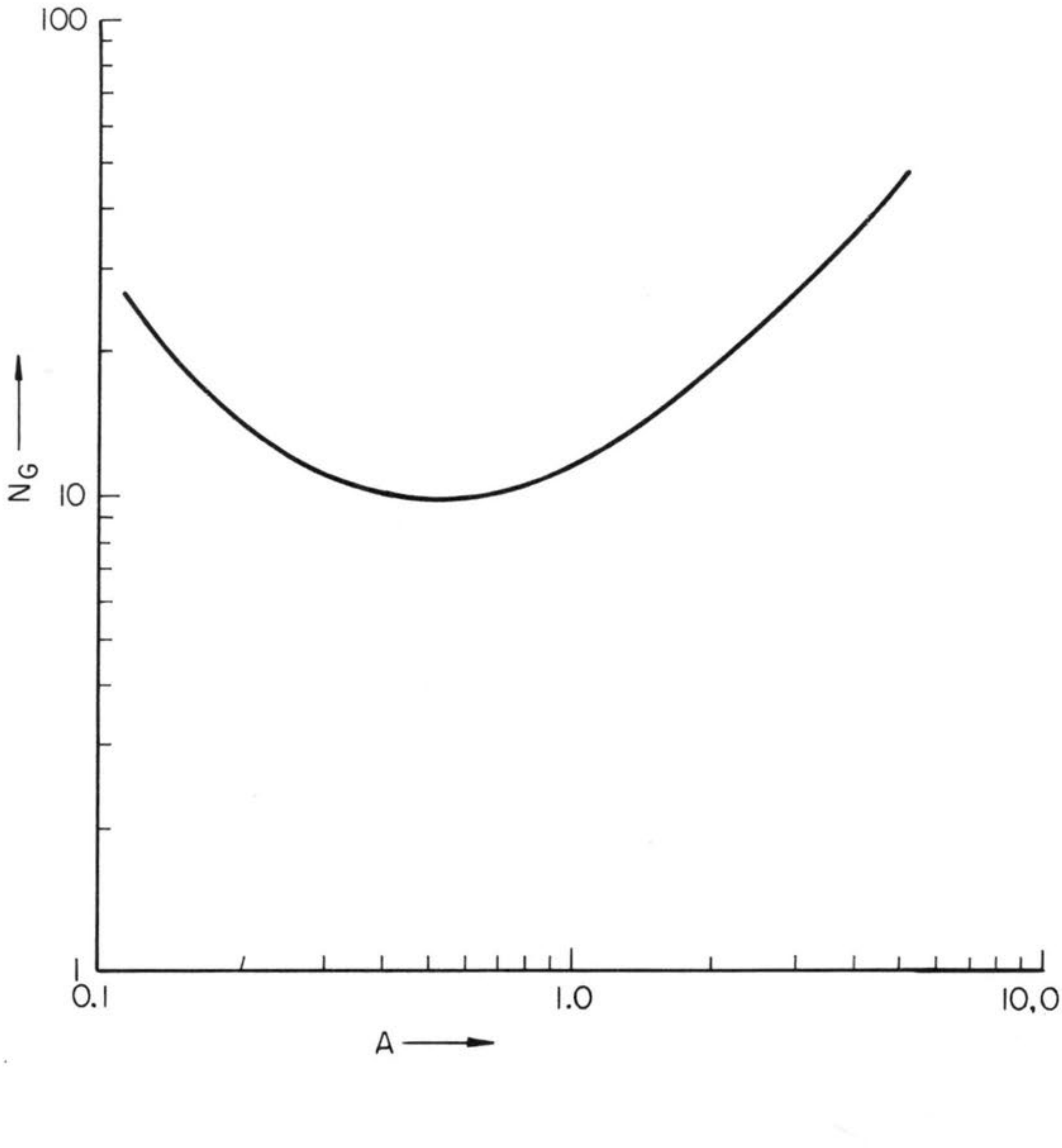

Fig. (18) Neutral Amplification Curve for Spin Up of a Cylinder in an Infinite Medium.

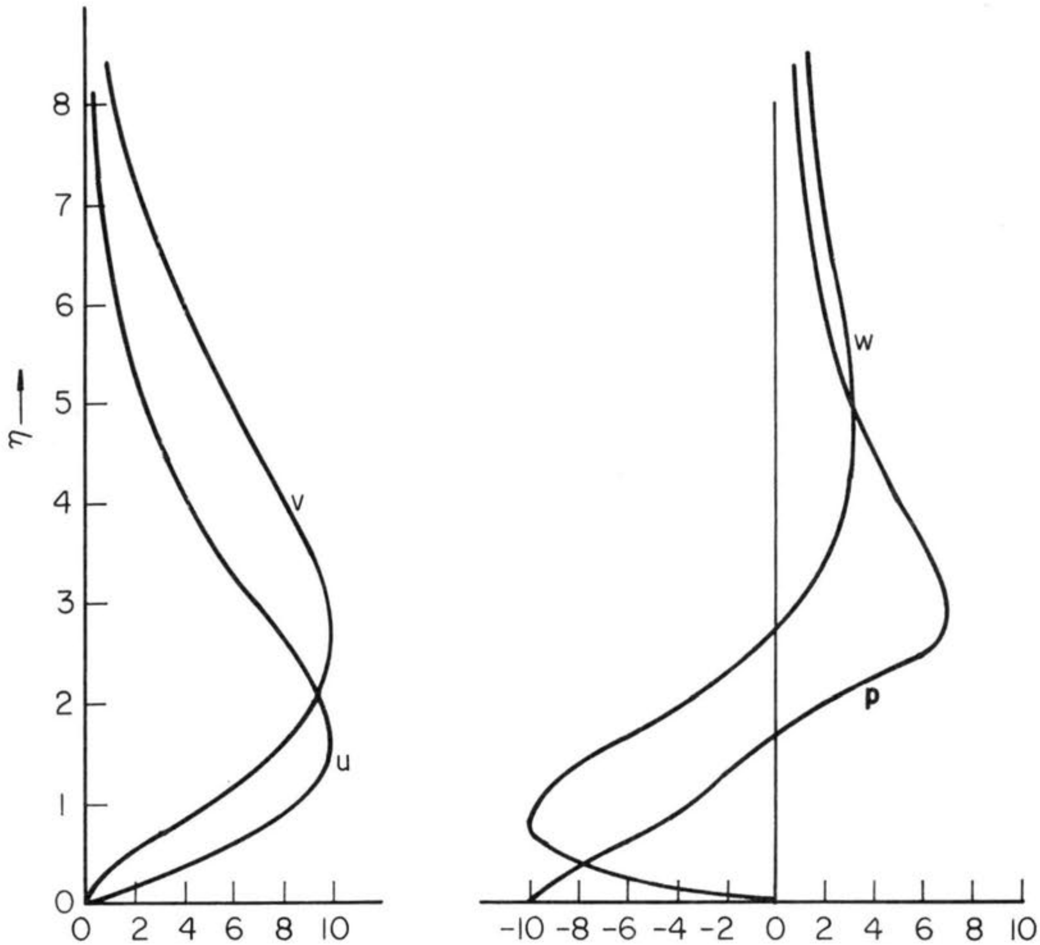

Fig. (19) Spin Up Problem - Normalized Eigenfunctions at Critical Conditions.

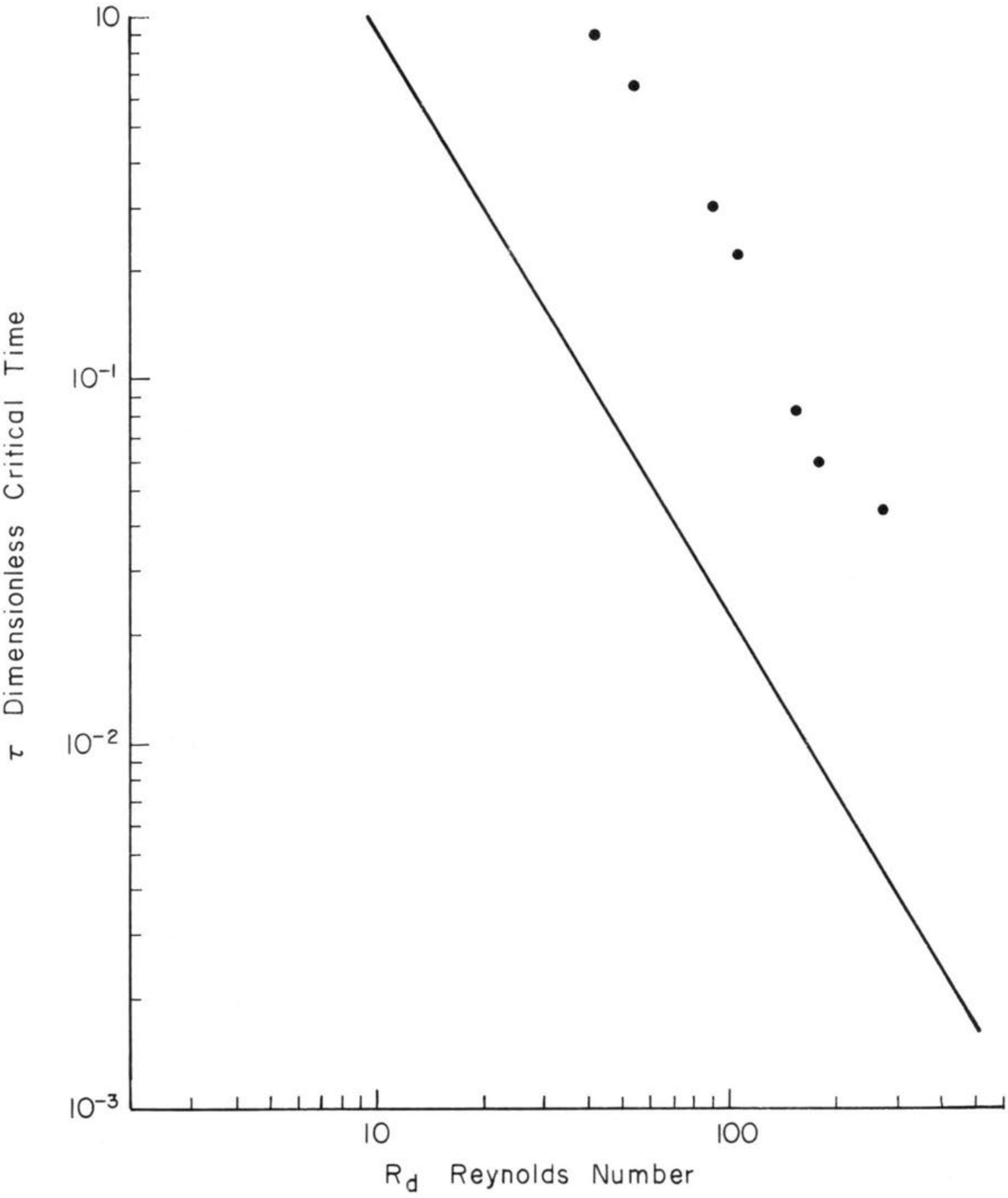

Fig. (20) Comparison Between Present Theory and Experiments of Kirchner and Chen (1970).

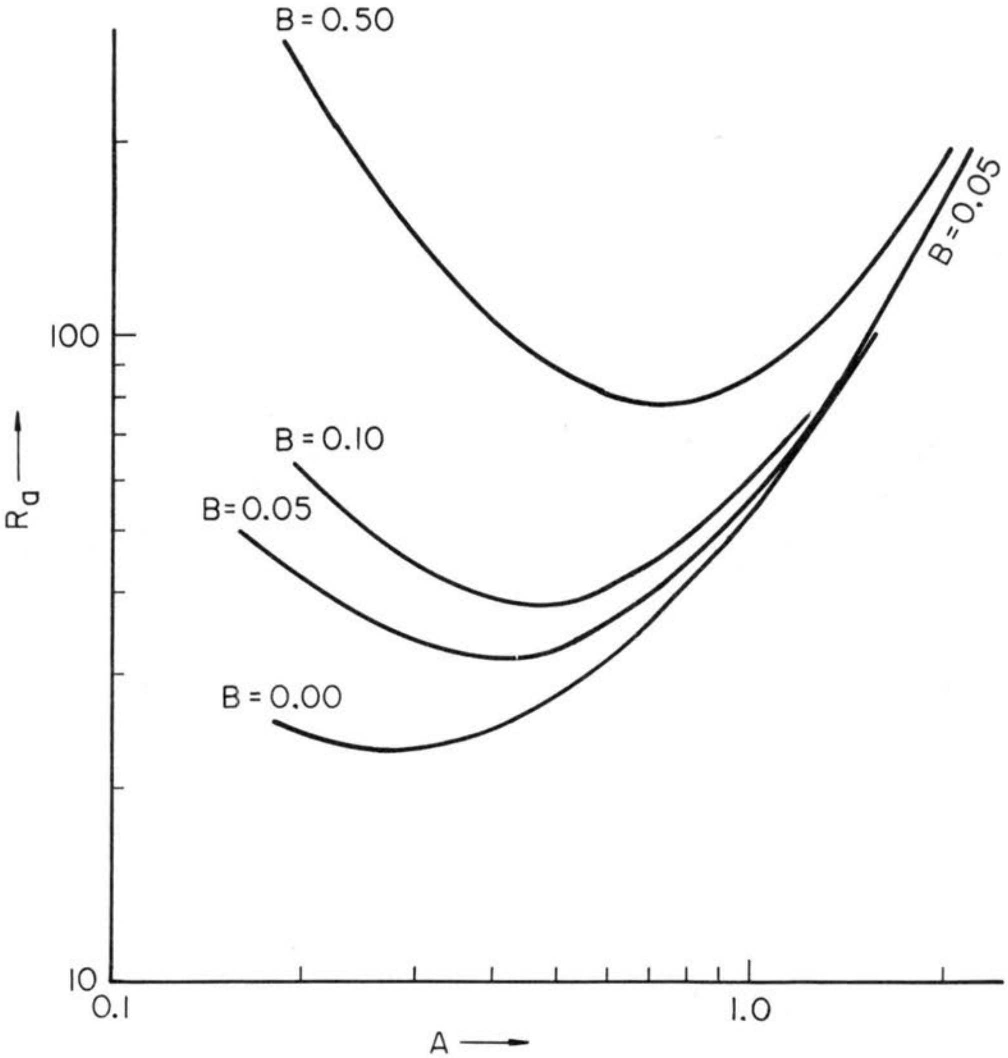

Fig. (21) Amplification Curves for the Stability of a Layer of Fluid Suddenly Heated from Below.

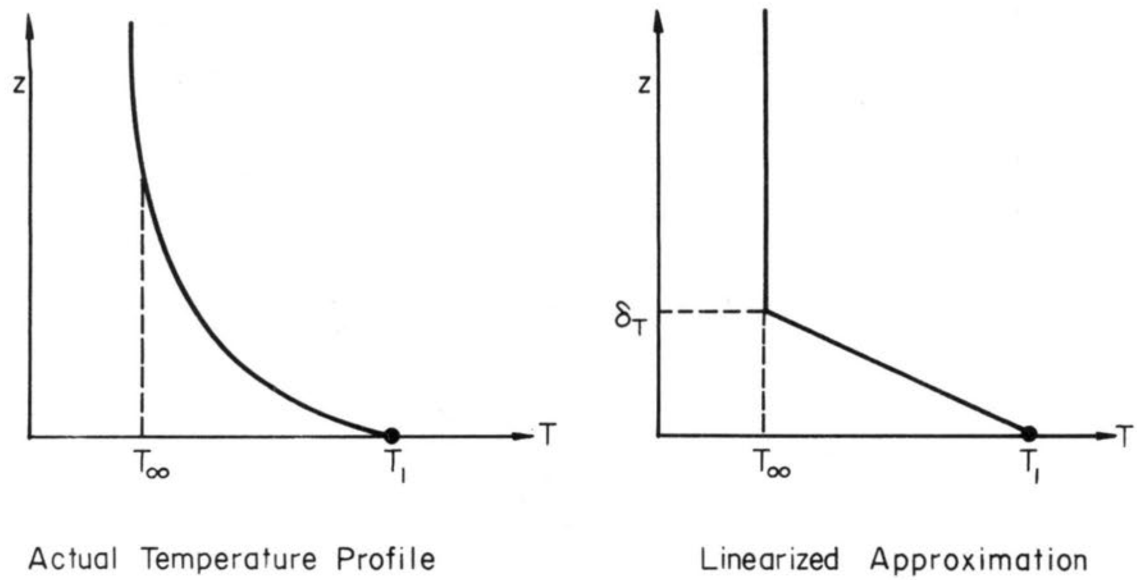

$$\int_0^\infty (T - T_\infty)\, dz = \frac{1}{2} (T_1 - T_\infty)\, \delta_T$$

Fig. (22) The Time Dependent Temperature Profile and Its Two Segment Approximation.

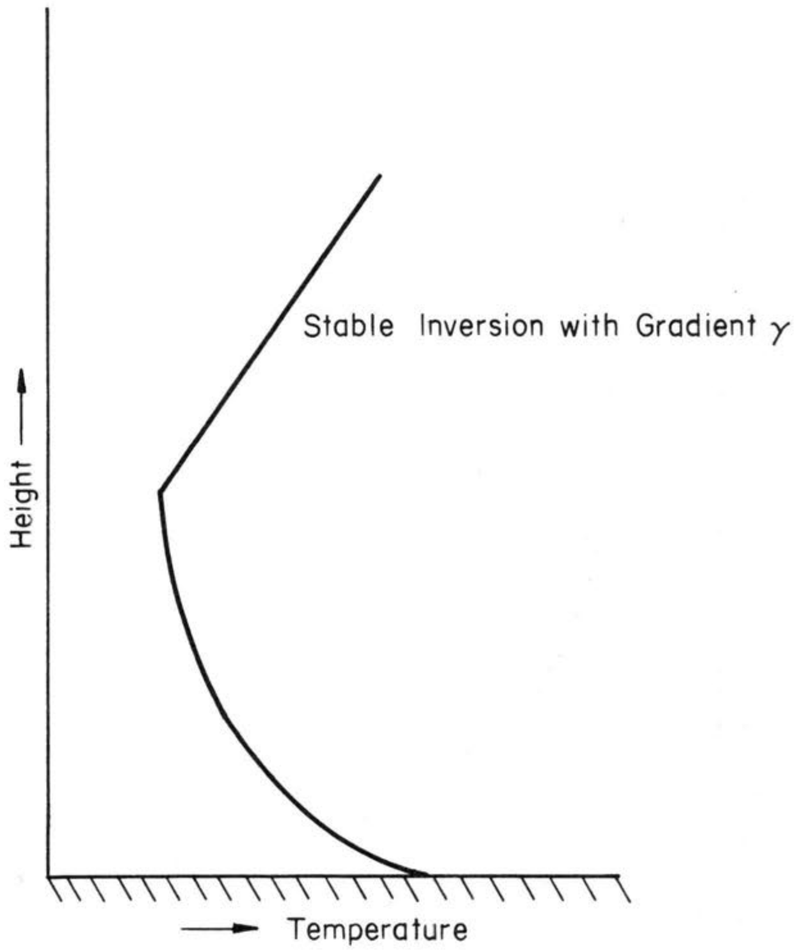

Fig. (23) Mean Temperature Profile with an Elevated Inversion. (Not to Scale)

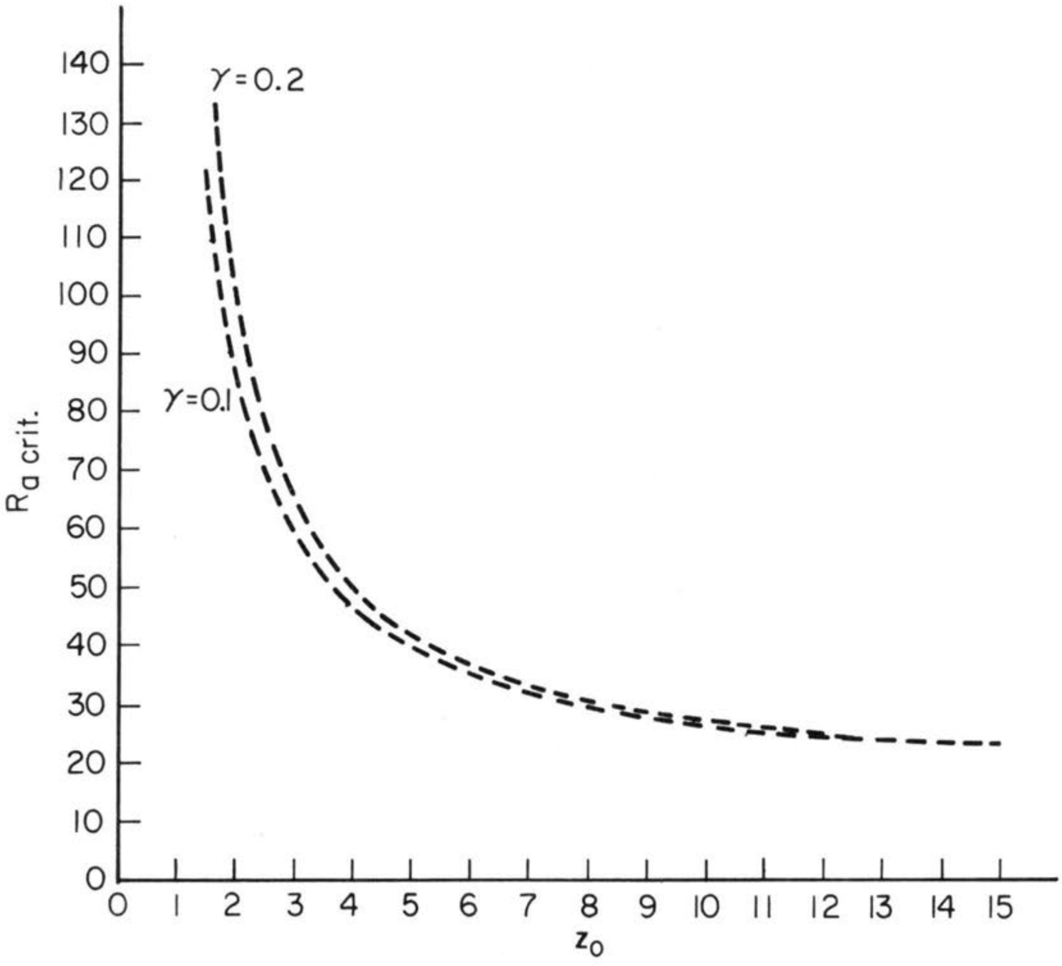

Fig. (24) Variation of Critical Rayleigh Number with Inversion Height.

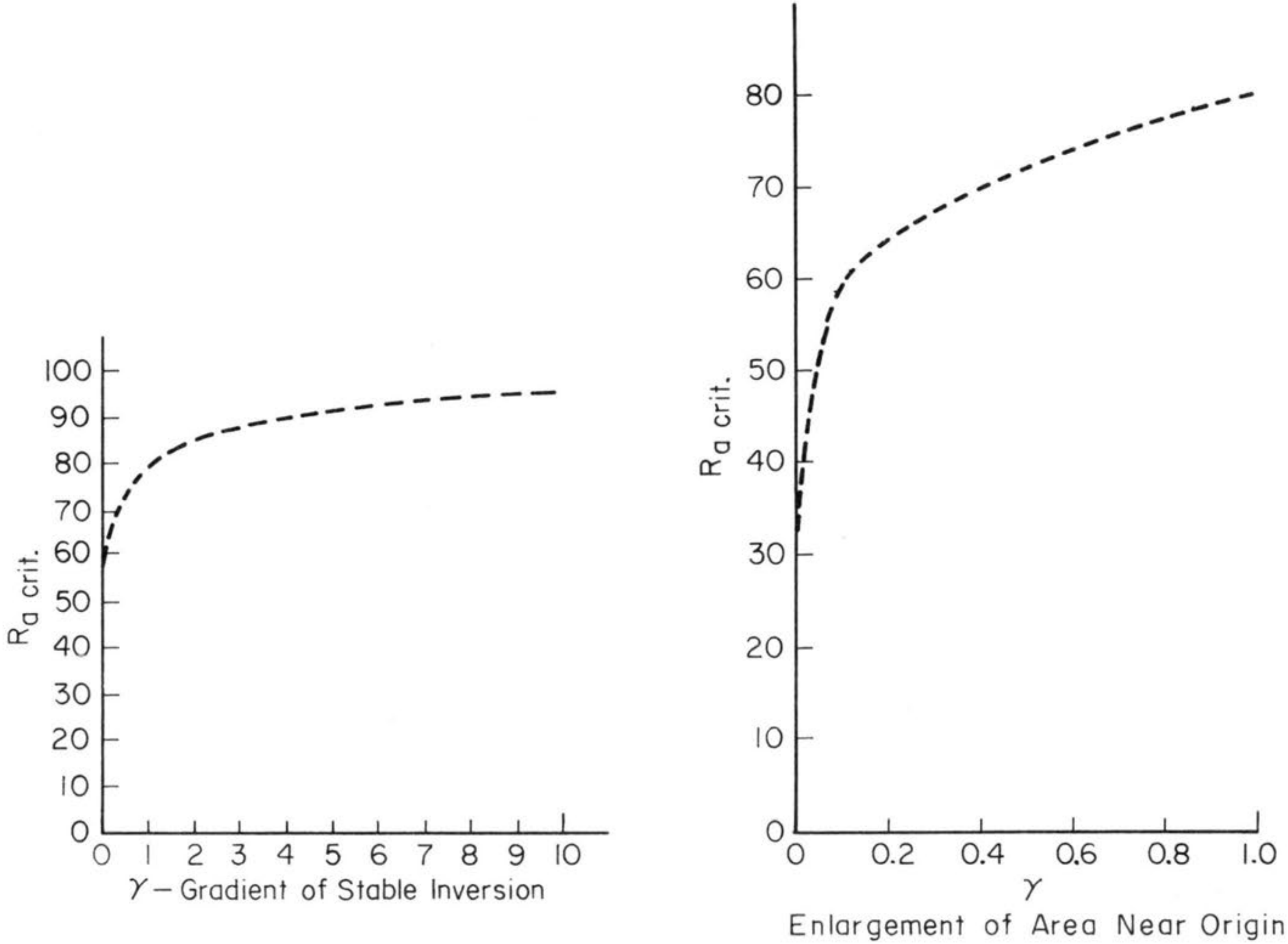

Fig. (25) Variation of Critical Rayleigh Number with Inversion Stability at Constant Inversion Height.

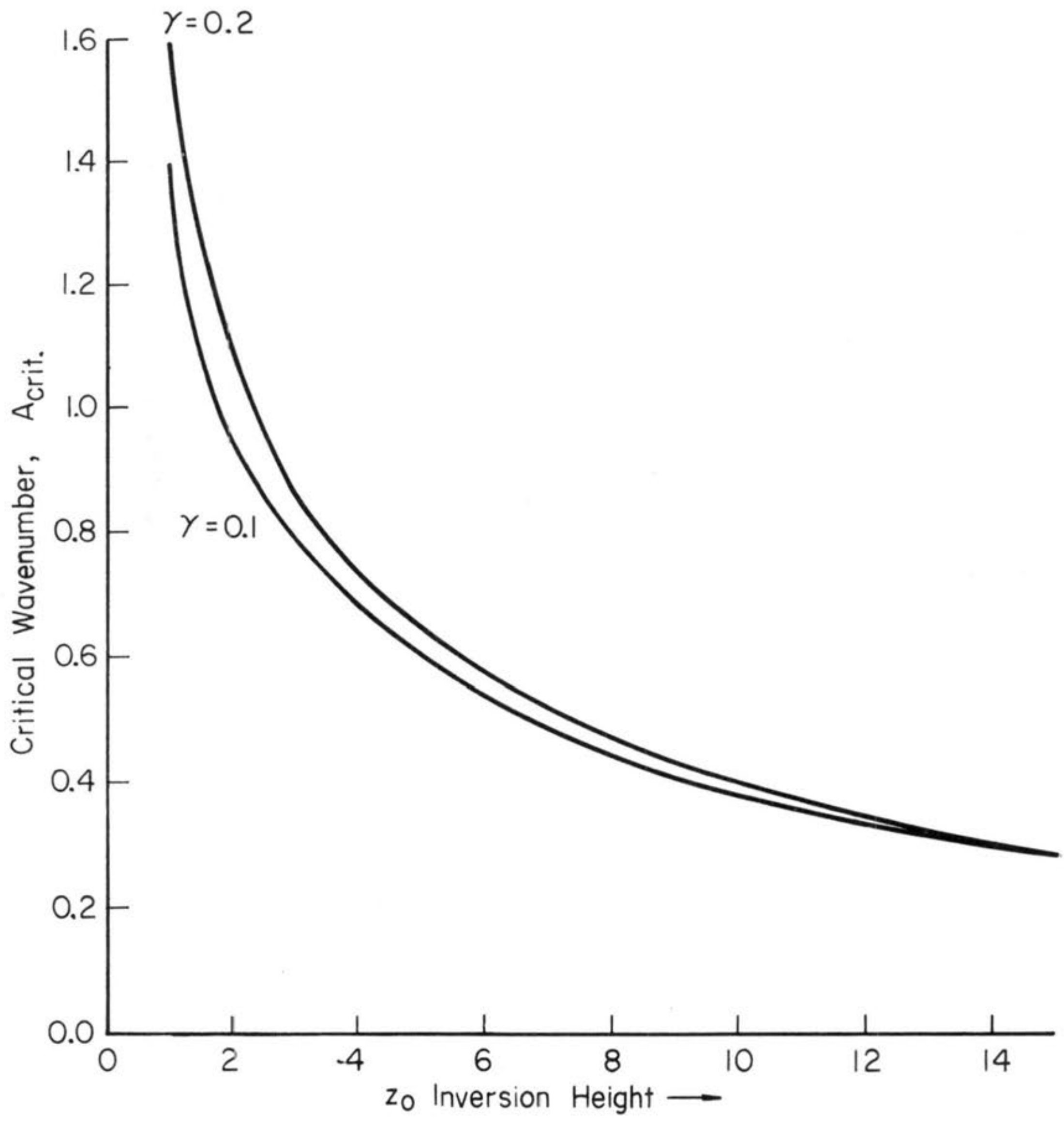

Fig. (26) Variation of Critical Wavenumber with Inversion Height.

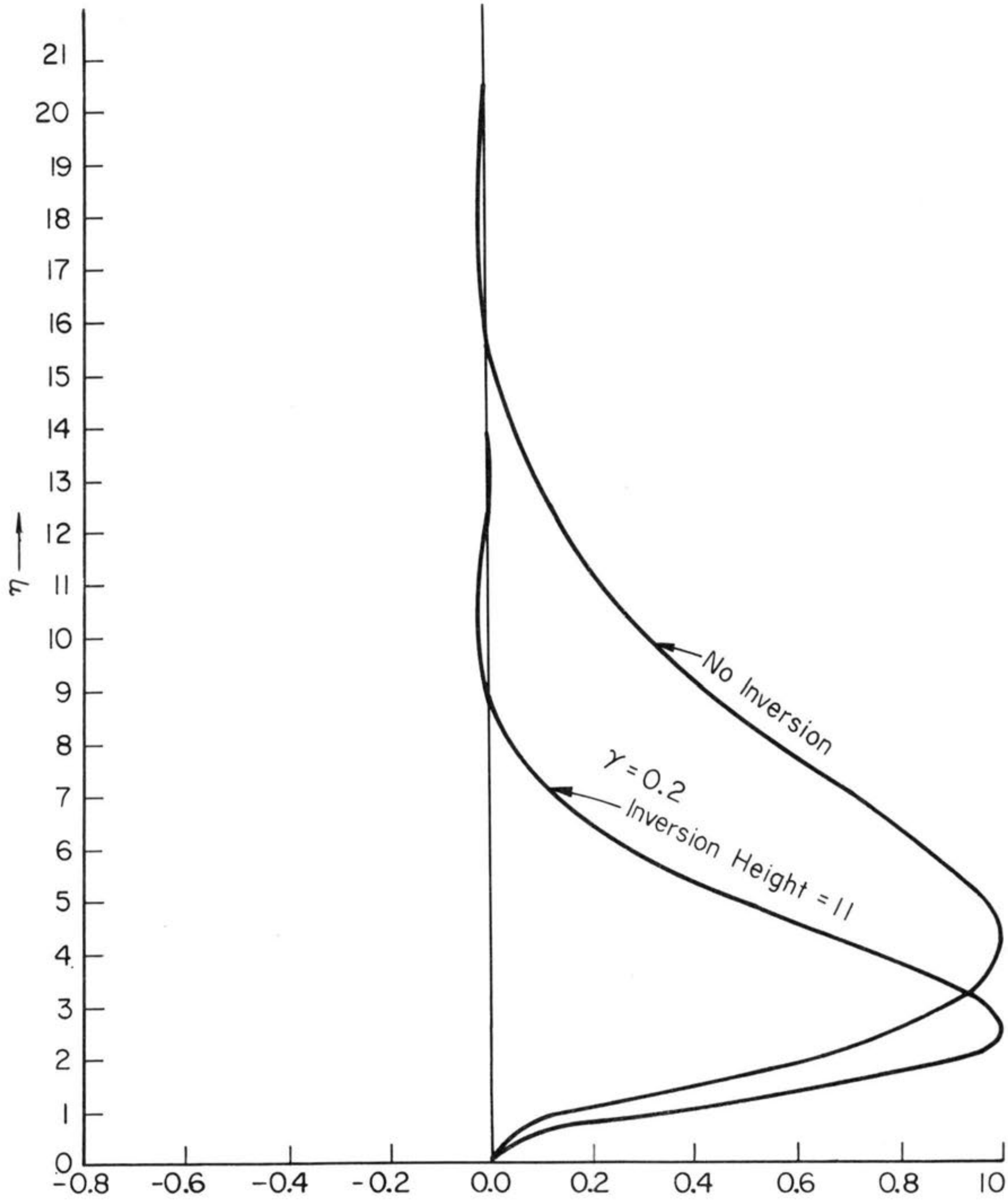

Fig. (27) Normalised $\overline{\tilde{v}\,\tilde{T}}$ Correlation at Critical Conditions.

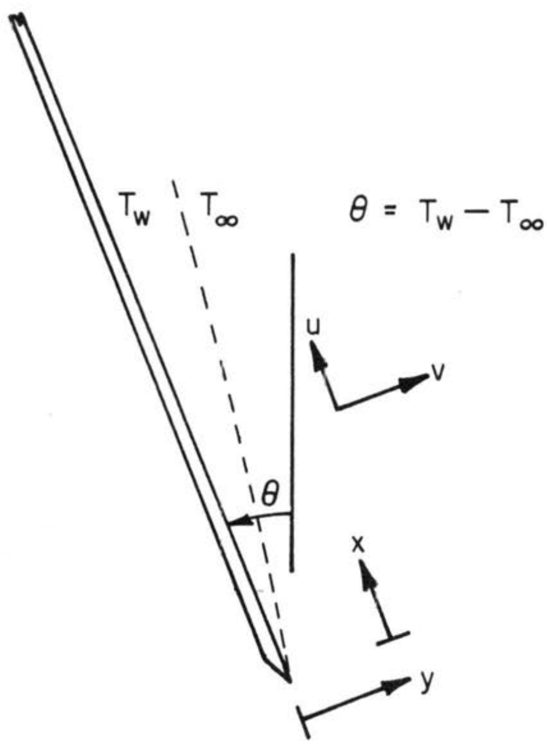

Fig. (28) Natural Convection from an Inclined Plate.

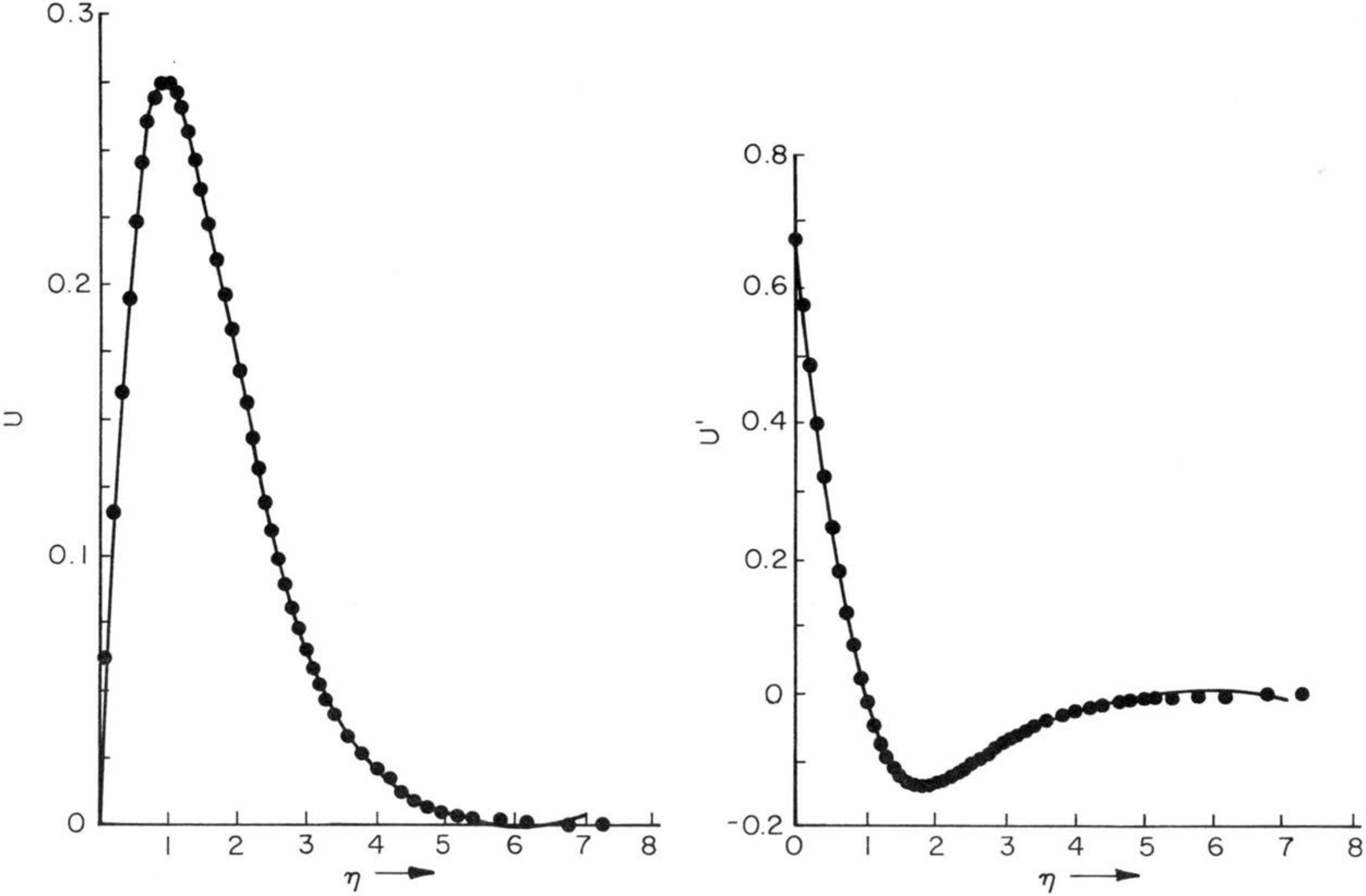

Fig. (29a) Similarity Solutions (points) of the Natural Convection Profiles along a Vertical Heated Plate and Polynomial Approximation (line).

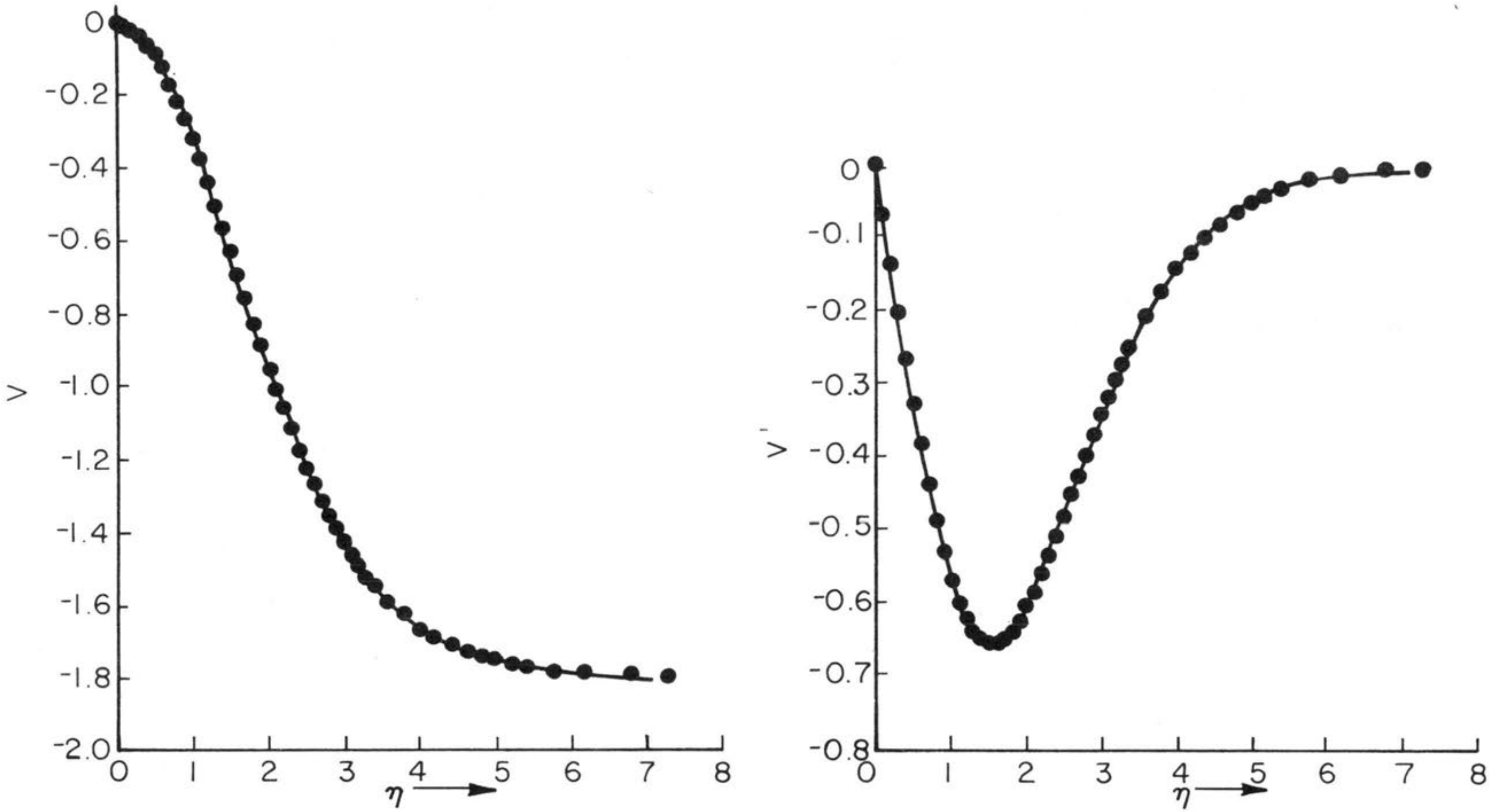

V
0
-0.2
-0.4
-0.6
-0.8
-1.0
-1.2
-1.4
-1.6
-1.8
-2.0
0 1 2 3 4 5 6 7 8
η
V'
0
-0.1
-0.2
-0.3
-0.4
-0.5
-0.6
-0.7
-0.8
0 1 2 3 4 5 6 7 8
η

Fig. (29b)

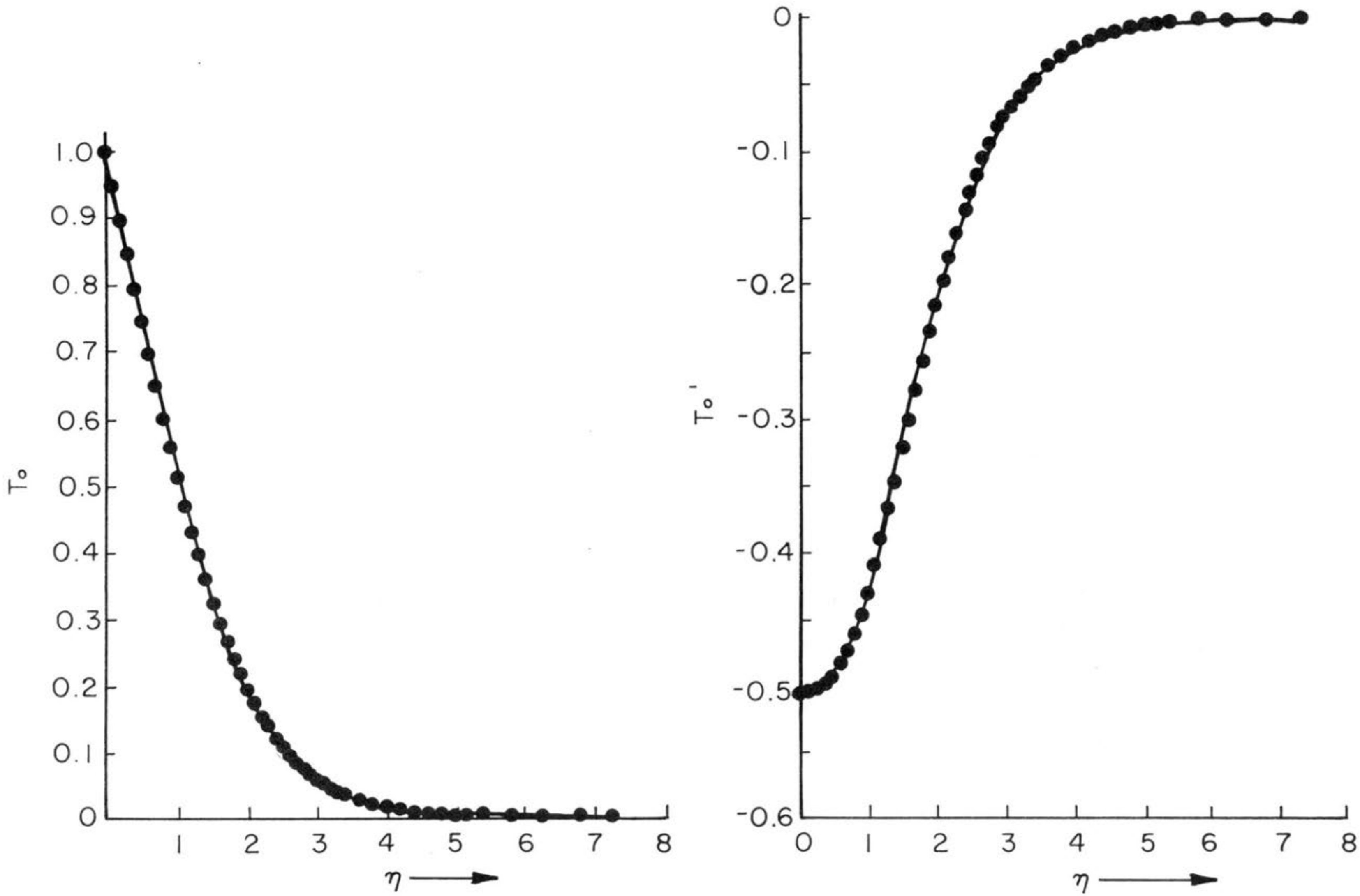
T₀
1.0
0.9
0.8
0.7
0.6
0.5
0.4
0.3
0.2
0.1
0
1
2
3
4
5
6
7
8
η
T₀'
0
-0.1
-0.2
-0.3
-0.4
-0.5
-0.6
0
1
2
3
4
5
6
7
8
η

Fig. (29c)

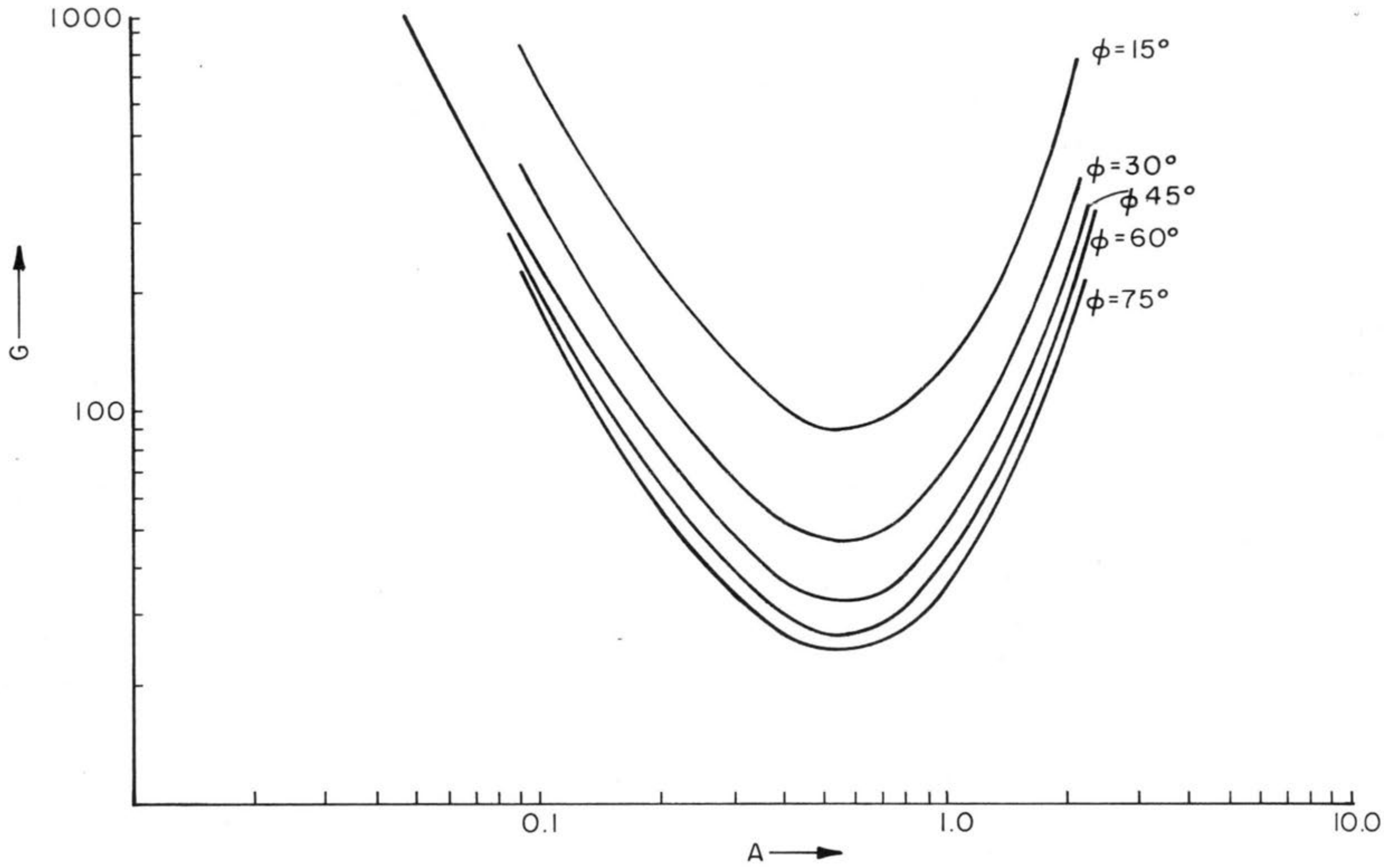

Fig. (30) Neutral Stability Curves for Different Inclination Angles
Prandtl Number = 0.72

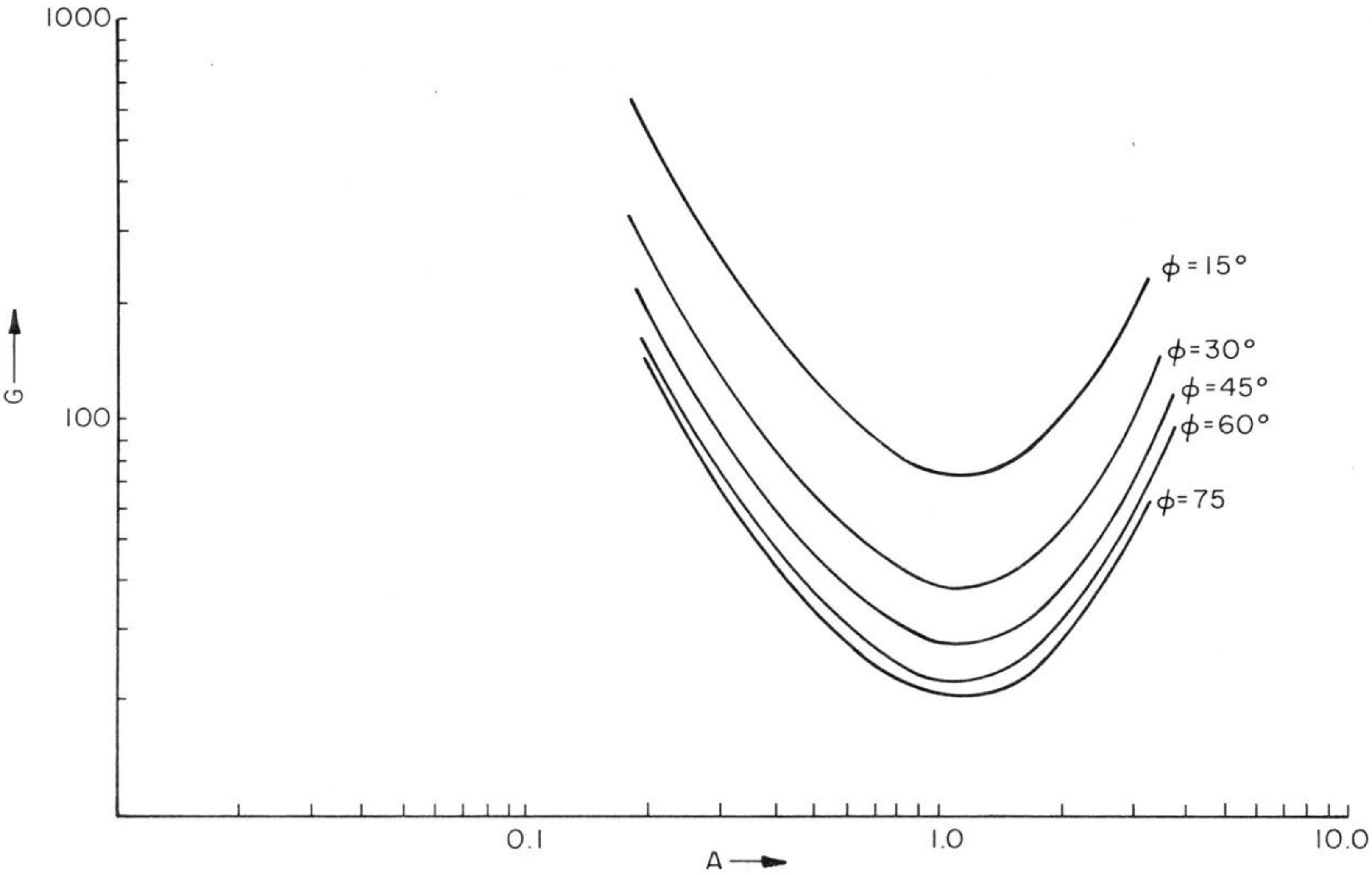

Fig. (31) Neutral Stability Curves for Different Inclination Angles
Prandtl Number = 10 .

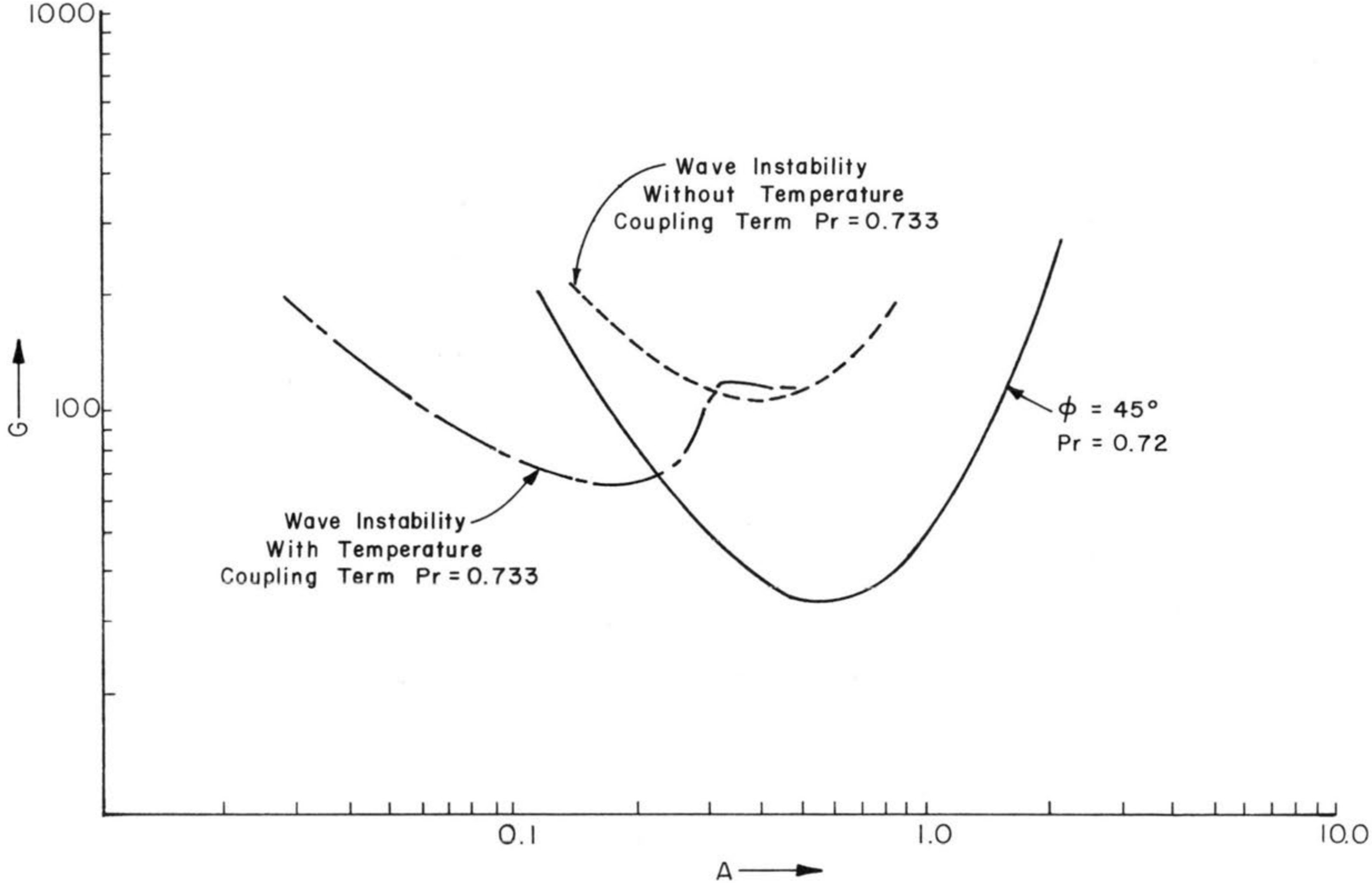

Fig. (32) Comparison of Neutral Amplification Curves for the Two and Three Dimensional Instabilities

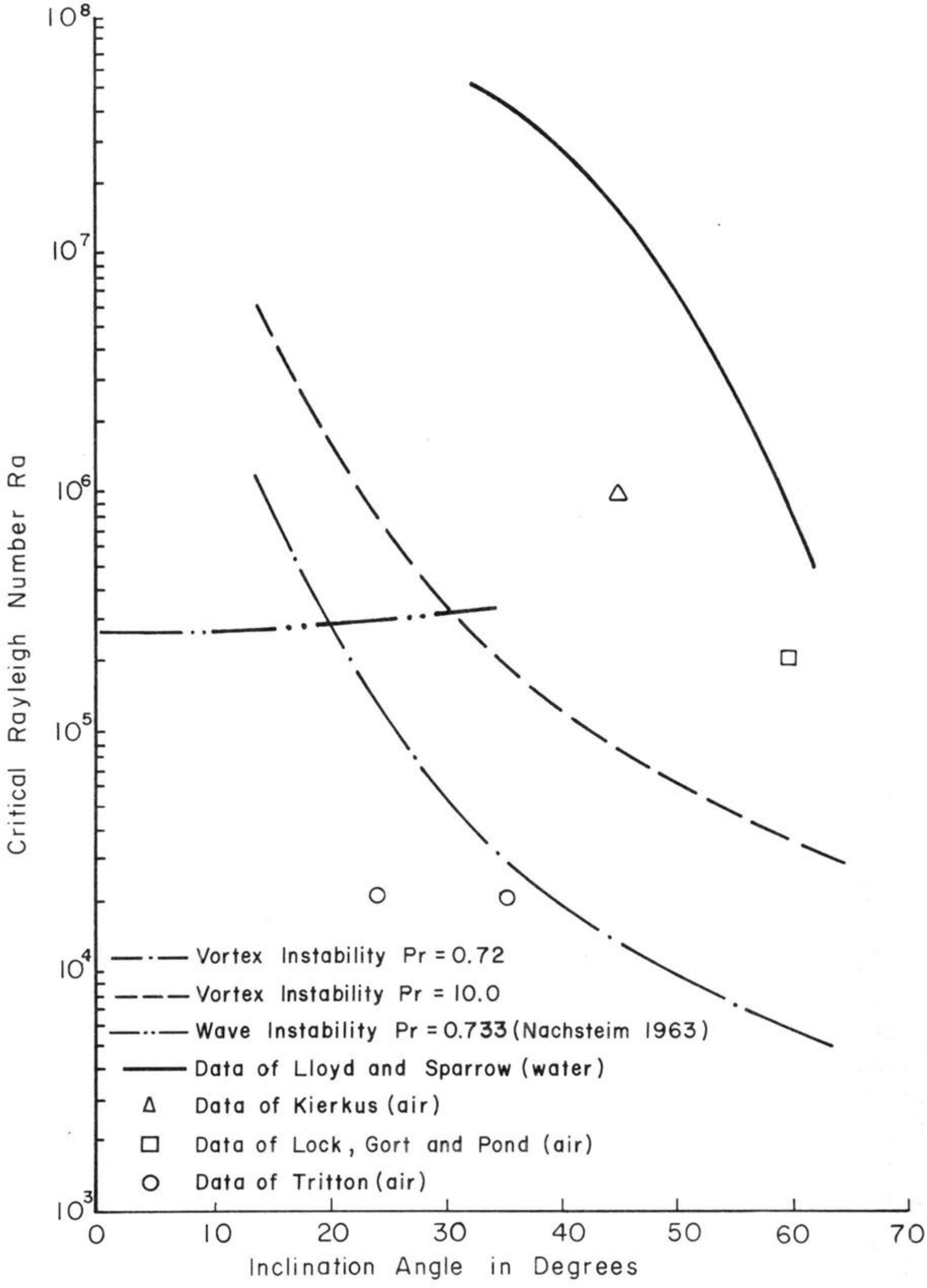

Fig. (33) Comparison of Theory with Experiment

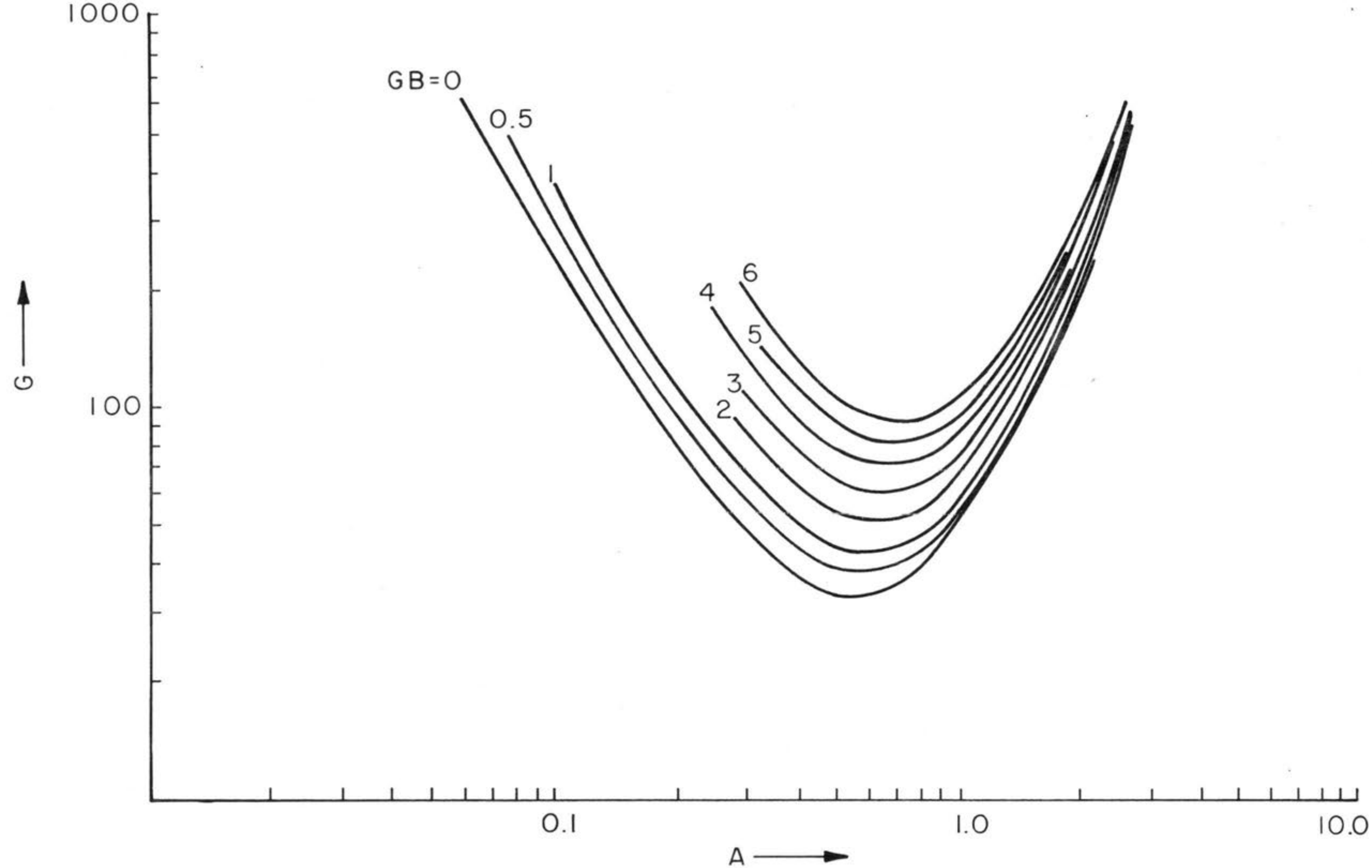

Fig. (34) Amplification Curves for $\phi = 45^{o}$ and Pr = 0.72

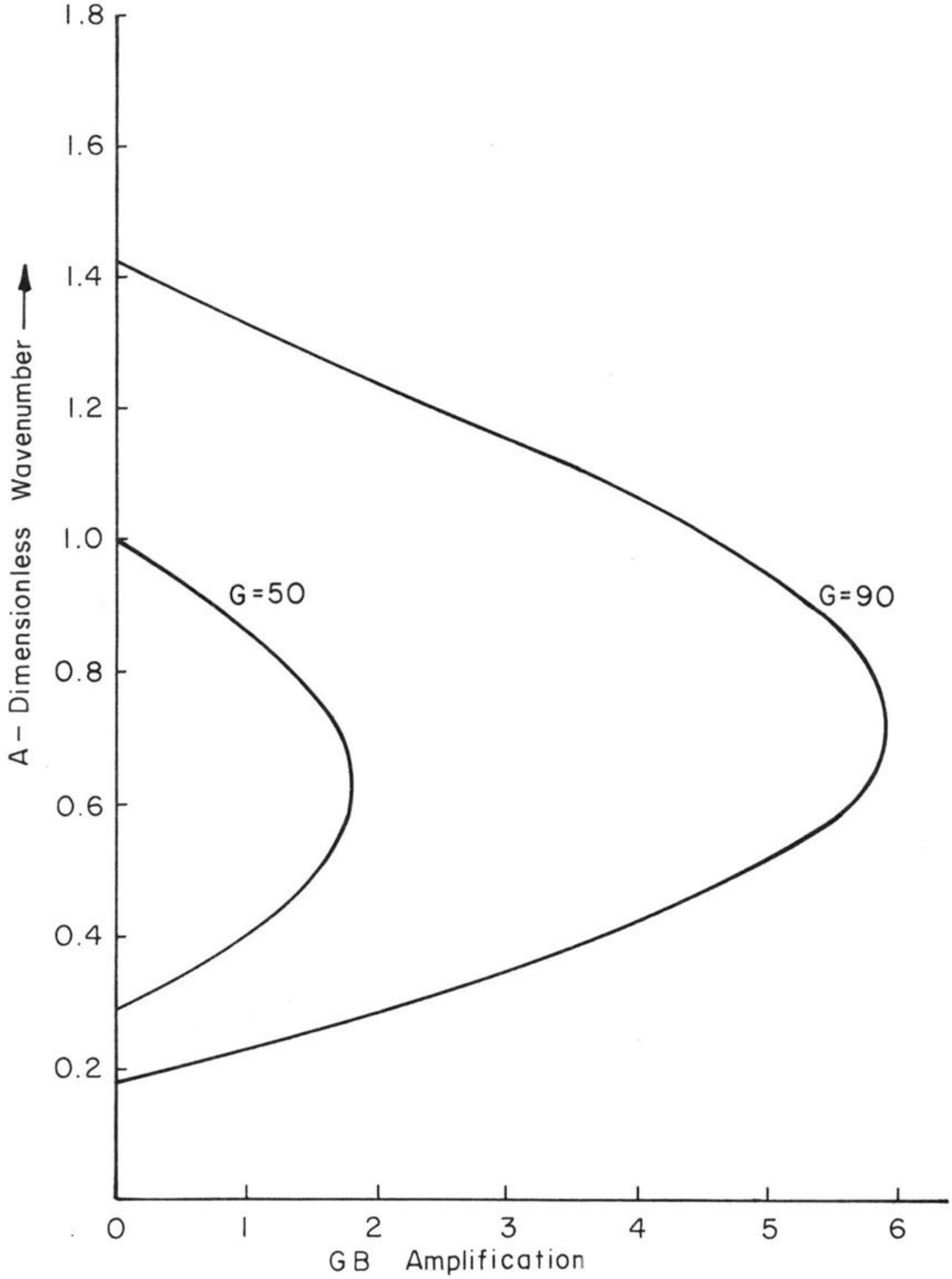

Fig. (35) Curves of Amplification versus Wavenumber Pr = 0.72

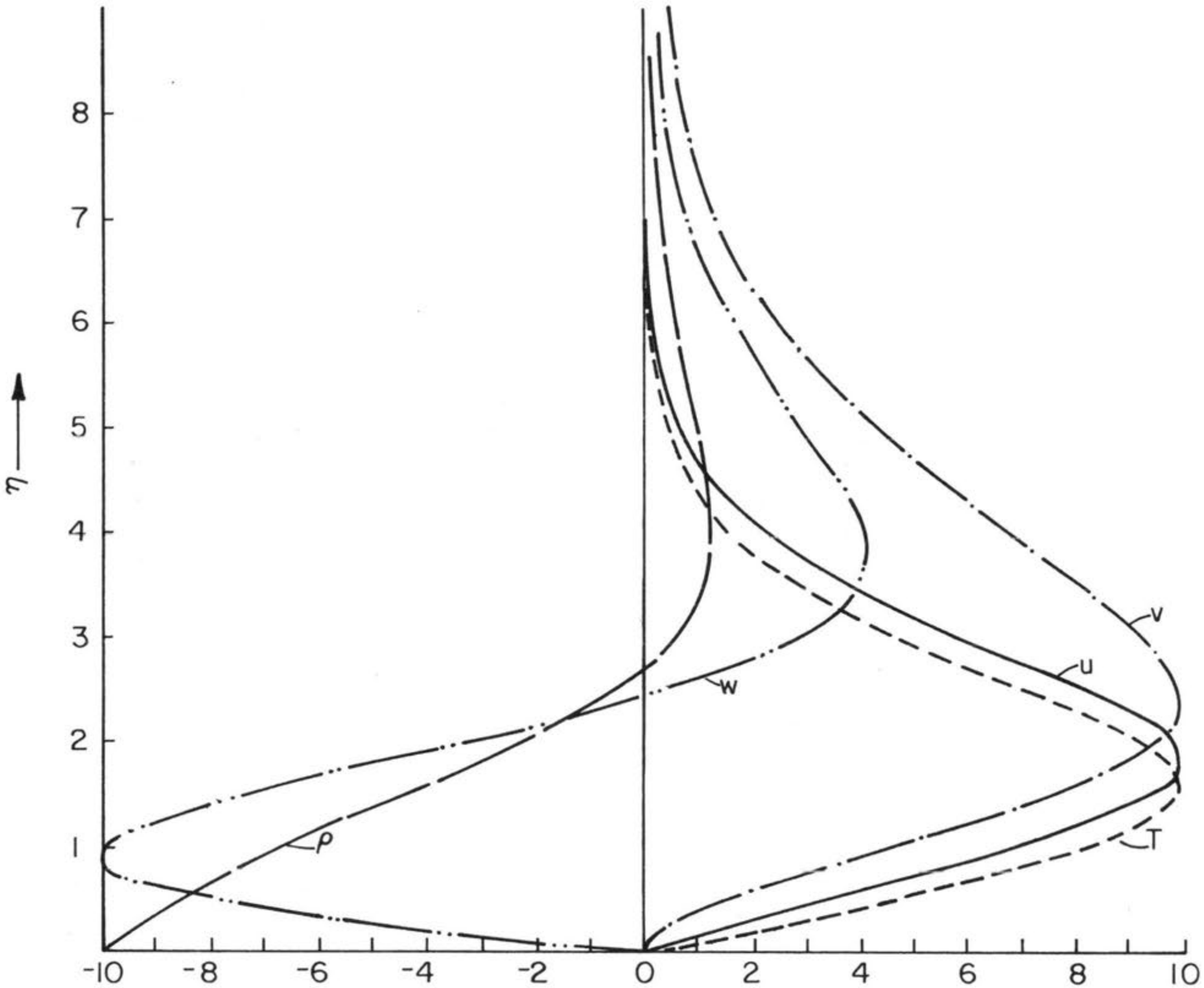

Fig. (36) Normalised Eigenfunctions at Critical Conditions
Pr = 0.72 ϕ = 45°

Unclassified

Security Classification

DOCUMENT CONTROL DATA - R&D

(Security classification of title, body of abstract and indexing annotation must be entered when the overall report is classified)

1. ORIGINATING ACTIVITY (Corporate author) Fluid Dynamics & Diffusion Laboratory College of Engineering, Colorado State University Fort Collins, Colorado 80521	2a. REPORT SECURITY CLASSIFICATION Unclassified 2b. GROUP

3. REPORT TITLE

THE STABILITY OF PARALLEL, QUASI-PARALLEL AND STATIONARY FLOWS

4. DESCRIPTIVE NOTES (Type of report and inclusive dates)

Technical Report

5. AUTHOR(S) (Last name, first name, initial)

Kahawita, René A. and Meroney, Robert N.

6. REPORT DATE	7a. TOTAL NO. OF PAGES	7b. NO. OF REFS
September 1973	162	67

8a. CONTRACT OR GRANT NO. N00014-68-A-0493-0001 b. PROJECT NO. NR 062-41416-6-68 (Code 438) c. d.	9a. ORIGINATOR'S REPORT NUMBER(S) CER73-74RK-RNM 9b. OTHER REPORT NO(S) (Any other numbers that may be assigned this report) THEMIS TECHNICAL REPORT NO. 24

10. AVAILABILITY/LIMITATION NOTICES

Distribution of this report is unlimited

11. SUPPLEMENTARY NOTES	12. SPONSORING MILITARY ACTIVITY
	Office of Naval Research U. S. Department of Defense Washington, D.C.

13. ABSTRACT

The methods of linear perturbation theory have been used to study the stability of various flows, among them being (i) The stability of boundary layers along concave heated walls; (ii) The stability of boundary layers along concave walls with suction; (iii) The stability of wall jets along concave and convex walls; (iv) The spin up of a two-dimensional cylinder in an infinite medium; (v) The stability of stationary layers of fluid with arbitrary temperature stratification; (vi) The stability of natural convection flow along inclined plates.

During the course of this work, three different solution techniques were employed; one of them was an approximate analytic technique, the remaining two were numerical. Three-dimensional spatially and temporally amplifying disturbances were considered in this study.

The results indicated that the normal velocity component of the mean flow in a boundary layer, although much smaller than the stream-wise component had a profound effect in reducing the stability of the flow. On the other hand, suction at the wall improved the stability characteristics. For the flow of parallel layers of fluid along heated walls with small curvature, it was found that a unique stability curve for neutral disturbances may be obtained if the quantity plotted along the abscissa is $Ra + K_S N_G^2$ where Ra is the Rayleigh number, N_G is the Goertler number and K_S is a constant which expresses the relative importance of the mean temperature and velocity profiles.

DD FORM 1 JAN 64 1473

Security Classification

14. KEY WORDS	LINK A		LINK B		LINK C	
	ROLE	WT	ROLE	WT	ROLE	WT
boundary layers						
flow stability						
linear perturbation theory						
wind tunnel experiments						
Rayleigh number						
Goertler number						

INSTRUCTIONS

1. ORIGINATING ACTIVITY: Enter the name and address of the contractor, subcontractor, grantee, Department of Defense activity or other organization *(corporate author)* issuing the report.

2*a*. REPORT SECURITY CLASSIFICATION: Enter the overall security classification of the report. Indicate whether "Restricted Data" is included. Marking is to be in accordance with appropriate security regulations.

2*b*. GROUP: Automatic downgrading is specified in DoD Directive 5200.10 and Armed Forces Industrial Manual. Enter the group number. Also, when applicable, show that optional markings have been used for Group 3 and Group 4 as authorized.

3. REPORT TITLE: Enter the complete report title in all capital letters. Titles in all cases should be unclassified. If a meaningful title cannot be selected without classification, show title classification in all capitals in parenthesis immediately following the title.

4. DESCRIPTIVE NOTES: If appropriate, enter the type of report, e.g., interim, progress, summary, annual, or final. Give the inclusive dates when a specific reporting period is covered.

5. AUTHOR(S): Enter the name(s) of author(s) as shown on or in the report. Enter last name, first name, middle initial. If military, show rank and branch of service. The name of the principal author is an absolute minimum requirement.

6. REPORT DATE: Enter the date of the report as day, month, year; or month, year. If more than one date appears on the report, use date of publication.

7*a*. TOTAL NUMBER OF PAGES: The total page count should follow normal pagination procedures, i.e., enter the number of pages containing information.

7*b*. NUMBER OF REFERENCES: Enter the total number of references cited in the report.

8*a*. CONTRACT OR GRANT NUMBER: If appropriate, enter the applicable number of the contract or grant under which the report was written.

8*b*, 8*c*, & 8*d*. PROJECT NUMBER: Enter the appropriate military department identification, such as project number, subproject number, system numbers, task number, etc.

9*a*. ORIGINATOR'S REPORT NUMBER(S): Enter the official report number by which the document will be identified and controlled by the originating activity. This number must be unique to this report.

9*b*. OTHER REPORT NUMBER(S): If the report has been assigned any other report numbers *(either by the originator or by the sponsor)*, also enter this number(s).

10. AVAILABILITY/LIMITATION NOTICES: Enter any limitations on further dissemination of the report, other than those imposed by security classification, using standard statements such as:

(1) "Qualified requesters may obtain copies of this report from DDC."

(2) "Foreign announcement and dissemination of this report by DDC is not authorized."

(3) "U. S. Government agencies may obtain copies of this report directly from DDC. Other qualified DDC users shall request through ________________."

(4) "U. S. military agencies may obtain copies of this report directly from DDC. Other qualified users shall request through ________________."

(5) "All distribution of this report is controlled. Qualified DDC users shall request through ________________."

If the report has been furnished to the Office of Technical Services, Department of Commerce, for sale to the public, indicate this fact and enter the price, if known.

11. SUPPLEMENTARY NOTES: Use for additional explanatory notes.

12. SPONSORING MILITARY ACTIVITY: Enter the name of the departmental project office or laboratory sponsoring *(paying for)* the research and development. Include address.

13. ABSTRACT: Enter an abstract giving a brief and factual summary of the document indicative of the report, even though it may also appear elsewhere in the body of the technical report. If additional space is required, a continuation sheet shall be attached.

It is highly desirable that the abstract of classified reports be unclassified. Each paragraph of the abstract shall end with an indication of the military security classification of the information in the paragraph, represented as *(TS)*, *(S)*, *(C)*, or *(U)*.

There is no limitation on the length of the abstract. However, the suggested length is from 150 to 225 words.

14. KEY WORDS: Key words are technically meaningful terms or short phrases that characterize a report and may be used as index entries for cataloging the report. Key words must be selected so that no security classification is required. Identifiers, such as equipment model designation, trade name, military project code name, geographic location, may be used as key words but will be followed by an indication of technical context. The assignment of links, rules, and weights is optional.

DISTRIBUTION LIST FOR UNCLASSIFIED TECHNICAL REPORTS ISSUED UNDER
CONTRACT N00014-68-A-0493-0001 TASK 062-414

October 1972

All addressees receive one copy unless otherwise specified

Defense Documentation Center
Cameron Station
Alexandria, Virginia 22314 (12 copies)

Technical Library
Naval Ship Research and
Development Laboratory
Annapolis, Maryland 21402

Professor Bruce Johnson
Engineering Department
Naval Academy
Annapolis, Maryland 21402

Library
Naval Academy
Annapolis, Maryland 21402

Professor W. P. Graebel
Department of Engineering Mechanics
College of Engineering
University of Michigan
Ann Arbor, Michigan 48108

Professor T. Francis Ogilvie
Department of Naval Architecture and
Marine Engineering
University of Michigan
Ann Arbor, Michigan 48108

Professor W. W. Willmarth
Department of Aerospace Engineering
University of Michigan
Ann Arbor, Michigan 48108

AFOSR (REM)
1400 Wilson Boulevard
Arlington, Virginia 22204

Professor S. Corrsin
Department of Mechanics and
Materials Science
The Johns Hopkins University
Baltimore, Maryland 21218

Professor R. B. Couch
Department of Naval Architecture
and Marine Engineering
The University of Michigan
Ann Arbor, Michigan 48105

Professor L. S. G. Kovasznay
Department of Mechanics and
Materials Science
The Johns Hopkins University
Baltimore, Maryland 21218

Professor O. M. Phillips
Department of Mechanics and
Materials Science
The Johns Hopkins University
Baltimore, Maryland 21218

Professor M. Holt
Department of Mechanical Engineering
University of California
Berkeley, California 94720

Professor E. V. Laitone
Department of Mechanical Engineering
University of California
Berkeley, California 94720

Librarian
Department of Naval Architecture
University of California
Berkeley, California 94720

Professor P. Lieber
Department of Mechanical Engineering
Institute of Engineering Research
Berkeley, California 94720

Professor J. R. Paulling
Institute of Engineering Research
Department of Naval Architecture
University of California
Berkeley, California 94720

Professor W. C. Webster
College of Engineering
Department of Naval Architecture
University of California
Berkeley, California 94720

Professor J. V. Wehausen
Institute of Engineering Research
Department of Naval Architecture
University of California
Berkeley, California 94720

Commander
Boston Naval Shipyard
Boston, Massachusetts 02129

Director
Office of Naval Research Branch
Office
495 Summer Street
Boston, Massachusetts 02210

Commander
Puget Sound Naval Shipyard
Bremerton, Washington 98314

Dr. Alfred Ritter
Cornell Aeronautical Laboratory, Inc.
P. O. Box 235
Buffalo, New York 14221

Professor G. Birkhoff
Department of Mathematics
Harvard University
Cambridge, Massachusetts 02138

Professor G. F. Carrier
Division of Engineering and
Applied Physics
Harvard University
Cambridge, Massachusetts 02139

Commanding Officer
NROTC Naval Administrative Unit
Massachusetts Institute of Technology
Cambridge, Massachusetts 02139

Professor M. A. Abkowitz
Department of Ocean Engineering
Massachusetts Institute of Technology
Cambridge, Massachusetts 02139

Professor A. T. Ippen
Department of Civil Engineering
Massachusetts Institute of Technology
Cambridge, Massachusetts 02139

Professor Phillip Mandel
Department of Ocean Engineering
Massachusetts Institute of Technology
Cambridge, Massachusetts 02139

Professor E. W. Merrill
Department of Chemical Engineering
Massachusetts Institute of Technology
Cambridge, Massachusetts 02139

Professor E. Mollo-Christensen
Department of Meteorology
Room 54-1722
Massachusetts Institute of Technology
Cambridge, Massachusetts 02139

Professor J. Nicholas Newman
Department of Ocean Engineering
Room 5-324A
Massachusetts Institute of Technology
Cambridge, Massachusetts 02139

Commander
Charleston Naval Shipyard
Naval Base
Charleston, South Carolina 29408

A. R. Kuhlthau, Director
Research Laboratories for the
Engineering Sciences
Thorton Hall, University of Virginia
Charlottesville, Virginia 22903

Director
Office of Naval Research Branch Office
536 South Clark Street
Chicago, Illinois 60605

Library
Naval Weapons Center
China Lake, California 93555

Professor R. V. Edwards
Division of Chemical Engineering
Case Western Reserve University
Cleveland, Ohio 44106

Professor J. M. Burgers
Institute of Fluid Dynamics and
Applied Mathematics
University of Maryland
College Park, Maryland 20742

Professor Pai
Institute of Fluid Dynamics and
Applied Mathematics
University of Maryland
College Park, Maryland 20742

Acquisition Director
NASA Scientific and Technical Information
P. O. Box 33
College Park, Maryland 20742

Technical Library
Naval Weapons Laboratory
Dahlgren, Virginia 22448

Computation and Analyses Laboratory
Naval Weapons Laboratory
Dahlgren, Virginia 22448

Dr. R. H. Kraichnan
Dublin, New Hampshire 03444

Commanding Officer
Army Research Office
Box CM, Duke Station
Durham, North Carolina 27706

Dr. Martin H. Bloom
Polytechnic Institute of Brooklyn
Long Island Graduate Center
Department of Aerospace Engineering and
Applied Mechanics
Farmingdale, New York 11735

Technical Documents Center
Building 315
U. S. Army Mobility Equipment Research and
Development Center
Fort Belvoir, Virginia 22060

Professor J. E. Cermak
Department of Atmospheric Sciences
Colorado State University
Fort Collins, Colorado 80521

Professor O. H. Shemdin
Coastal and Oceanographic Engineering
Department
University of Florida
Gainesville, Florida 32601

Technical Library
Webb Institute of Naval Architecture
Glen Cove, Long Island, New York 11542

Professor E. V. Lewis
Webb Institute of Naval Architecture
Glen Cove, Long Island, New York 11542

Dr. J. P. Breslin
Davidson Laboratory
Stevens Institute of Technology
Castle Point Station
Hoboken, New Jersey 07030

Mr. C. H. Henry
Stevens Institute of Technology
Davidson Laboratory
Castle Point Station
Hoboken, New Jersey 07030

Dr. D. Savitsky
Davidson Laboratory
Stevens Institute of Technology
Castle Point Station
Hoboken, New Jersey 07030

Dr. A. Strumpf
Davidson Laboratory
Stevens Institute of Technology
Castle Point Station
Hoboken, New Jersey 07030

Dr. J. P. Craven
University of Hawaii
1801 University Avenue
Honolulu, Hawaii 96822

Professor J. F. Kennedy, Director
Iowa Institute of Hydraulic Research
State University of Iowa
Iowa City, Iowa 52240

Professor L. Landweber
Iowa Institute of Hydraulic Research
State University of Iowa
Iowa City, Iowa 52240

Professor E. L. Resler
Graduate School of Aeronautical Engineering
Cornell University
Ithaca, New York 14851

Dr. Y. H. Pao
Flow Research, Inc.
1819 South Central Avenue
Suite 72
Kent, Washington 98031

Dr. D. E. Ordway
Sage Action, Incorporated
P. O. Box 416
Ithaca, New York 14850

Professor John Miles
c/o I.G.P.P.
University of California, San Diego
La Jolla, California 92038

Director
Scripps Institute of Oceanography
University of California
La Jolla, California 92037

Professor A. T. Ellis
University of California, San Diego
Department of Aerospace and
Mechanical Engineering Science
La Jolla, California 92037

Dr. Coda Pan
Mechanical Technology Incorporated
968 Albany-Shaker Road
Latham, New York 12110

Mr. P. Eisenberg, President
Hydronautics, Incorporated
8210 Pindell School Road
Laurel, Maryland 20810

Mr. M. P. Tulin
Hydronautics, Incorporated
8210 Pindell School Road
Laurel, Maryland 20810

Commander
Long Beach Naval Shipyard
Long Beach, California 90802

Professor John Laufer
Department of Aerospace Engineering
University Park
Los Angeles, California 90007

Dr. F. H. Harlow
University of California
Los Alamos Scientific Laboratory
P. O. Box 1663
Los Alamos, New Mexico 87544

Professor J. M. Killen
St. Anthony Falls Hydraulic Laboratory
University of Minnesota
Minneapolis, Minnesota 55414

Lorenz G. Straub Library
St. Anthony Falls Hydraulic Laboratory
University of Minnesota
Minneapolis, Minnesota 55414

Professor J. Ripkin
St. Anthony Falls Hydraulic Laboratory
University of Minnesota
Minneapolis, Minnesota 55414

Dr. E. Silberman
St. Anthony Falls Hydraulic Laboratory
University of Minnesota
Minneapolis, Minnesota 55414

Superintendent
Naval Postgraduate School
Attn: Library
Monterey, California 93940

Professor A. B. Metzner
Department of Chemical Engineering
University of Delaware
Newark, New Jersey 19711

Technical Library
Naval Underwater Systems Center
Newport, Rhode Island 02840

Office of Naval Research
New York Area Office
207 W. 24th Street
New York, New York 10011

Professor V. Castelli
Department of Mechanical Engineering
Columbia University
New York, New York 10027

Professor H. Elrod
Department of Mechanical Engineering
Columbia University
New York, New York 10027

Engineering Societies Library
345 E. 47th Street
New York, New York 10017

Professor J. J. Stoker
Institute of Mathematical Sciences
New York University
251 Mercer Street
New York, New York 10003

Society of Naval Architects and
Marine Engineers
74 Trinity Place
New York, New York 10006

Miss O. M. Leach, Librarian
National Research Council
Aeronautical Library
Montreal Road
Ottawa 7, Canada

Technical Library
Naval Coastal System Laboratory
Panama City, Florida 32401

Dr. J. W. Hoyt
Naval Undersea R & D Center
Pasadena Laboratory
3202 E. Foothill Boulevard
Pasadena, California 91107

Technical Library
Naval Undersea R & D Center
Pasadena Laboratory
3203 E. Foothill Boulevard
Pasadena, California 91107

Professor A. J. Acosta
Department of Mechanical Engineering
California Institute of Technology
Pasadena, California 91109

Professor H. Liepmann
Graduate Aeronautical Laboratory
California Institute of Technology
Pasadena, California 91109

Professor M. S. Plesset
Department of Engineering Science
California Institute of Technology
Pasadena, California 91109

Professor A. Roshko
California Institute of Technology
Graduate Aeronautical Laboratories
Pasadena, California 91109

Professor T. Y. Wu
Department of Engineering Science
California Institute of Technology
Pasadena, California 91109

Director
Office of Naval Research Branch Office
1030 E. Green Street
Pasadena, California 91106

Naval Ship Engineering Center
Philadelphia Division
Technical Library
Philadelphia, Pennsylvania 19112

Technical Library
Philadelphia Naval Shipyard
Philadelphia, Pennsylvania 19112

Professor R. C. MacCamy
Department of Mathematics
Carnegie Institute of Technology
Pittsburgh, Pennsylvania 15213

Dr. Paul Kaplan
Oceanics, Inc.
Technical Industrial Park
Plainview, New York 11803

Technical Library
Naval Missile Center
Point Mugu, California 93441

Technical Library
Naval Civil Engineering Laboratory
Port Hueneme, California 93041

Commander
Norfolk Naval Shipyard
Portsmouth, Virginia 23709

Dr. H. N. Abramson
Southwest Research Institute
8500 Culebra Road
San Antonio, Texas 78228

Editor
Applied Mechanics Review
Southwest Research Institute
8500 Culebra Road
San Antonio, Texas 78206

Dr. Andrew Fabula
Code 600, Building 106
Naval Undersea R & D Center
San Diego, California 92132

Office of Naval Research
San Francisco Area Office
760 Market Street, Room 447
San Francisco, California 94102

Library
Pearl Harbor Naval Shipyard
Box 400, FPO
San Francisco, California 96610

Technical Library
Hunters Point Naval Shipyard
San Francisco, California 94135

Librarian
Naval Ordnance Laboratory
White Oak
Silver Spring, Maryland 20910

Mr. J. Enig
Room 3-252
Naval Ordnance Laboratory
White Oak
Silver Spring, Maryland 20910

Fenton Kennedy Document Library
The Johns Hopkins University
Applied Physics Laboratory
8621 Georgia Avenue
Silver Spring, Maryland 20910

Professor E. Y. Hsu
Department of Civil Engineering
Stanford University
Stanford, California 94305

Dr. Byrne Perry
Department of Civil Engineering
Stanford University
Stanford, California 94305

Dr. R. L. Street
Department of Civil Engineering
Stanford University
Stanford, California 94305

Professor R C. Di Prima
Department of Mathematics
Rensselaer Polytechnic Institute
Troy, New York 12181

Professor J. Lumley
Department of Aerospace Engineering
Pennsylvania State University
University Park, Pennsylvania 16802

Dr. J. M. Robertson
Department of Theoretical and
Applied Mechanics
University of Illinois
Urbana, Illinois 61803

Technical Library
Mare Island Naval Shipyard
Vallejo, California 94592

Code 438
Office of Naval Research
Department of the Navy
Arlington, Virginia 22217 (3 copies)

Code 461
Office of Naval Research
Department of the Navy
Arlington, Virginia 22217

Code 463
Office of Naval Research
Department of the Navy
Arlington, Virginia 22217

Code 466
Office of Naval Research
Department of the Navy
Arlington, Virginia 22217

Code 468
Office of Naval Research
Department of the Navy
Arlington, Virginia 22217

Code 473
Office of Naval Research
Department of the Navy
Arlington, Virginia 22217

Code 481
Office of Naval Research
Department of the Navy
Arlington, Virginia 22217

Code 2627
Naval Research Laboratory
Washington, D. C. 20390 (6 copies)

Library, Code 2629 (ONRL)
Naval Research Laboratory
Washington, D. C. 20390 (6 copies)

Code 6170
Naval Research Laboratory
Washington, D. C. 20390

Code 4000
Director of Research
Naval Research Laboratory
Washington, D. C. 20390

Code 8030 (Maury Center)
Naval Research Laboratory
Washington, D. C. 20390

Code 8040
Naval Research Laboratory
Washington, D. C. 20390

Code 031
Naval Ship Systems Command
Washington, D. C. 20360

Code 0341
Naval Ship Systems Command
Washington, D. C. 20360

Code 0322 (L. Benen)
Naval Ship Systems Command
Washington, D. C. 20360

Code 0321 (J. Schuler)
Naval Ship Systems Command
Washington, D. C. 20360

Code 2052
Naval Ship Systems Command
Washington, D. C. 20360

Code 6034
Naval Ship Engineering Center
Center Building
Prince George's Center
Hyattsville, Maryland 20782

Code 6101E
Naval Ship Engineering Center
Center Building
Prince George's Center
Hyattsville, Maryland 20782

Code 6110
Naval Ship Engineering Center
Center Building
Prince George's Center
Hyattsville, Maryland 20782

Code 6114
Naval Ship Engineering Center
Center Building
Prince George's Center
Hyattsville, Maryland 20782

Code 6120E
Naval Ship Engineering Center
Center Building
Prince George's Center
Hyattsville, Maryland 20782

Code 6136
Naval Ship Engineering Center
Center Building
Prince George's Center
Hyattsville, Maryland 20782

Dr. A. Powell (Code 01)
Naval Ship Research & Development Center
Bethesda, Maryland 20034

Mr. W. M. Ellsworth (Code 11)
Naval Ship Research & Development Center
Bethesda, Maryland 20034

Dr. W. E. Cummins (Code 15)
Naval Ship Research & Development Center
Bethesda, Maryland 20034

Dr. H. R. Chaplin (Code 16)
Naval Ship Research & Development Center
Bethesda, Maryland 20034

Mr. G. H. Gleissner (Code 18)
Naval Ship Research & Development Center
Bethesda, Maryland 20034

Mr. R. Wermter (Code 152)
Naval Ship Research & Development Center
Bethesda, Maryland 20034

Dr. W. B. Morgan (Code 154)
Naval Ship Research & Development Center
Bethesda, Maryland 20034

Mr. J. B. Hadler (Code 156)
Naval Ship Research & Development Center
Bethesda, Maryland 20034

Library (Code 5641)
Naval Ship Research & Development Center
Bethesda, Maryland 20034

Mr. S. F. Crump (Code 1505)
Naval Ship Research & Development Center
Bethesda, Maryland 20034

Dr. P. Pien (Code 1521)
Naval Ship Research & Development Center
Bethesda, Maryland 20034

Mr. Paul Granville (Code 1541)
Naval Ship Research & Development Center
Bethesda, Maryland 20034

Mr. J. McCarthy (Code 1552)
Naval Ship Research & Development Center
Bethesda, Maryland 20034

Dr. Nils Salvesen (Code 1552)
Naval Ship Research & Development Center
Bethesda, Maryland 20034

Dr. M. Strasberg (Code 1901)
Naval Ship Research & Development Center
Bethesda, Maryland 20034

Code 03
Naval Air Systems Command
Department of the Navy
Washington, D. C. 20360

AIR 5301
Naval Air Systems Command
Department of the Navy
Washington, D. C. 20360

AIR 604
Naval Air Systems Command
Department of the Navy
Washington, D. C. 20360

Code ORD 03
Naval Ordnance Systems Command
Department of the Navy
Washington, D. C. 20360

Code ORD 035
Naval Ordnance Systems Command
Department of the Navy
Washington, D. C. 20360

Code ORD 05413
Naval Ordnance Systems Command
Department of the Navy
Washington, D. C. 20360

Code ORD 9132
Naval Ordnance Systems Command
Department of the Navy
Washington, D. C. 20360

CNM PM-1
Strategic Systems Project Office
Department of the Navy
Washington, D. C. 20360

Technical Division (CNM PM 11-20)
Deep Submergence Systems Project Office
Department of the Navy
Washington, D. C. 20360

Oceanographer of the Navy
Washington, D. C. 20390

Commander
Naval Oceanographic Office
Washington, D. C. 20390

Dr. A. L. Slafkosky
Scientific Advisor
Commandant of the Marine Corps (CODE AX)
Washington, D. C. 20380

Librarian Station 5-2
Coast Guard Headquarters
NASSIF Building
400 7th Street, S.W.
Washington, D. C. 20591

Office of Research and Development
Maritime Administration
441 G Street, N.W.
Washington, D. C. 20235

Division of Ship Design
Maritime Administration
441 G Street, N.W.
Washington, D. C. 20235

National Science Foundation
Engineering Division
1800 G Street, N.W.
Washington, D. C. 20550

Dr. G. Kulin
National Bureau of Standards
Washington, D. C. 20234

Science & Technology Division
Library of Congress
Washington, D. C. 20540

Chief of Research & Development
Office of Chief of Staff
Department of the Army
Washington, D. C. 20310

Professor A. Thiruvengadam
Department of Mechanical Engineering
The Catholic University of America
Washington, D. C. 20017

Dr. A. S. Iberall, President
General Technical Services, Inc.
451 Penn Street
Yeadon, Pennsylvania 19050

Commander
Portsmouth Naval Shipyard
Portsmouth, New Hampshire 03801